UNIVERSITAT DE BARCELONA

Analysis of Reelin function in brain development and in adult neurogenesis

Análisis de la función de Reelina en el desarrollo del cerebro y la neurogénesis adulta

Alba del Valle Vílchez Acosta

UNIVERSITAT DE BARCELONA

FACULTAT DE BIOLOGIA

DEPARTAMENTO DE BIOLOGIA CEL·LULAR, FISIOLOGIA I IMMUNOLOGIA

PARC CIENTÍFIC DE BARCELONA

Analysis of Reelin function in brain development and in adult neurogenesis

Alba del Valle Vílchez Acosta

Barcelona, 2019

Programa Doctorado Biomedicina

UNIVERSITAT DE BARCELONA

FACULTAT DE BIOLOGIA

DEPARTAMENTO DE BIOLOGIA CEL·LULAR, FISIOLOGIA I IMMUNOLOGIA

PARC CIENTÍFIC DE BARCELONA

Analysis of Reelin function in brain development and in adult neurogenesis

Análisis de la función de Reelina en el desarrollo del cerebro y la neurogénesis adulta

Programa Doctorado Biomedicina

Memoria presentada por Alba del Valle Vílchez Acosta, licenciada en Biotecnología, para optar al grado de Doctora por la Universitat de Barcelona.

Los Estudios de tercer ciclo se han enmarcado en el programa de **Doctorado en Biomedicina** de la Universitat de Barcelona. El proyecto de Tesis Doctoral está inscrito al Departamento de Biologia Cel·lular, Fisiologia i Immunologia de la Facultat de Biologia de la Universitat de Barcelona. El trabajo experimental y la redacción de la memoria que se presentan han estado dirigidos por el Dr. Eduardo Soriano García y la Dra. Yasmina Manso Sanz.

Barcelona, septiembre de 2019

Dr. Eduardo Soriano García

Dra. Yasmina Manso Sanz

Doctoranda

Alba del Valle Vílchez Acosta

A mi abuela Valle,
A mis padres y a Jorge.

Je suis de ceux qui pensent que la science est d'une grande beauté. Un scientifique dans son laboratoire est non seulement un technicien : il est aussi un enfant placé devant des phénomènes naturels qui l'impressionnent comme des contes de fées.

Maria Salomea Skłodowska-Curie (Varsovia-Passy)

Caminante, son tus huellas
el camino y nada más;
Caminante, no hay camino,
se hace camino al andar.

Antonio Machado (Sevilla-Colliure)

ACKNOWLEDGMENT

Este capítulo de mi vida está a punto de cerrarse y me gustaría dedicar unas breves palabras de agradecimiento a todas aquellas personas que han sido partícipes y han hecho posible que esta tesis llegue al final de su recorrido.

En primer lugar me gustaría dar las gracias al Dr. Eduardo Soriano, gracias por abrirme las puertas del laboratorio, por confiar en mí y por darme la oportunidad de poder realizar esta tesis. A la Dra. Yasmina Manso, gracias por enseñarme tanto, gracias por tus consejos y gracias por haberme guiado durante todo este tiempo. Muchas gracias a los dos por haber dirigido esta tesis.

A los compañeros del laboratorio, GRACIAS a todos, a los que siguen y a los que ya se fueron. En especial me gustaría dar las gracias a Ash, porque sin ti nos volveríamos locos. A Núria, por dejarnos de herencia tú trabajo. A Sere y a Dani (ciao ragazzi!), por vuestra ayuda y vuestra alegría. También me gustaría dar las gracias a todos los estudiantes que han pasado por el laboratorio, Laia, Berta, Lorena, muchísimas gracias por vuestro trabajo. Berta, esto se merece unas buenas croquetas!.

También me gustaría agradecer a todo el personal de plataformas técnicas y estabularios sin los cuales hubiera sido imposible realizar todo este trabajo. En especial a las chicas de microscopía del Clínic (María, Elisenda y Anna) y del Parc. También al personal de los estabularios, David, Laia. Muchísmas gracias por todo.

Gracias también al Dr. Víctor Borrell por permitirme realizar una estancia en su laboratorio. Gracias Adri, Ana, Salma, Lucía, Cristina… por haberme acogido y ayudado durante mi estancia. Gracias también a Michael, quién diría que el destino nos volvería a juntar! Grazie di tutto!

La lista de todos los que me habéis ayudado durante estos cuatro años es muy larga, a todos GRACIAS.

Pero para llegar hasta aquí el camino fue largo y me gustaría agradecer a todas las personas que me han ayudado a recorrerlo.

En primer lugar a Matilde, a Luisa, al Dr. Juanjo, porque la vida es como una carrera de obstáculos pero uno nunca se rinde hasta que no cruza la meta. Des personnes de Paris… Angelique, Danica, Carola, Human, Joan… merci pour tout.

Gracias a mis Biotecs, por compartir conmigo 5 años tan increíbles. A mis pilimilitrini, Angie, Clara, por ser siempre, porque siempre es un hasta luego. Parras, Paula, porque nuestros caminos se sigan cruzando.

A los planarios, por ser mi alegría en Barcelona. Por hacerme sentir un poquito más en casa. Gracias Giulia, Carles, Liska, Sara, Arantxa, Aleix…

Gracias a ti Jordi, y a tu familia, por cuidarme tanto. Angeleta, por enseñarme la cuina catalana. A ti Jordi, gracias por traerme hasta aquí y por descubrir conmigo tantas cosas. Gracias por confiar siempre en mí.

Gracias a todos los que de una forma u otra han hecho que Barcelona fuese mi segunda casa. Gracias Cone, por ayudarme siempre. Gracias Elena, por traer un poco de sur al norte. Gracias Ana y Nathan, por enseñarme las buenas sorpresas que te da la vida. Gracias a mis Andaluzas, por levantarme el ánimo cuando más lo necesitaba. Gracias Marta, por estar siempre dispuesta a todo. Gracias a Andreu, por compartir conmigo el mejor congreso. Gracias a ti

Artur, Arturitooo, porque siempre nos quedará Bruno Mars... Y gracias a todos los que habéis compartido conmigo tantos momentos durante estos años.

A mis amigos de siempre, los de Pinoloko (sí tenía que aparecer), porque de allí venimos y mira dónde estamos. Fernan, Javi, Sergio, gracias por ser y estar, por hacerme querer volver siempre, por recordarme quién soy. Gracias Sergio, por tener siempre un momento para mí. A los tres, gracias de todo corazón.

Si he llegado hasta aquí sin duda ha sido gracias a la PhD family. Gracias Marc, porque gracias a tí uno aprende a relativizar las cosas XD. A ti Cris… tengo tantas cosas que agradecerte que podría escribir otra tesis. Ha sido una suerte tenerte de compañera de tesis.

Gràcies Toni, per haver sigut el meu company en moltíssims aspectes. Gràcies perquè sense tu, ara no seria qui soc. Especialment, gràcies per escoltar les meves reflexions infumables sobre el món de la Reelina, sense els teus consells i la teva paciència aquesta tesi no seria el que és.

Por último, quiero dar las gracias a mi familia. Pepa, Sole, tita Antonia, abuela, Gabi, Sandra, Reyes, Cristóbal, María… Gracias porque sin vosotros no sería quien soy.

Gracias Papá, Mamá y Jorge por todo. Gracias Jorge por ser el mejor hermano del mundo. Crecer a tu lado ha sido la mejor experiencia de mi vida. Gracias Papá, por ser como dicen los Carapapas mi primer amor. Gracias Mamá, por enseñarme lo que significan las alas, y ayudarme a volar siempre. GRACIAS por ser mi hogar, y por vuestro apoyo incondicional, esta tesis es de los cuatro.

A tots, gràcies.

A todos, gracias.

ABSTRACT

Reelin is a large extracellular matrix glycoprotein with a crucial role both during brain development, where it is key for neuronal migration and for the formation of the layered structure of cerebral cortex and cerebellum, and in the adulthood, where it is involved in adult synaptic plasticity, including neurogenesis in the dentate gyrus and dendritogenesis amongst other processes. Reelin acts through the binding to its canonical receptors (apolipoprotein E receptor 2, ApoER2; and very low density lipoprotein receptor, VLDLR) which trigger a complex signaling cascade involving numerous kinases and the adaptor protein Dab1. At the embryonic stage, Reelin is expressed mainly by Cajal-Retzius cells on the developing brain whereas at perinatal stages its expression gradually disappears from Cajal-Retzius cells and starts to be expressed by GABAergic interneurons of the cortex and hippocampus.

In the neocortex, postmitotic neurons migrate in an ordered sequence that determines the normal "inside-out" layer formation. The malpositioning of cortical neurons is a result of abnormal migration and could cause severe layering malformations with functional consequences related with neurodevelopmental diseases such as Schizophrenia, Autism and Epilepsy. In this context, one of the most studied models has been the *reeler* mouse which presents a characteristic phenotype caused by an autosomal mutation in the *Rln* gene. The *reeler* mouse presents several morphological defects including a failed pre-plate splitting that causes a roughly inverted neuronal layering in the cortex, mispositioning of pyramidal neurons as well as granular cells on the dentate gyrus and profound cerebellar hypoplasia. However the study of the effects of Reelin signaling in the adult brain is difficult in the *reeler* mouse model due to the failed migration and mispositioning during development. Thus, to unravel the function of Reelin at different developmental stages (from embryonic to adult) as well as to gain insight in the potential distinct contribution of Reelin from different cell-types, we have generated three Reelin deficient conditional transgenic lines which allow us to ubiquitously delete Reelin in a temporally-controlled manner (Cre fR/fR) or selectively remove Reelin from Cajal-Retzius cells (CR fR/fR) or GABAergic interneurons (Gad fR/fR).

Analysis of the cortical organization using layer-specific markers reveals that, unlike the *reeler* mouse, none of our transgenic lines shows the characteristic inversion of cortical layers. Moreover, our data strongly indicates that Reelin from Cajal-Retzius cells is important for the typical inside-out laminar cortical development but seems to be dispensable for pre-plate splitting. Furthermore, our results suggest that the absence of Reelin during early postnatal and adult stages seems to impact on the well-defined laminar structure of the cortex, leading to an invasion of layer I by late-born neurons from layer II-III. Regarding the hippocampus, our results suggest, on the one hand, a differential contribution of Reelin expressed by Cajal-Retzius cells and by GABAergic interneurons in the formation of the laminar structures of the hippocampus. On the other hand, temporally-controlled removal of Reelin at postnatal stages demonstrates that it is essential for the correct formation of the hippocampus whereas in the adult seems to be key for several aspects of hippocampus neurogenesis, including neuronal positioning in the dentate gyrus and dendritic orientation at different maturation stages of adult new-born granule cells. Finally, our findings also support the importance of Reelin expression for proper Purkinje cell migration, but not for granule cell disposition in the cerebellum at early postnatal and adult stages.

Taken altogether, our results suggest a causal relation between the absence of Reelin and structural alterations in the hippocampus, cortex and cerebellum, either at developments stages or adult stages.

TABLE OF CONTENTS

Table of Contents

Index of Figures and Tables

2. Role of Reelin expressed by GAD65 interneurons in corticogenesis and hippocampus formation

3. Analysis of the conditional loss of Reelin signaling in early postnatal development and adult stages in the cortex, hippocampus and cerebellum

Index of abbreviations

aa	amino acid
AD	Alzheimer disease
ADAMTS	a desintegrin and metalloproteinase with trombospondin motifs
AIS	axon initial segment
Akt	Ak thymona
AMPA	α-amino-3-hydroxy-5-methyl-4-isoxazolepropionic acid
ApoE	apoliprotein E
ApoER2	apoliprotein E receptor 2
APP	amyloid precursor protein
BDNF	brain-derived neurotrophic factor
BMP	bone morphogenic protein
BLBP	brain lipid-binding protein
CA	Cornus Ammonis
CAM	cell adhesion molecule
CAMKK	calmodulin-dependent protein kinase kinase
CAMKI	calmodulin-dependent protein kinase I
cAMP	cyclic adenosine monophosphate
Ca^{2+}	Calcium ion
CNS	central nervous system
CLASP2	cytoplasmic linker-associated protein 2
CP	cortical plate
CR	Calretinin
CRC	Cajal-Retzius cell
CSF	cerebrospinal fluid
Ct	C-terminus
CTR	carboxyl terminal region
Cul5	Cullin 5
C3G	C3 glomerulopathy
Dab1	disabled-1
DCX	Doublecortin
DG	dentate gyrus
DNE	dentate neuroepithelium
EC	entorhinal cortex
ECM	extracellular matrix
EGF	epidermal growth factor
EGL	external granular layer
FGF	fibroblast growth factor
GABA	gamma-aminobutyric acid
GAD	glutamic acid descarboxilase
GC	granule cell
GCL	granule cell layer
GFAP	glial fibrillary acidic protein
GSK3β	glycogen synthase kinase-3β
HP	hippocampal plate
IGL	inner granular layer
IGF	insulin-like growth factor
IP	intermediate progenitor
IPB	infra-pyramidal blade

IZ	intermediate zone
Kb	kilobases
KDa	kilodaltons
LIMK1	LIM motif-containing protein kinase 1
Lis1	Lissencephaly 1
LKB1	liver kinase B1
LTD	long-term depression
LTP	long-term potentiation
MAPS	microtubule assembly-promoting proteins
MARK2	microtubule affinity-regulating kinase 2
ML	molecular layer
MMP	matrix metalloproteinases
MTLE	mesial temporal lobe epilepsy
MTOC	microtubule-organizing center
mTOR	mammalin target of rampamycin
MZ	marginal zone
NMDA	N-methyl-D-aspartate
NPC	neural precursor cell
NGF	nerve growth factor
NT	neurotrophin
Nt	N-terminal
OB	olfactory bulbs
OML	outer molecular layer
PC	Purkinje cell
pDab1	phosphorylated Dab1
PI3K	phosphoinositide 3-kinase
PIP_3	phosphatidylinositol triphosphate
PKA	protein kinase A
PNNs	perineuronal nets
PP	preplate
PSA-NCAM	polysialyted-neural cell adhesion molecule
RA	retinoic acid
Rac1	Ras-Releated C3 Botulinum Toxin Substrate 1
Rap1	Ras-related protein 1
RG	radial glia
RMS	rostral migratory stream
SDM	secondary dentate matrix
SFKs	Src-family kinases
SGZ	subgranular zone
Shh	Sonic hedgehog
slm	stratum lacunosum moleculare
SNPs	single-nucleotide polymorphisms
so	stratum oriens
SOCS	cytokine signalling proteins
Sox2	sry-related HMG box transcription factor
sp	stratum pyramidale
SP	subplate
SPB	supra-pyramidal blade
Sp1	Specific protein 1
sr	stratum radiatum
SVZ	subventricular zone
Tag1	transient axonal glycoprotein-1

TDM	tertiary dentate matrix
TGF	transforming growth factor
TH	tyrosine hydroxylase
tPA	tissue plasminogen activator
TRK	tropomyosin receptor kinases
TSP1	thrombospondin-1
VLDLR	very low density lipoprotein receptor
VZ	ventricular zone

INTRODUCTION

1. The development of the nervous system.

1.1. Compartmentalization of the nervous system.

In the mammalian embryo, the formation of the neural tube defines the first appearance of the central nervous system (CNS). Its development is the result of the process of neurulation, in which the outer surface of the embryo (or ectoderm) folds giving rise to the formation of the neural tube. At the time that neurulation ends the longitudinal anterior-posterior (or rostral-caudal) axis of the embryo is already established. About fifty percent of the caudal end becomes spinal cord. This area is organized in repeated segments called neuromeres. Conversely, the rostral part of the neural tube that becomes the cephalic portion or brain, acquires a suprasegmental organization meaning that its setup does not repeat. Nevertheless, small portions of this suprasegmental structure acquire a pattern of segmental organization such as the motor and the sensory components. The molecular basis behind this kind of organization is due to the restricted pattern of expression of genes from the Hox and Pax family amongst others, and the presence of inductive signals that control changes in gene expression such as retinoic acid (RA), fibroblast growth factor (FGF), transforming growth factor (TGF), Sonic hedgehog (Shh) hormone or signalling through Wnt family (Leung & Shimeld, 2019)(Lakoma *et al.*, 2011)(Nikolopoulou *et al.*, 2017)(Franco & Muller, 2011).

Later on during development, the cephalic neural tube differentiates into three primordial vesicles: the prosencephalon or forebrain, the mesencephalon or midbrain and the rhomboencephalon or hindbrain in a rostral-caudal axis. In a next step, the prosencephalon is subdivided into the telencephalon and diencephalon, and the rhomboencephalon becomes subdivided into the metencephalon and myelencephalon. These five secondary vesicles define the major structural divisions of the adult brain: the cortex, hippocampus and olfactory cortices originate from the telencephalon, the thalamus and hypothalamus are derived from the diencephalon, and the cerebellum is developed from the metencephalon **(Figure I.1.1.)** (Sotelo, 2004)(Greene & Copp, 2014).

Taking into account the circumferential dimension of the neural tube, differentiation in the dorsal-ventral axis correlates with the functional organization of the CNS into sensory and motor areas. Both, the longitudinal (rostral-caudal) and the circumferential (dorsal-ventral) axis control the expression of different molecular markers that define a grid-like pattern of domains in the wall of the neural tube.

An additional level of complexity is given by a series of changes in the radial dimension of the neural tube that generates a variety of laminar structures. In order to understand how this lamination pattern takes place it is necessary to consider the cellular processes through which each cell goes through including cell proliferation, cell migration, cell differentiation and cell death.

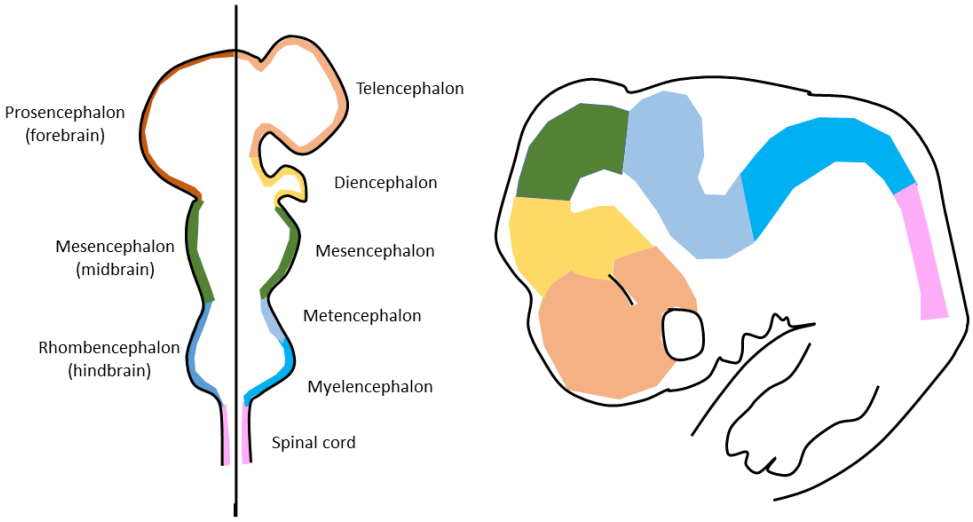

Figure I.1.1. | Longitudinal differentiation of the neural tube. Left, schematic representation of the lateral view of the neural tube. In the left side, the three primordial vesicles, the prosencephalon, the mesencephalon and the rhombencephalon are represented. On the right side, the five secondary vesicles that will give rise to the adult brain, telencephalon, diencephalon, mesencephalon, metencephalon and myelencephalon, and the spinal cord are showed. **Right,** sagittal section of an embryo showing the distribution of the five secondary vesicles and the spinal cord. Adapted from: (Sotelo, 2004)

1.2. Cell proliferation

The majority of the cells of the CNS (neurons and glia) are produced in the ventricular zone (VZ). Progenitor cells in the VZ are known as neural precursor cells (NPCs). During its cell-cycle, precursor cells in the VZ remain attached to both the ventricular and the pial surfaces. With each cell-cycle these neural precursors proliferate as neural stem cells or stop proliferation to become postmitotic neuroblasts and migrate out of VZ. In some parts of the CNS such as the neocortex, a second proliferative zone appears the subventricular zone (SVZ). Proliferative cells in the SVZ are no attached to the ventricular or pial surfaces (Gelman & Marin, 2010). In the VZ, NPCs can divide symmetrically to expand their population or asymmetrically (Obernier & Alvarez-Buylla, 2019)(Laumonnerie & Solecki, 2018). There are several modes of asymmetrical division:

- Neurogenic division: a postmitotic neuroblast and another progenitor cell are generated.
- Asymmetric progenitor division: the division gives rise to a progenitor cell and an intermediate progenitor (IP) cell that migrates to other proliferative region such as the SVZ.
- Gliogenic division: the division results in a postmitotic neuroblast and a glial cell that migrates away from the VZ to become astroglia.

1.3. Cell migration

Since proliferation occurs in zones different than the ultimate destination of the neurons, new-generated postmitotic neurons have to migrate to reach their final position. In the CNS, several principle types of migration have been proposed based on the route of migration and the ways in which cells interact during migration: radial migration, tangential migration and chain migration. However neurons often switch between these types of migration, suggesting that besides cell-intrinsic mechanisms, extracellular cues can influence the choice of a particular migration mode. Depending on the distance, the migration mode could be divided into "outside-to-inside" migration or "inside-to-outside" displacement. In the outside-to-inside mode, neurons are displaced from the border of the proliferative zone by newly produced cells. Thus, the last generated neurons are located closer to the proliferative area while the earliest are placed further away. One of the regions where this type of displacement is present in the dentate gyrus (DG) of the hippocampus. Conversely, in the inside-to-outside mode of migration, new generated neurons migrate long distances away from the proliferative area bypassing the previously generated cells. This pattern of migration is generally referred to as neuronal migration and is present in the cerebral and cerebellar cortices (Super *et al.*, 1998) (Franco & Muller, 2011).

1.3.1. Formation of the neocortex

In the adult cerebral cortex neurons are arranged into six well defined cortical layers generated in an inside-to-outside manner. There are two main types of cortical neurons: the projection pyramidal neurons and the local interneurons. Projecting neurons are located in layers III, IV, V and VI. They are excitatory neurons that use glutamate as a transmitter. The cortical interneurons, on the other hand, are inhibitory gamma-aminobutyric acid (GABA)-containing cells that remain distributed along the cortex. Both cell types are born in distinct progenitor niches of the embryonic telencephalon, and are displaced in their final position by using two different migration programs, the radial and the tangential migration modes respectively (Cooper, 2008)(Zhou *et al.*, 2007).

1.3.1.1. Radial migration

Cortical projection neurons are generated in the VZ and the SVZ of the telencephalon. The cortical migration from the proliferative zone is guided by a particular type of glial cell, the radial glia (RG) cell. Cortical development progresses through an early phase of progenitor expansion, a middle neurogenic phase of radial expansion and a final phase of gliogenesis (Lakoma *et al.*, 2011). Once a postmitotic neuroblast has been born within the VZ/SVZ zone, it starts the cortical migration to reach its final position in the developing cortex. The earliest born neurons arrange in the transient preplate (PP), the most primary structure in the developing cortex, and are followed by other neurons that form the cortical plate (CP). In mice, the PP is formed by embryonic day 11.5 (E11.5). A day later, the PP is splitted into a superficial layer, the marginal zone (MZ) and an inner layer, the subplate (SP) **(Figure I.1.2.)**. The MZ contains Cajal-Retzius cells (CRC) that synthesize and secrete the extracellular matrix protein

Reelin, which has relevant functions in the control of neuronal migration (Chai & Frotscher, 2016) (Olson, 2014) (Zhou *et al.*, 2007). Cortical CRC are originated at the border of the developing palium and migrate towards the MZ by using tangential migration (Borrell & Marin, 2006) (Anstotz *et al.*, 2018) (Olson, 2014).

In parallel, an additional area between the SP and the VZ/SVZ is originated, the intermediate zone (IZ), that contains the axons of the primitive neurons. Neurons that form the primitive PP use somal traslocation as migration mode, whereas CP migrating neurons employ locomotion mode. Neurons that migrate using somal translocation extend a long, branched leading process to the pial surface that gets progressively shorter as the cell soma moves upward. In the locomotion mode, newly born projection neurons move from their birthplace through the SVZ/IZ towards the CP, adopting a multipolar morphology with short, unbranched and multiple leading and trailing processes that extend and retract rapidly (Tabata & Nakajima, 2003). This multipolar phase is transient and is followed by a switch to bipolar morphology, with a long leading process oriented toward the MZ and a shorter trailing process to VZ/SVZ. Locomotion through CP is RG-dependent. RG are polarized cells with a short basal process oriented to the VZ and a long apical process anchored at the pial surface that not only serve as precursors but also provide the scaffold for migrating neurons. Once the leading processes of migrating neurons reach the MZ, they disengage from their glial support and undergo terminal translocation in order to attain their final positions (Cooper, 2008).

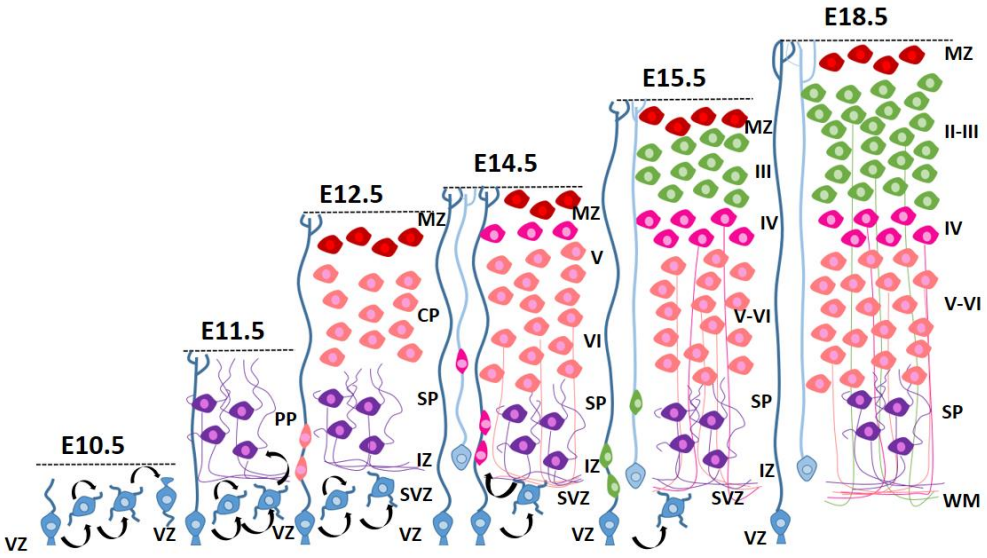

Figure I.1.2. |Phases underlying inside-out cortical lamination of the mouse neocortex. After the asymmetric division of radial glia, progenitors (blue cell) are generated. The first cohort of cells (purple) exit the ventricular zone (VZ) and form the transient preplate (PP). After PP splitting at embryonic day 12.5 (E12.5), the second cohort of neurons (pink cells) occupy the cortical plate (CP), giving rise to the Cajal-Retzius (red cells) containing-marginal zone (MZ) and to the deeppest layer, the subplate (SP). Just beneath the SP the intermediate zone (IZ) is established. As the inside-out migration continues, the six layered neocortex becomes evident, with earlier born neurons (pink cells) placed in the lower part of the cortex (layers VI, V and IV) and later born neurons (green cells) occupying upper positions (layers II-III). WM, white matter. Adapted from: (Santana & Marzolo, 2017).

1.3.1.2. Tangential migration

The inhibitory interneurons arise from the medial and caudal ganglionic eminences and the preoptic area of the ventral telencephalon (Gelman & Marin, 2010)(Zhou *et al.*, 2007). In mice, these interneurons are generated during a period that extends from E12.5 until birth. Then, they migrate tangentially to the radial glia scaffold from the ganglionic eminences towards the developing cortex using different migratory routes: the MZ, the SP or the IZ/SVZ (Nadarajah & Parnavelas, 2002)(Sekine *et al.*, 2014)(Bartolini *et al.*, 2017). The final position of the distinct interneurons subtypes is defined by their place of origin more than their time of birth. Thus, a series of spatially and temporally regulated transcription factors control the generation of interneurons diversity. Once in the cortex, migrating interneurons spread throughout the cortex using radial migration and following an inside-to-outside sequence that correlates with the final position occupied by projection neurons born at the same time. In addition, interactions with projection neurons enable the final laminar distribution of interneurons in the CP. Either by using radial or tangential migration, migrating cortical neurons share common principles and molecular mechanisms that can be arranged into three synchronized steps: extension of the leading process, nucleokinesis and retraction of the trailing process (Rahimi-Balaei *et al.*, 2018)(Cooper, 2008).

- Formation and extension of the leading process: oriented neuronal migration requires the regulation of both the actin and the microtubule cytoskeleton in the leading process of migrating neurons. A large number of chemoattractants and chemorepellents molecules and their receptors control the cytoskeleton dynamics.
- Nucleokinesis: refers to the mechanism of nuclear translocation towards the leading process. This displacement relies on actin and microtubules cytoskeletal rearrangements and is mediated by dynein and kynesin regulatory factors, such as Lissencephaly 1 (Lis1). In addition, during nucleokinesis, nuclear translocation is powered by the centrosome displacement and the molecule doublecortin (DCX) has been propose to mediate coupling of the nucleus to the centrosome.
- Retraction of the trailing process: the trailing process morphology varies between interneurons and projection neurons. Whereas radially migrating neurons extend an extensive proto-axon, interneurons spread out only a minor trailing process.

1.3.2. Formation of the hippocampus.

In the adult brain, the hippocampus is a crucial structure for cognitive abilities such as learning and memory (Deng *et al.*, 2010). The hippocampus is a laminar structure comprising mainly the Ammon's horn (the hippocampus proper) and the DG. Each of these highly ordered fields consists of only one layer of principal neurons, the pyramidal cells and the granule cells, respectively. The hippocampus is functionally connected to related brain regions including the subiculum, presubiculum, parasubiculum and the entorhinal cortex that together form the hippocampal formation (Khalaf-Nazzal & Francis, 2013)(Forster *et al.*, 2006). The formation of the hippocampus, begins in response to the expression of the active molecules bone morphogenic protein (BMP) and Wnt and the lack of expression of the transcription factor Lhx2 emanating from the cortical hem (Urban & Guillemot, 2014)(Gil & Del Rio, 2019).

1.3.2.1. Development of the Ammon's horn

The Ammon's horn which is compartmentalized into the cornus Ammonis (CA)-1 (CA1), CA2 and CA3, is vertically subdivided into stratum orients (so), stratum pyramidale (sp), stratum radiatum (sr) and stratum lacunosum-moleculare (slm)(Toni & Schinder, 2015). In mice, pyramidal neurons that will form the Ammon's horn are generated in the Ammonic neuroepithelium from E12 to E18 **(Figure I.1.3.)**. These newly born neurons leave the VZ/SVZ and become multipolar post-mitotic cells within the IZ and migrate radially towards the hippocampal plate (HP) adopting a bipolar morphology. In the MZ of the developing Ammon's horn, CRC aid in the correct migration of pyramidal neurons and in the layering of the hippocampus. In contrast to the neocortical migration, migrating neurons in the HP change their migration scaffold (RG fibers) giving rise to a zigzag displacement (Hayashi *et al.*, 2015). In addition, there are some differences in the migration mode between CA1 and CA3 pyramidal neurons. The CA3 region present a U-shaped curve with one end elongated toward the DG. Considering that neurons at this end must migrate long distances from the VZ, formation of CA3 occurs one day later that formation of CA1 (Zhao *et al.*, 2018).

1.3.2.2. Development of the dentate gyrus

The DG formation, which presents a birthdate-dependent outside-to-inside pattern, represents an exception compared to the general development of the cerebral cortex (Super *et al.*, 1998). Moreover, the DG is one of the two brain regions where adult neurogenesis takes place. In mice, dentate granule precursors are generated at E13.5 and E14 in the primary dentate neuroepithelium (DNE), located in the dentate notch **(Figure I.1.3.)** (Seki *et al.*, 2014). By E15.5 new born granule cells (GC) from the dentate notch migrate out and form the secondary dentate matrix (SDM) where they keep proliferating (Berg *et al.*, 2018). Then, the earlier-born neurons migrate from the SDM towards the hippocampal fissure where CRC are located, forming a first migratory route toward the outermost part of the future dentate granule cells layer. First the dentate granule cells migrate along RG fibers and become arranged in the supra-pyramidal blade (SPB) of the DG. Later on, they shift the migrating stream to form the infra-pyramidal blade (IPB) by postnatal day 14 (P14). In the late embryonic and early postnatal stages there is a second wave of migrating dentate granular cells from the SDM towards the hilus, where they maintain their proliferating activity in the tertiary dentate matrix (TDM). During this time, the TDM generates its own RG scaffold which is radially oriented from the hilus. Dentate GC generated in the TDM become the inner part of the dentate granule cell layer. GCs display apical dendrites projecting through the ML, and axons oriented to the hilus (Toni & Schinder, 2015). In the adulthood, the proliferative activity in TDM is restricted to the subgranular zone (SGZ) by the border of the granular layer, and is one of the locations of adult neurogenesis (Li & Pleasure, 2005)(Urban & Guillemot, 2014)(Hayashi *et al.*, 2015) (Fan *et al.*, 2018).

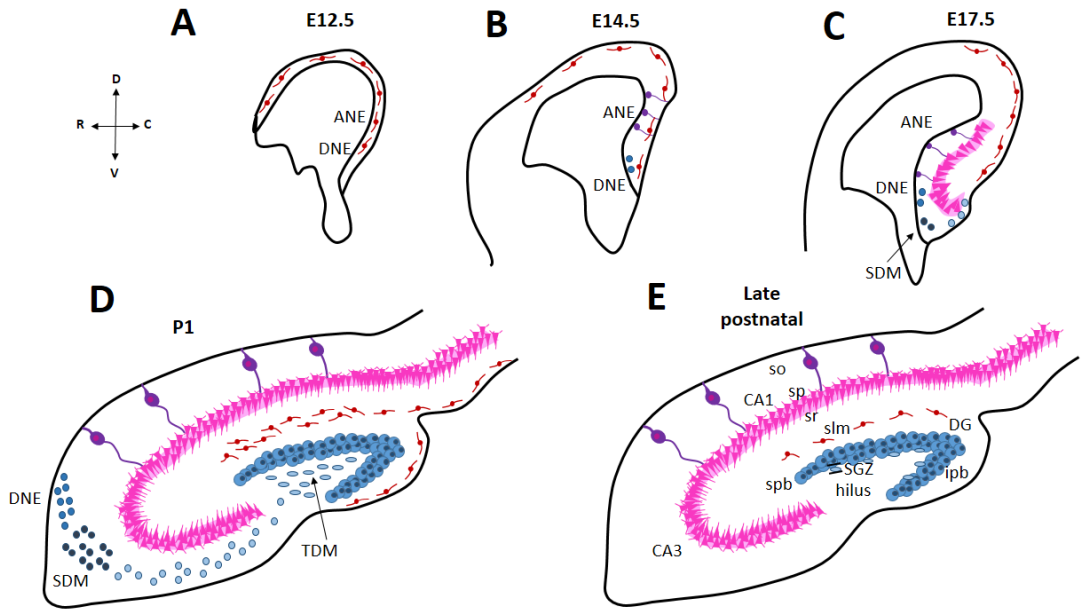

Figure I.1.3. | Development of the mouse hippocampus. (A-E) Schematic representation of coronal sections of the hippocampus development at embryonic day 12.5 (E12.5) (A), E14.5 (B), E17.5 (C) postnatal day 1 (P1) (D) and adult (E). **(A)** Cajal-Retzius cells (red) originated in the dentate neuoepithelium (DNE) are placed surrounding the pial surface. **(B)** Dentate granule precursors (blue circles) are generated in the DNE. **(C)** Granule precursors cells (dark blue) start to migrate generating the secondary dentate matrix (SDM) while the hippocampal fissure is formed. In the Ammon's neuroepithelium (ANE) radial glia precursors (purple) start to generate postmitotic pyramidal neurons (pink). **(D)** The dentate precursor cells form the tertiary dentate matrix (TDM) (light blue) and the dentate gyrus (DG) start to arrange. **(E)** Both blades of the DG are generated and granule precursors reach the subgranular zone (SGZ). Cajal-Retzius cells on the hippocampal fissure partially disappear. R, rostral; D, dorsal; V, ventral; C, caudal; spb, supra pyramidal blade; ipb, infra pyramidal blade; so, stratum oriens; sp, stratum pyramidale; sr, stratum radiatum; slm, stratum lacunosum moleculare. Adapted from: (Seki *et al.*, 2014)

1.3.2.3. Hippocampal connectivity

The hippocampus is functionally connected in a "tri-synaptic" circuit. The sequence is originated in the entorhinal cortex (EC) where the axons from neurons located in this area transmit sensory information to the distal dendritic segments of the granule cells of the DG, following the medial and lateral perforant pathway **(Figure I.1.4.)** (Khalaf-Nazzal & Francis, 2013). The perforant network maturates following a stereotyped sequence in which the correct laminar specificity of hippocampal afferent fibre projections is controlled by specific molecular interactions between the ingrowing fibres and their targets. Transient CRC in the MZ serve as temporary targets for ingrowing entorhinal projections, previous to the connection with their final targets, the granule cell dendrites (Super *et al.*, 1998) (Del Rio *et al.*, 1997)(Forster *et al.*, 2006). Granule cells of the DG have mossy fibres that end on the proximal dendrites of CA3 pyramidal cells. These mossy fibres also interact with mossy cells and other interneurons in the hilus. Axon of CA3 neurons converge onto CA1 pyramidal cells via Schaffer collateral projections, and finally information flows to the subicullum and back to the EC.

Inputs from the EC carry sensory information to the DG that in turn, leads to the production of episodic memories (Toni & Schinder, 2015). In addition, GC dendrites are innervated by associational and commissural fibers coming up from the glutamatergic mossy cells of the ipsilateral and contralateral hilus (Song *et al.*, 2016)(Gil & Del Rio, 2019)(Del Turco *et al.*, 2004).

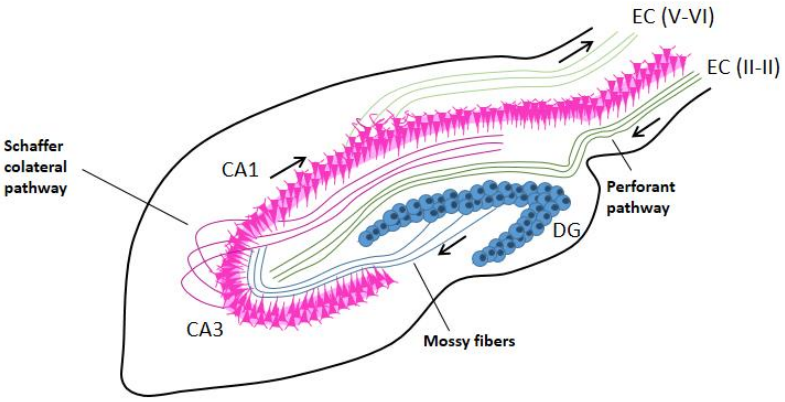

Figure I.1.4. | Neural circuitry in the mouse hippocampus. Schema of the hippocampal trisynaptic circuit. Entorhinal cortex (EC) fibers (in green) follow the perforant pathway up to the dendritic segments of granule cells (blue cells) in the dentate gyrus (DG). Mossy fibers of granule cells (in blue) connect with CA3 pyramidal neurons (pink cells) which in turn project their axons (in pink) to CA1 pyramidal cells via Schaffer collateral projections. Finally, CA1 pyramidal fibers come back to the EC. Adapted from: (Deng *et al.*, 2010).

1.3.2.4. Hippocampal interneurons

Besides principal excitatory granule neurons that form the trisynaptic circuit, other major components in the hippocampus are the diverse interneurons (Song *et al.*, 2016). Hippocampal interneurons are remarkably diverse in their location, morphology, targets and expression of proteins. Like their neocortical counterparts, these interneurons are originated in the medial and caudal ganglionic eminences in two different waves of neurogenesis between E11-E17. These hippocampal interneurons migrate using tangential migration through both MZ and IZ/SVZ migratory paths towards their final destination. The first interneurons reach the CA1 field, then the CA3 at E16 and at E17 the DG. The final positioning of hippocampal interneurons still continues in early postnatal stages (Khalaf-Nazzal & Francis, 2013). Between hilar GABAergic interneurons, basket cells that are located in the SGZ contact with GC somas and express parvalbumin. Other GABAergic interneurons residing in the hilus participate in the regulation of the hilar-perforant, hilar-commisural or molecular-perforant paths (Song *et al.*, 2016) (Flames & Marin, 2005) (Toni & Schinder, 2015).

1.3.3. Formation of the cerebellum

The cerebellum is a laminated structure responsible for the control of motor coordination and also some non-motor functions such as emotion, cognition and language (Rahimi-Balaei *et al.*, 2018). Anatomically, the adult cerebellum is composed of three main layers: the outermost one is the molecular layer, the deepest one is the granular layer and the region between the molecular and the granular layer is the Purkinje cell (PC) layer. The cerebellum contains relatively few cell types that can be classified into inhibitory GABAergic and excitatory glutamatergic neurons. The two main principal neurons in the cerebellum are the inhibitory PC, located into the Purkinje layer, and the glutamatergic granule cells that are placed in the granular cell layers (Marzban *et al.*, 2015). In the developing cerebellum, two cell proliferation compartments are formed: the ventricular neuroepithelium and the external granular layer (EGL) **(Figure I.1.5.)** (Sathyanesan *et al.*, 2019).

1.3.2.5. Ventricular zone

In mice, the first cerebellar neurons, PC and deep nuclear neurons, are originated in the VZ from E11 to E13. Then, they migrate to the cerebellar plate or PC plate, following a radial migration along the processes of RG. The PCs have a pivotal role in the organization of the cerebellar circuit. In one hand, PCs have a mitogenic role, regulating proliferation of granule cells precursors through secretion of Shh. In the other hand, they also receive the imput of the main afferents conveying information to the cerebellum, the Mossy and the climbing fibers. Climbing fibers are originated in the inferior olivary nucleus and contact with the dendritic compartment of the PC while Mossy fibers project indirectly to the PC through parallel fibers. Inhibitory projections from PC are directed to deep nuclei and represent the only output from the cerebellum (Sotelo, 2004) (Marzban *et al.*, 2015).

1.3.2.6. External granular layer

In the mouse embryo, the external granule layer cell precursors are originated in the rhombic lip by E10. At E13, these EGL precursors initially migrate tangentially toward the pial surface where they remain proliferating to produce granule cells until E16, forming the external granule layer. Later in development, postmitotic granule cells extend their axons among the molecular layer while the soma migrate following an inward radial migration toward their final position in the inner granular layer (IGL). By P15, the EGL disappears and the granule cells only occupy the IGL (Sotelo, 2004) (Rahimi-Balaei *et al.*, 2018).

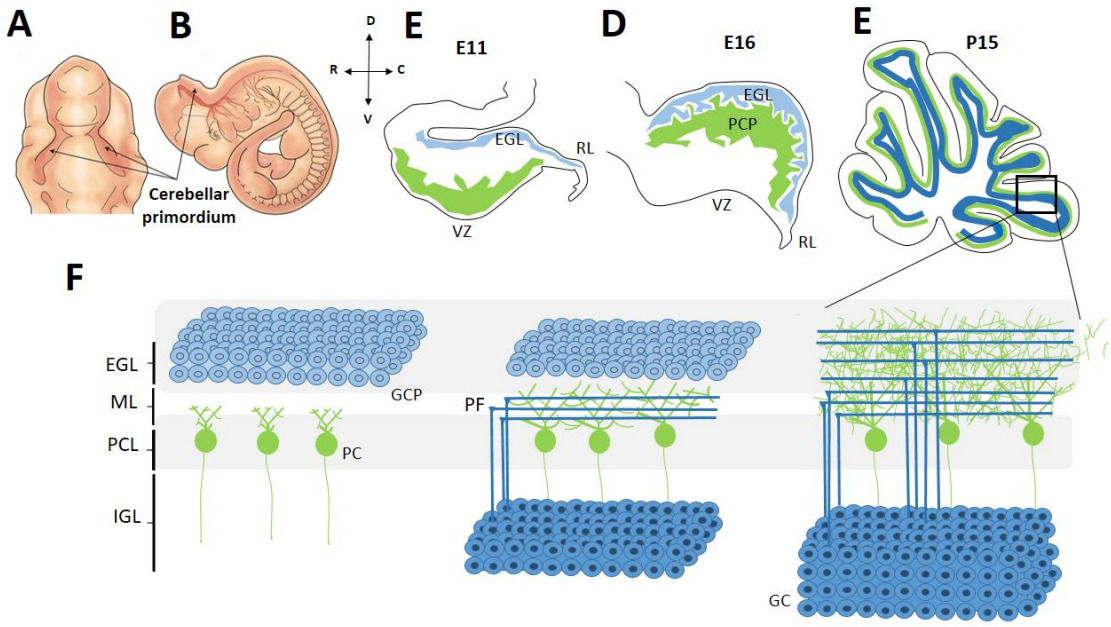

Figure I.1.5. | Development of mouse cerebellum. (A-B) Coronal (A) and sagittal (B) aspect of the mouse embryo at embryonic day 10 (E10) showing the location of the cerebellar primordium (indicated by arrows). **(C-E)** Schematic representation of sagittal sections of the early cerebellar development at E10-13 (C), E16-17 (D) and postnatal day 15 (P15) to adult (E). **(F)** Representacion of cellular events within the cerebellar cortex. Purkinje cells (PC) extend their dendritic fibers to the cerebellar pial surface contacting with the parallel fibres (PF), while granule cell precursor (GCP) from the external granule layer (EGL) become mature granule cells (GC) and inward migration towards the inner part of the granule layer (IGL). R, rostral; D, dorsal; V, ventral; C, caudal; VZ, ventricular zone; RL, Rhombic lip; PCP, Purkinje cell plate; ML, molecular layer; PCL, Purkinje cell layer. Adapted from: (Sathyanesan *et al.*, 2019).

1.4. Cell differentiation

Once a new generated neuron leaves the proliferative area and reaches its final destination, it undergoes an extensive maturation process. During differentiation, each neuron becomes polarized: an axon is projected to the appropriate target cell and dendrites are extended in order to establish the pattern of synaptic connections (Lewis *et al.*, 2013).

1.4.1. Neuronal polarization

The establishment and maintenance of neuronal polarization is crucial for the correct development and function of the CNS. Neurons are compartmentalized into two morphological and functional processes, axons and dendrites, that control the directional information flow though the CNS (Lewis *et al.*, 2013)(Laumonnerie & Solecki, 2018). In general, neurons determine their polarity in a stochastic manner, meaning that multiple neurites are initially extended but just the leading and the trailing processes are finally established (Lanoue & Cooper, 2019). Neurites growth is regulated in the growth cones by two cytoskeletal components, the actin and the microtubules filaments. Accordingly with the distribution of these cytoskeletal components the growth cone can be divided into three regions: a central

domain containing microtubules, a peripheral region rich in actin filaments that contains filopodia and lamellopodia-like structures, and the contractile transition zone (Namba *et al.*, 2015). It has been proposed that the axon specification may occurs based on neurite length due to the accumulation of a growth-promoting protein, as the primary event during neuronal polarization. Usually, the growth promoting neurite accumulates most of the polarity molecules, whereas the others are maintained in a growth inhibitory state due to the efficiency of a feedback-loop network (Schelski & Bradke, 2017). During axon specification, an increased number of microtubules with enriched plus-end-out orientation is present in the nascent axon compared to other neurites **(Figure I.1.7.)**. The plus end is a crucial site for tubulin polymerization while the minus end is the anchoring place of the microtubule-organizing center (MTOC) and is associated with tubulin depolymerization. The orientation of the microtubules determines the contribution of microtubule-dependent motor proteins such as kinesins and dyneins. These motor proteins are responsible for the anterograde and retrograde transport of cytosolic proteins, membrane structures and organelles that determine neuronal polarity. Another important issue for axonal specification is the formation of the axon initial segment (AIS). The AIS is an actin rich structure essential for the formation of a cytoplasmatic diffusion barrier between the axonal and somatodendritic compartments. Thus, the AIS acts as a cytoplasmatic filter controlling the polarized transport in axon and dendrites (Namba *et al.*, 2015)(Lewis *et al.*, 2013). Several molecular mechanisms have been described to regulate neuronal polarization including both intracellular signalling molecules and extracellular cues. The majority of these cues modulate cytoskeletal organization, thus determining cell morphology and motility (Schelski & Bradke, 2017).

1.4.1.1. Intracellular signalling pathways

Several signalling pathways controlling cytoskeletal dynamics have been identified to control the feedback-loop network and to promote neurite growth in the axonal growth cone **(Figure I.1.6.)** (Takano *et al.*, 2015)(Namba *et al.*, 2015):

PI3K pathway

Activation of phosphoinositide 3-kinase (PI3K) induces the production of phosphatidylinositol triphosphate (PIP_3). PIP_3 is located in the tips of the growth cones where it controls the cytoskeletal dynamics. Moreover, PIP_3 indirectly activates thr Akt/GSK3β pathway.

Rho pathway

Ras-Releated C3 Botulinum Toxin Substrate 1 (Rac1), Cdc42, and RhoA are members of the Rho family of small GTPases. The active form of these Rho GTPases triggers the activation of a variety of specific downstream effectors that govern the directionality of cytoskeletal dynamics (Lanoue & Cooper, 2019). Cdc42, which is activated by PIP_3 via PI3K, induces Rac1 activation. Activated Rac1 can bind to PI3K, acting as a positive feedback loop for axon specification. In addition, Cdc42 induces cofilin activation, promoting actin turnover in the axonal growth cone. Furthermore, Rac1 also plays a pivotal role in axon specification through regulation of actin polymerization. Conversely, RhoA acts as a growth-inhibiting factor and is degraded in the axonal growth cone during axon specification and elongation (Schelski & Bradke, 2017).

Ras/Akt/GSK3β pathway

The glycogen synthase kinase-3β (GSK3β) is constitutively active and its inactivation depends on Akt activation. GSK3β inactivation leads to the activation of microtubule assembly-promoting proteins (MAPs) such as Tau, MAP1B and CRMP-2.

CAMKK pathway

Calcium (Ca^{2+}) is a signal involved in mediating responses to axon guidance molecules. Ca^{2+} release induces the activation of the Ca^{2+}/calmodulin-dependent protein kinase I (CAMKI) and Ca^{2+}/calmodulin-dependent protein kinase kinase (CAMKK). CAMKI can activate microtubule affinity-regulating kinase 2 (MARK2) that phosphorylates several MAPs such as Tau, MAP2 or DCX. Thus, the appropriate regulation of MARK2 is essential for neuronal migration and neuronal polarization since it controls both axon specification and axon elongation.

cAMP pathway

The increasing levels of cyclic adenosine monophosphate (cAMP) induce axon specification via protein kinase A (PKA)-dependent phosphorylation of liver kinase B1 (LKB1). Phosphorylation of LKB1 is also involved in neurites outgrowth and neuronal migration.

1.4.1.2. Extracellular signals

These intracellular signalling pathways are controlled and regulated by some local extracellular cues that instruct neurites to become axons by promoting axon extension or repressing axon growth in favour of dendritic development.

- **Neurotrophins (NT):** consist of a family of structurally related proteins, including the nerve growth factor (NGF), the brain-derived neurotrophic factor (BDNF), neurotrophin-3 (NT-3) and neurotrophin-4 (NT-4) (Ledda & Paratcha, 2017). NTs bind to the tropomyosin receptor kinases (TrKs) activating their downstream signalling molecules. Among all the neurotrophines, BDNF and NT-3 induce axon specification in either paracrine or autocrine ways. First, BDNF-induced signalling leads the increasing production of cAMP, activating PKA and LKB1. Second, Trk signals to PI3K which increases the accumulation of Trk in the membrane of the axon cone. In addition, accumulation of cAMP induces BDNF release, thereby activating TrK, and leading to PI3K activation and TrK accumulation in a positive feebdack loop. Furthermore, NTs recruit Ras in the tip of the future axon that also signals PI3K. Thus, the BDNF/TrK signalling also promotes dendrite morphogenesis via PI3K/AKT/GSK3β (De Vincenti *et al.*, 2019)(Schelski & Bradke, 2017)(Namba *et al.*, 2015).
- **TGFβ:** Upon the binding of TGFβ with its receptors, two different pathways can be activated. On the one hand, TGFβ receptors regulate the degradation of RhoA which in turn controls actin filaments dynamics via cofilin. On the other hand, the transcription of CRMP-2 is also controlled by TGFβ.
- **Extracellular matrix (ECM) proteins:** Several ECM proteins such as Laminin and Reelin are implicated in the control of neuronal polarization. Two possible

mechanisms could be underlying the process. On the one hand, mechanical tension can induce neurite elongation. On the other hand, cell-to-cell interactions can activate intracellular signalling cascades (Namba *et al.*, 2015).

- **HRas**: accumulated in the tip of the longest neurite, promote neurite growth through a positive feedback loop involving PI3K (Schelski & Bradke, 2017).

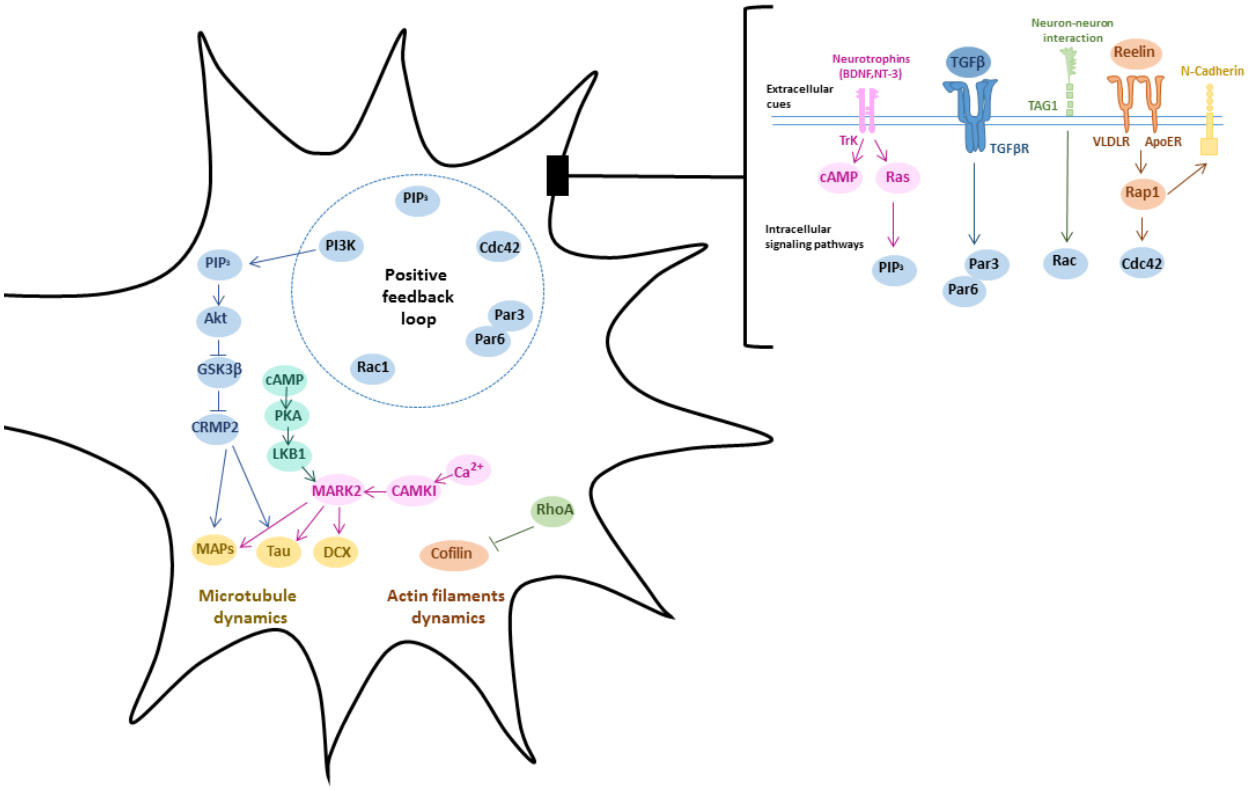

Figure I.1.6. | Signalling pathways involved in neuronal polarization. Adapted from (Namba *et al.*, 2015)(Schelski & Bradke, 2017).

1.4.2. Neuronal maturation

The principal element of neuronal polarity which is the cytoskeletal configuration differs between the axon and the dendritic compartments. While axons extend a long process to their appropriate targets, dendrites arborize to form specific synapses (Ledda & Paratcha, 2017) (Lanoue & Cooper, 2019).

1.4.2.1. Axogenesis

The axon is a unique long process responsible for the signal transduction to other neurons by releasing neurotransmitters. The axon development, which starts during neuronal migration with the extension of the trailing process, can be divided into three fundamental steps: axon specification during neuronal polarization, axon guidance and growth, and finally axon branching and presynaptic development (Lewis *et al.*, 2013).

Axon elongation requires the local disruption of actin organization in the growth cone and the microtubule polymerization. The dymanic organization of the actin cytoskeleton is controlled by different actin-associated complex such as Arp2/3, Ena/VASP or ADF/cofilin. This actin instability allows axon to elongate by creating space for microtubules to penetrate from the central domain into the peripheral regions of the growth cone. The contribution of microtubule dynamics to axon growth is not limited to microtubule invasion but also involves microtubule polymerization and stabilization. Among all the MAPs, Tau and MAP1B regulate microtubule stability during axon specification and branching. Furthermore, axon elongation requires the transport and addition of new membrane lipids, proteins, cytoskeleton elements and organelles along the axon that is controlled through phosphorylation of Tau (Lewis *et al.*, 2013).

The last step of axon growth is the axon branching which allows a single axon to innervate multiple postsynaptic targets (He *et al.*, 2018). Axonal branching is known to occur when most presynaptic contacts with postsynaptic partners are established (Lewis *et al.*, 2013). As well as for the elongation of the axon, axonal branching requires actin and microtubule reorganization events. In addition, cell-autonomous spontaneous activity in the form of calcium waves and spontaneous vesicular release is also required for terminal axon branching. Finally refinement pruning occur during synapse formation (Ledda & Paratcha, 2017).

1.4.2.2. Dendritogenesis

The dendritic compartment is composed of multiple branched processes and their dendritic spines that receive signals from other neurons through multiple neurotransmitter receptors. The dendrite growth, anatomy, connectivity and electrical properties determine the ultimate function of each neuron. While axon specification occurs at the same time that a newborn neuron migrates, dendrite morphogenesis is incompatible with neuronal migration (Ledda & Paratcha, 2017) (Prigge & Kay, 2018). Several factors arrest the dendritic morphogenesis during migration including cytoskeletal regulators, Sema3E, N-cadherin or transcription factors such as Sox11 (He *et al.*, 2018)(Prigge & Kay, 2018). In addition, loss of polarization switches migration of neurons towards dendrite genesis. During the process of dendrite morphogenesis some fundamental steps can be distinguish:

- Dendrite extension: Once the neuron arrives to its final destination, local cues derived from extracellular matrix or neighbouring dendrites from the same cell or partner neurons and glia, determine branch formation and stabilization. Local guidance cues such as Wnt and Netrin control branch extension by actin filament extension. The regulation of actin polymerization is controlled by the Rho GTPases family of proteins. Furthermore, microtubule nucleation and extension are essential for dendrite growth and branching. In contrast to axon, microtubules in the dendrites that are labelled with MAP2, are less stable, thinner and present a complex array of orientations (Lewis *et al.*, 2013) (Lanoue & Cooper, 2019).
- Dendrite branching: extension and retraction processes of the nascent dendritic branches allow the neurons to explore. Establishment of new dendritic branches

comes from the extension of actin-rich dynamic filopodial protusions. In addition, dendritic filopodia also contain a branched actin network controlled by actin-associated complexes such as Arp2/3 and Ena/VASP (Lanoue & Cooper, 2019)(Prigge & Kay, 2018).

- Dendritic self-avoidance/ dendritic tilling: expression of repulsive receptor DSCAM and protocadherins prevent self-contacts between sister dendrites or the axon in the same neuron (dendritic self-avoidance). In addition, dendrites from different neurons with redundant function are also avoided (dendritic tilling). Between others, Contactin5/Caspr4 and cadherins mediate and stabilize dendritic contacts with their correct presynaptic arbors whereas repulsive semaphorins and plexins prevent straying of direction-selective circuit dendrites (Prigge & Kay, 2018) (Lanoue & Cooper, 2019) (Ledda & Paratcha, 2017).
- Dendrite maturation: dendrites differentiate into specific synaptic structures, the dendritic spines. The dendritic spines represent the subcellular postsynaptic compartments where neuronal inputs are received. They consist in actin-rich dynamic structures that can grow or contract in an experience-dependent way (He *et al.*, 2018).
- Dendrite pruning: this includes the refinement of the dendritic connections to ensure that only those dendrites that are properly innervated will last for long periods (Ledda & Paratcha, 2017). Moreover, dendrites within the same neuron can receive different types of synapses becoming molecularly and functionally different (Prigge & Kay, 2018).

1.4.3. Neuronal synaptogenesis

The proper functioning of the CNS depends on highly accurate and specific connectivity of neuronal circuits. The synapses can be either excitatory or inhibitory, depending if the neurotransmitter released is glutamate or GABA, respectively. Each neuron of the CNS can receive both GABAergic and glutamatergic synaptic inputs. The major components of excitatory postsynaptic compartments consist in AMPA and NMDA receptors (AMPAR and NMDAR), which are able to bind glutamate. Conversely, $GABA_A$ is the main receptor in inhibitory synapses (Carleton *et al.*, 2003) (Waites *et al.*, 2005) (Wasser & Herz, 2017).

During development, growing axons must navigate long distances before contacting target cells. Several types of cues regulate the temporal and spatial specificity of synaptogenesis triggering the formation of the synapse in a specific target region:

- Diffusible factors: a variety of proteins such as members of the Wnt and FGF families and BDNF neurotrophins that are synthesized by target neurons promoting synaptogenic priming. In addition, the surrounding glia also secretes synaptogenic factors including cholesterol bound to apolipoprotein E (ApoE) and thrombospondin-1 (TSP1) (He *et al.*, 2018)(De Vincenti *et al.*, 2019).
- Cell adhesion molecules (CAMs): different classes of CAMs such as cadherins and protocadherins can control target specification. They are found in the pre and

postsynaptic plasma membranes and specifically at the initial axo-dendritic contact sites.

- Inducers of synapse formation: Include Narps and EphrinB that clusters postsynaptic molecules, and Syn-CAM and neuroligin implicated in the formation of functional presynaptic active zones.

Subsequent to target recognition and synapse induction, several pre and postsynaptic components must be assembled into the synapse junctions. During the assembly of presynaptic compartment a number of different vesicles carrying synaptic vesicle proteins such as syntaxin and SNAP25 are clustered. Conversely, in the postsynaptic compartment, the recruitment of scaffolding proteins of the PSD-95 family as well as AMPA and NMDA receptors seems to occur primarily. The next feature of synaptic development is the synaptic maturation. During this stage, synapse expands in size and change in form, from shaft synapses to spine synapses. Spine morphology is controlled by several mechanisms including cadherins, proteins of the Rho and Ras family of GTPases and the ephrin system. Once synaptogenesis occurs, the synaptic activity determines whether these new synapsis are permanent or eliminated. The activity-dependent pruning of synapses is important for normal brain development and for removal of connections to fine tune brain networks (Ferrer-Ferrer & Dityatev, 2018)(Frotscher *et al.*, 2014) (Castillo *et al.*, 2011).

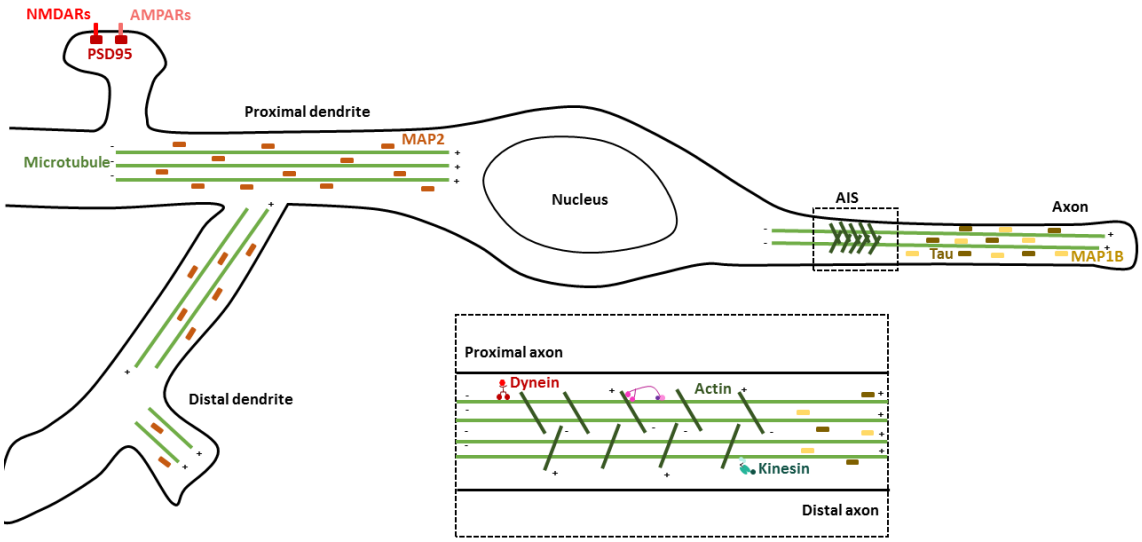

Figure I.1.7. | Neuronal polarization and trafficking of axonal and somatodendritic elements. Neurons are polarized into the axon and the dendritic compartment. Polarity maintenance is controlled in the axon initial segment (AIS) that regulates the trafficking of specific proteins. In the axonal compartment microtubules are oriented uniformly, with the plus end away from the cell body while in the somatodendritic compartment microtubules are oriented in both directions. In the AIS, motor proteins such as dynein, and kinesin restric the specific transport of proteins to either the axon or the dendrites. Adapted from: (Lewis *et al.*, 2013).

1.5. Cell death

In mice, many of the neurons generated embryonically are eliminated through programmed cell death (PCD). The main functions of PCD are to eliminate errors and developmentally transient structures, to limit the number of progenitor pools and to control the matching of neurons during synaptogenesis. In the mammalian brain, two major waves of PCD occur. The first one is confined to proliferative areas, where many of the precursor cells are eliminated. The second one, referred as post-mitotic cell death, is thought to occur mainly during synaptogenesis. In the postnatal cerebellum, PCD is responsible to reduce the pool of progenitor cells as well as to remove erroneously migrated Purkinje cells. In the neocortex, approximately thirty per cent of the interneurons are eliminated. In addition, regarding CRC, approximately the third part of the total number of cells disappear by apoptosis at P8 when the cortical migration is complete. Furthermore, elimination of neurons with ectopic position is also observed in the developing cerebral cortex. In the hippocampus, a transient layer of neurons in the stratum oriens is eliminated by PCD at the time of birth Similar to the neocortex, CRC population in the hippocampus gradually die in the molecular layers of both the hippocampus proper and dentate gyrus from P7 and thereafter (Anstotz *et al.*, 2018) (Mosley *et al.*, 2017) (Soriano & Del Rio, 2005) (Chai & Frotscher, 2016).

Because neurons must be properly integrated and synaptically connected with their targeted neurons, PCD and adult neurogenesis are continuously active, controlling changes in neural networks (Kim & Sun, 2011).

2. Adult brain plasticity

2.1. Adult neurogenesis

Neurogenesis is the process by which new functional neurons are generated from precursor cells and integrated in pre-existent circuits. Neurons continue to be generated in the adult vertebrate brain throughout life. Adult neurogenesis recapitulates the same process of embrionic neurogenesis, from proliferation and face specification to finally fuctional synaptic integration through migration and axonal and dendritic development. In adult mouse brain, the neurogenic niches are restricted to the subependymal zone of the lateral ventricles, also called SVZ and the SGZ of the DG in the hippocampus. In these neurogenic niches a variety cell types and cellular structures such as astrocytes, mature neurons, axon projections and blood vessels maintain the appropriate environment that modulates the behavoiur of adult stem cells. The addition of new generated neurons on the preexisting complex circuitry of the adult brain confers crucial brain functions implicated in memory, learning and olfactory processing (Song *et al.*, 2016)(Urban & Guillemot, 2014)(Obernier & Alvarez-Buylla, 2019) (Kang *et al.*, 2016).

2.1.1. Adult neurogenesis in the SVZ

The SVZ can be seen as a prolongation of the embryonic VZ of the telencephalon. In the adult mouse brain, the SVZ is located along the walls of the lateral ventricles in close proximity with the striatum and recives the influence of striatal GABAergic interneurons projections (Song *et al.*, 2016). Neurogenesis in the olfactory bulbs (OB) improves olfactory memory, olfactory fear conditioning and mating and social recognition. The importance of the sense of smell during mammalian evolution reflexes the needed of adaptative mechanisms in the form of neurogenesis, migration and maturation of new neurons in the OB and their synaptic plasticity. Interestingly, one of the forms of this plasticity may reside in the type of neurotransmitter released by newly formed cells (Obernier & Alvarez-Buylla, 2019)(Ming & Song, 2011) .

In the SVZ of adult mice, different populations of adult NSCs, called type-B1 cells, are able to generate a variety of cells, including periglomerular and granule interneurons in the OB and astrocytes. The different populations of type-B1 cells present a especific pattern of location within the SVZ, recognizable by the differential expression of specific transcription factors along the anteroposteior and dorsoventral axes. However, all the progeny cells migrate rostrally towards their final destination in the OB using the rostal migratory stream (RMS) where they differentiate **(Figure I.2.1.)** (Urban & Guillemot, 2014). Morphologically, type B1 cells ressemble embryonic radial glia, since they present an apical process in contact with the cerebrospinal fluid (CSF) and a ventricle basal process with end-feet on blood vessels. Several regulatory cues provided by the CSF, such as insuline-like growth factor (IGF)-2, BMP, RA or Shh, regulate type B1 cell proliferation, suggesting that the apical contact is essential for the regulation of the adult neurogenesis in the SVZ (Obernier & Alvarez-Buylla, 2019). In addition,

a number of different factors influence germinal activity within the SVZ including mitogens, growth factors, cellular interactions and even neurotransmitters. Many of these cues are secreted by ependymal and microglial cells of the CSF and the blood vessel, respectively, that penetrate into the SVZ (Urban & Guillemot, 2014)(Lim & Alvarez-Buylla, 2016).

During adult neurogenesis, dividing type B1 cells generate, after asymmetrical division, a transitory intermediate progenitor (also called type C cell) and another type B1 cell. Then, the type C cell is simmetrically divided becoming a neuroblast (type A cells). Type B1 cells also generate proliferative astrocytes (called B2 cells)(Obernier & Alvarez-Buylla, 2019). Type C cells divide three or four times before generating type A cells. Type A cells form chains of themselves and migrate long distances through a tube formed by astrocytes up to the OB, where they integrate into the pre-existing prexisting circuitry (Ming & Song, 2011). Certain cell-surface molecules such as polysialyted-neural cell adhesion molecule (PSA-NCAM) and integrins seem to be required for efficient chain migration. In additon, type A cells release GABA, which activates $GABA_A$ receptors in type B1 cells reducing proliferation and favouring migration and maturation (Song *et al.*, 2016)(Berg *et al.*, 2018). Once in the OB, type A cells leave the tangentially oriented RMS and start radial migration within the different layers of the OB to complete their differenciation into neurons. In the OB the majority of the new generated cells differentiate into granule interneurons becoming the largest subtype of neurons in the OB. The OB interneuron population is comprised of several cellular phenotypes accordingly to their morphology, location, synaptic properties and neurochemistry. The granule interneurons are located in the granule cell layer and they are mostly GABAergic interneurons, while periglomerular interneurons are located more peripherally in the glomerular layer and they can be subdivided according to the expression of calbindin, calretinin, glutamic acid descarboxilase (GAD) or tyrosine hydroxylase (TH) (Lim & Alvarez-Buylla, 2016). Once the newly generated neurons arrive to the OB, they have to become functionally integrated into the adult neural networks. During the tangential migration in the RMS, type A cells expressed $GABA_A$ and α-amino-3-hydroxy-5-methyl-4-isoxazolepropionic acid (AMPA) receptors. Once in the OB after ending radial migration, adult-generated granule interneurons begin to develop the dendritic arbor and express functional N-methyl-D-aspartate (NMDA) receptors. These receptors respond to local neuronal activity and accelarate the maturation and differentiation of new generated neurons. First, new neurons receive GABAergic synapses and then glutamatergic ones, concurring with the increase in number and length of newborn GC dendrites. Only after new born neurons become connected, spikes formation occurs. This adult mechanism of sequential maturation protects preestasblished functional networks and contributes to adult plasticity. The global process of neurogenesis takes about two weeks, and within a month after, more than half of the new generated neurons that reach their mature state die. This represents a selective mechanism for rapid modification of the circuitry in response to a changing environment (Carleton *et al.*, 2003)(Andrade *et al.*, 2007).

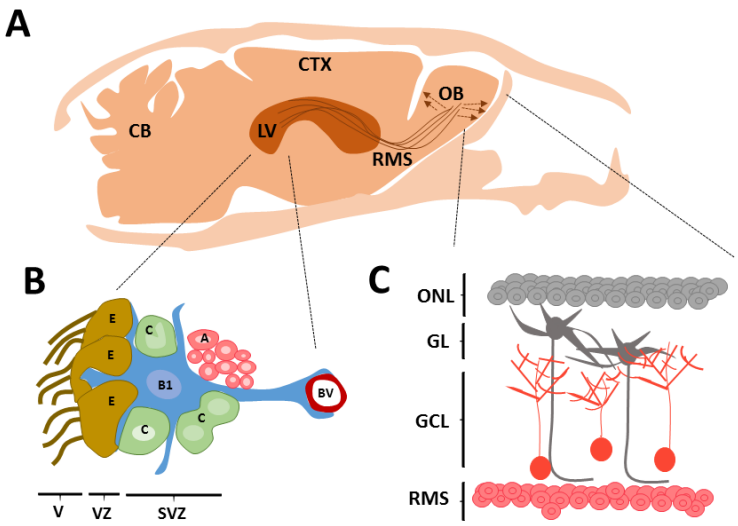

Figure I.2.1. | Overview of the adult ventricular-subventricular zone (V-SVZ) neurogenesis in the olfactory bulb (OB). (A) The diagram represents a sagittal section of adult mouse pointed the V-SVZ where adult neurogenesis takes place. Neuroblasts (type A cells) born in the V-SVZ migrate through the rostral migratory stream (RMS) towards the olfactory bulb (OB) where they differentiate. **(B)** Diverse cellular components of the V-SVZ. Type B1 cell (blue) presents a basal process with end-feet on blood vessels (BV) and an apical process in contact with ependymal cells (E) of the cerebrospinal fluid. Once divided, type B1 cells generate a transitory intermediate progenitor or type C cells (green), which rapidly divide becoming neuroblast or type A cells (red). **(C)** The layered structure of the OB. Tangentially migrated type A cells leave the RMS and start to differentiate into granule interneurons (red) or periglomerular interneurons (grey) which are finally placed in the granule cell layer (GCL) and glomerular layer (GL), respectively. ONL, olfactory nerve layer. Adapted from: (Lim & Alvarez-Buylla, 2016).

2.1.1. Adult neurogenesis in the DG

Adult hippocampal neurogenesis in the DG contributes to increasing the plasticity of the dinamic neural network, by changing the number and the intensity of synaptic contacts in an activity dependent manner. Adult hippocampal neurgenesis gives rise only to one type of neuron, the GCs. In the hippocampus, adult newborn granule neurons are generated locally within the SGZ, beneath the granule cell layer (GCL). These new type of cells that are formed during adult hippocampal neurogenesis migrate into the GCL of the DG and become glutamatergic GC, the principal excitatory cells in the DG (Song *et al.*, 2016)(Kempermann & Gage, 2015). After the cell-cycle exit, the new generated neurons extend mossy fibers through the hilus towards the CA3 layer providing excitatory input to the pyramidal cells. Around two-three weeks post-mitosis, GCs also begin to form synapses with hilar mossy cells. Finally, within four-six weeks after birth, adult generated GCs form synapsis with inhibitory interneurons in the DG itself and in the CA3 region. The first inputs on new granule cells come from local GABAergic inhibitory interneurons, followed by the glutamatergic input from mossy cells in the hylus and finally, from neurons on the entorhinal cortex, three to four weeks after birth **(Figure I.2.2.)** (Cope & Gould, 2019)(Kempermann & Gage, 2015)(Song *et al.*, 2016) (Toni & Schinder, 2015).

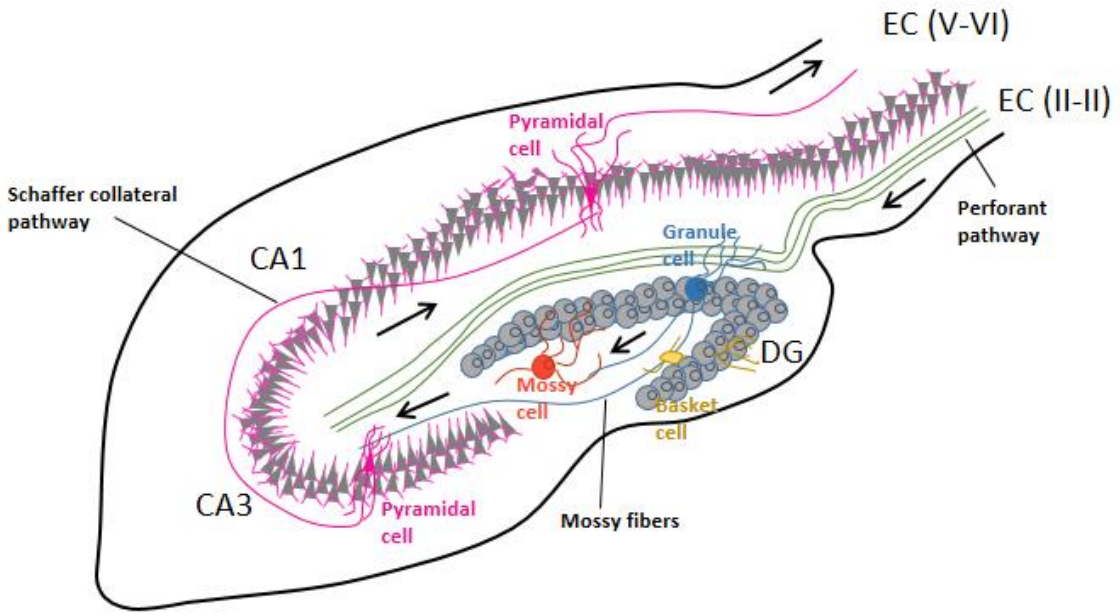

Figure I.2.2. | Overview of the network formation of new-generated granule neurons. First, new generated granule neurons project mossy fibers towards CA3 pyramidal neurons, which in turn porject Schaffer colateral fibers to CA1 pyramidal neurons and then back to the entorhinal cortex (EC). On the input side, new generated neurons recive their first contacts from local interneurons such as basket cells, followed by the glutamatergic input from mossy cells. Finally, new generated granule cells come in contact with the perforant path, composed of axon from the EC neurons. Adapted from: (Toni & Schinder, 2015).

Self-renewing and multipotent NSCs give rise to both neurons and astrocytes, but not oligodedrocytes in the adult hippocampus. These adult NSCs are induced very early at postnatal stages in a restricted region close to the ventral part of the hippocampus, in proximity with the lateral ventricles, having a separate origen from embryonic NSCs (Urban & Guillemot, 2014) (Berg *et al.*, 2018). The development of newborn neurons in the adult hippocampus can be divided into four different phases: a precursor cell phase, an early survival phase, a post-mitotic maturation phase, and finally a late-phase of maturation and maintenance **(Figure I.2.3.)** (Kempermann & Gage, 2015).

2.1.2.1. The precursor cell phase

A number of different morphologically identifiable precursor cells participate in adult hippocampal neurogenesis. During the first step of adult neurogenesis, the so-called precursor cell phase, there is an expansion of the pool of these neural progenitors. These neural stem cells (called type 1 progenitors) possess radial-glia like properties. Morphologically they present a long process the extends throughout out the GCL and short branching into the ML with no synaptic contacts, and antigenically, they are recognizable by the expression of glial fibrillary acidic protein (GFAP), sry-related HMG box transcription factor (Sox2), brain lipid-binding protein (BLBP) and nestin. Type 1 progenitors are capable of both asymmetric and symmetric divisions. The asymmetric division gives rise to intermediate progenitor cells, the

type 2 cells. This type of progenitors, that present short processes, divide more rapidly to amplify the progenitor population. Intermediate progenitors can be subdivided into type 2a and type 2b by the expression of different markers. Type 2a cells still express glial markers but they lack the radial glia appearance of type 1 progenitors. In the intermediate progenitor stage, the cell decides which will be its final fate. When this fate is neuronal, type 2a cells progress over type 2b cells, which expresses markers of neuronal phenotypes such as Prox1 and Tbr2, but still maintains self-renewing properties. Type 2b cells divide to generate a neuroblast (type 3 progenitors) which maintain the proliferative capacity at the time that start to maturate and migrate into the GCL. Type 3 progenitors show slow proliferative activity and express neuronal markers such as DCX and PSA-NCAM from proliferative stages to a period of postmitotic maturation (Kempermann & Gage, 2015)(Toni & Schinder, 2015)(Berg *et al.*, 2018) (Rodriguez-Iglesias *et al.*, 2019).

2.1.2.2. The early survival phase

After the proliferative stages, the early survival phase marks the cell-cycle exit, when the type 3 cells differentiate into immature GCs at the same time that they start to express postmitotic markers such as NeuN and Calretinin. The number of NeuN positive cells decreases within a few days by an apoptotic process, before new postmitotic neurons establish synaptic contacts with CA3 neurons or receive dendritic inputs from the entorhinal cortex (Urban & Guillemot, 2014). Once the new generated neurons go through this phase (arround the second week after birth), they will be persistenly integrated into the DG network for a long period of time (Kempermann & Gage, 2015). This is the major migration time, in which GCs occupy their final position within the inner half of the GCL. At the beginning of this stage, new granule cells are depolarized in response to GABA because of their high expression of the sodium-potassium-chloride co-transporter that maintains high levels of intracellular chloride, and in the fourth week after neuronal birth, this depolarization is switched to a hyperpolarization, an event that coincides with the expansion of the dendritic arborisation and the synaptic integration of new GCs (Toni & Schinder, 2015)(Song *et al.*, 2016) (Zhao *et al.*, 2008) (Christian *et al.*, 2014).

2.1.2.3. The postmitotic maturation phase

This stage is related with the onset of glutamatergic synaptogenesis. The exact time of maturation is dependent on the activity of local circuits. Glutamartergic synaptogenesis depends on NMDA-receptor mediated cell-autonomous activity. At the time of synaptic integration, perforant path terminals start to form contacts with dendrites of new GCs and spines start to develop. This time coincides with the transition of excitatory GABAergic inputs to being inhibitory (Deng *et al.*, 2010) (Christian *et al.*, 2014). During functional dendrites maturation, new GCs express calretinin. Once they become fully integrated in the existing network, the new cells start to express calbindin (Kempermann & Gage, 2015).

2.1.2.4. The late maturation phase

This period begins once glutamatergic synaptic connections have been established, and comprises a phase of increasing synaptic plasticity, a mechanism that has long been implicated in learning and memory. Within four-six weeks after birth, new born granule neurons present a lower induction threshold and increased amplitude of LTP, being highly excitable. Finally, new granule cells integrate in the GCL to the existing GABAergic and glutamatergic circuitry, becoming indistinguishable from the other granule neurons from the eighth week of age (Song *et al.*, 2016)(Deng *et al.*, 2010)(Ming & Song, 2011)(Christian *et al.*, 2014).

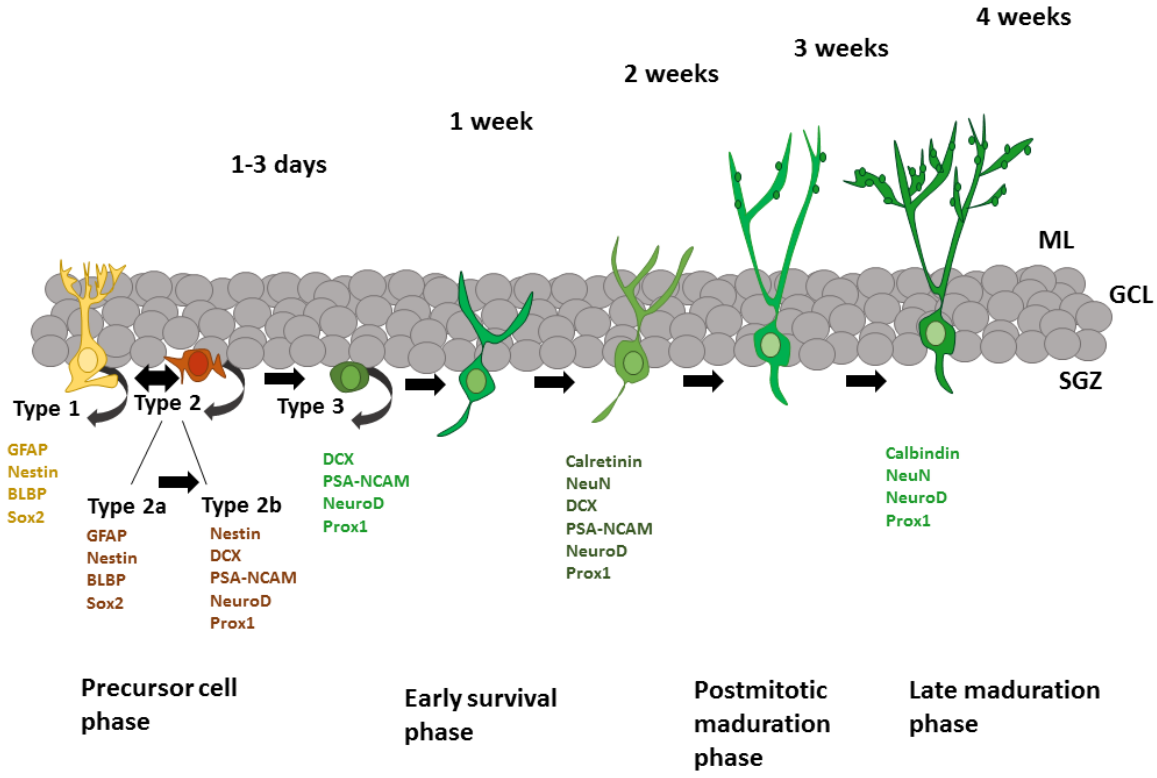

Figure I.2.3. | Overview of adult hipponcampal neurogenesis in the subgranular zone (SGZ) of the dentate gyrus. Schematic representation of the different developmental phases of the adult hippocampal neurogenesis and integration of newborn neurons in the adult dentate gyrus. The different markers of each neuronal phenotype are showed. ML: molecular layer; GCL: granule cell layer; SGZ: subgranular zone. Adapted from: (Kempermann & Gage, 2015)(Toni & Schinder, 2015).

2.1.2.5. Regulation of adult neurogenesis in the DG

The whole process of formation and maturation of the new-born neurons goes on for seven-eight weeks in the adult mouse brain, mean while it can be affected by a number of environmental and pathological conditions (Song *et al.*, 2016). In contrast to embryonic neurogenesis, hippocampal adult neurogenesis is highly regulated in each step of the neurogenic process by the neuronal activity and the local envioronment of the neurogenic niche. The major cellular components of the SGZ neurogenic niche include the endothelial

cells, astrocytes, ependymal cells, microglia, mature neurons, the adult neural precursor cells and their progeny (Ming & Song, 2011). These cellular components are embedded in an extracellular matrix and present cell-to-cell contacts. Among all the cellular components, the vascular cells play a prominent role facilitating proliferation (Kempermann & Gage, 2015). In addition, similar to the SVZ, a number of both intrinsic and extrinsinc mechanisms signal the neurogenic niche to regulate adult neurogenesis in the hippocampus, including Shh, Wnt, BMPs, growth factors, adhesion molecules, neurotrophins and neurotransmitters (Ming & Song, 2011). Local interneurons release GABA which regulates cell proliferation and maturation, dendritic development and synaptic integration of newly generated granule neurons. In addition, glutamate regulates survival of newly generated neurons through a NMDAR-dependent mechanism during the formation of the spines. Although synaptic currents are absent in type 1 precursors, these progenitors express both GABA and glutamate receptors and local GABA release by parvalbumin interneurons induces their quiescence. Furthermore, activation of GABAergic parvalbumin interneurons by mature GC is essential for the increase of the number of spines and the complexity of dendrites of the new-generated neruons (Song *et al.*, 2016) (Urban & Guillemot, 2014)(Rodriguez-Iglesias *et al.*, 2019).

2.1.3. Functions of adult neurogenesis

Functional neurogenesis is modulated by experience and enriched environments. Furthermore, aging has been found to decrease adult neurogenesis in the DG (Rossi *et al.*, 2008). On the other hand, other physiological stimuli, such as physical exercise and enriched environment promote cell proliferation and survival respectively (Nishijima *et al.*, 2013)(Colangelo *et al.*, 2019). Learning also promotes neurogenesis but only hippocampus-dependent tasks are positive regulators of neurogenesis (Ming & Song, 2011).

In general, impaired adult neurogenesis has been related with some cognitive deficits that are often a hallmark of patients with psychiatric disorders such as major depression, schizophrenia, anxiety disorders and addictive behaviours, but also with some neurodegenerative diseases such as Alzheimer's and Parkinson's disease (Kang *et al.*, 2016). Adult hippocampal neurogenesis confers an extra degree of plasticity that is essential for certain types of spatial learning and object recognition (Urban & Guillemot, 2014)(Deng *et al.*, 2010). Furthermore, adult hippocampal neurogenesis also plays important roles in anxiety and stress regulation and some aspects of social behaviour (Cope & Gould, 2019). Functionally, the adult mouse hippocampus can be subdivided into the dorsal region, supporting spatial learning and memory, and the ventral one, involved in emotional behaviour and motivation, and adult neurogenesis has been implicated in all these functions (Christian *et al.*, 2014) (Berg *et al.*, 2018). Reduced number of new neurons and reduced hippocampal volume have been associated with excessive anxiety under stress conditions, and impairments in social behaviours (Kang *et al.*, 2016) (Cope & Gould, 2019). Under pathological situations, such as stroke and trauma, neurogenesis is increased even if each of these conditions is associated with reduced cognitive functions (Ming & Song, 2011). One possible interpretation is that damage-induced adult neurogenesis gives rise to abnormal synaptic connectivity. For instance, seizures enhance cell proliferation in both adult SGZ and SVZ, but they also lead to abnormal morphogenesis of the new-born neurons in the SGZ: they present hilar basal ectopic dendrites

and also aberrant migration to the hilus. Proliferation is also increased in stroke, and even if the resulting new-born neurons migrate to the infarct sites, the majority of them fail to survive over long periods. Moreover, treatment with antidepressant leads to induced proliferation at the same time that causes cognitive decline as well as increased anxiety (Cope & Gould, 2019)(Christian *et al.*, 2014). On the other hand, cell proliferation is decreased in stress and diabetes. Regarding neurodegenerative diseases, impaired proliferation has been described in Alzheimer's and in Parkinson's disease (Zhao *et al*., 2008). In summary, dysfunction of the hippocampus by disturbed adult hippocampal neurogenesis may represent in most cases a loss-of function due to decreased new-neurons production and integration, but also a gain-of-function with the consequent aberrant development and morphogenesis of the new-generated neurons (Christian *et al.*, 2014).

2.2. Synapse plasticity

New-born GCs go through a critical period of structural synaptic plasticity from the second to the eighth week after birth. The hippocampal function is influenced by differences in the connectivity but also by differences in non-neuronal components that regulate their connections (Cope & Gould, 2019). Regulation of synaptic connectivity involves at least four main cellular or molecular components: the presynaptic neuron, the postsynaptic neuron, glia and the ECM, which together make up the tetrapartite synapse. Glial cells and extracellular matrix molecules participate in adult neurogenesis and plasticity either by direct contact or by the secretion of several factors.

2.2.1. Glial cells

Among the glial cell subtypes, the more relevant ones for adult neurogenesis and plasticity are:

- Astrocytes: they control stem cell proliferation and their survival, but also influence the differentiation and integration of adult-born neurons into the hippocampal circuitry and in the OB. In additon, the vesicular release of trophic factors and anti-inflammatory cytokines in response to damage and disease also contributes to regulate adult neurogenesis. Astrocytes also release signaling molecules such as glutamate or GABA, influencing dendritic branching and synaptic activity in a process known as gliotrasmission (Rodriguez-Iglesias *et al.*, 2019) (Cope & Gould, 2019).
- Microglia: it is present in the mouse hippocampus from postnatal day 15 (P15). In the adult hippocampus, microglia cells maintain the homeostasis of the neurogenic niche at the time that they modulate neurogenesis through the secretion of differents molecules such as cytokines or trophic factors (Rodriguez-Iglesias *et al.*, 2019). Thus, microglia could have both promoting and detrimental effects on adult hippocampal neurogenesis exerting their action by multiple processes:
    - Trogocytosis: microglia cells limit axonal growth by actively removing axonal fragments by phagocitosis.
    - Release of soluble factors: microglia cells release several components of the extracellular matrix such as BDNF, IGF-1, several interleukines and TNF-α.

- Synaptic pruning: microglia have been described to be involved in the elimination of presynaptic and postsynaptic dendritic spine elements and in the relocation of dendritic spines.

2.2.2. Extracellular matrix molecules

Molecules from ECM facilitate the communication between neurons and glia due to the incorporation of secreted signaling factors in the common extracellular space. In addition, the ECM can form highly plastic structures around the cell body and the proximal dendrites called perineuronal nets (PNNs). These specialized structures are implicated in restraining synaptic plasticity and promoting synaptic stability in the adult brain. Specifically, PNNs may attract or repel axons of new neurons (Cope & Gould, 2019). Between the many components of the ECM, the more relevant ones for adult neurogenesis and plasticity are:

- Chondroitin sulfate proteoglicans: they are essential for new neuron formation and maturation since they are able to bind neurotrophic factors such as FGF-2 and BDNF.
- Reelin: in the adult hippocampus is mainly secreted by GABAergic interneurons. Reelin deficiency inhibits aldult neurogenesis, while its overexpression has been shown to stimulate it (Pujadas *et al.*, 2010).
- Matrix metalloproteinases: they regulate the amount of neurotrophins, such as nerve growth factor (NGF) (Colangelo *et al.*, 2019). They could also modulate the ECM structural plasticity, promoting or restricting the glia-neuron interaction.
- Tenascin-R: through its interaction with other ECM components and receptors, tenascin-R has been shown to modulate adult neurogenesis (Cope & Gould, 2019).

2.2.3. Functions of synapse plasticity

At the molecular level, adult synaptic plasticity underlies changes in synaptic strength in the form of long-term potentiation (LTP) and long-term depression (LTD), after increases or decreases of neurotransmitter release, respectively. LTP is known to occur as an increase in postsynaptic glutamate sensitivity and is correlated with the growth of the spines (Colgan & Yasuda, 2014) (Castillo, 2012). The global process of LTP induccion ocurrs as follows:

- First, calcium influx is produced after activation of NMDA receptors.
- Increasing levels of Ca^{2+} transiently activate Ca^{2+}/calmodulin-dependent kinase II (CaMKII).
- Activated CamKII initiates a signaling cascade that triggers the incorporation of additional AMPA receptors at the synapse as well as the remodeling of the spine structure through changes in actin cytoskeleton dynamics.

In addition, LTD of NMDA receptor-mediated transmission can be also induced in some synapses in response to the free Ca^{2+} concentration (Hunt & Castillo, 2012). Moreover, presynaptic forms of LTP and LDT co-exist together with postsynaptic forms of adult plasticity (Castillo, 2012).

3. Reelin

3.1. Molecular biology: The gene, mRNA and protein

In the mouse, the *reelin* gene (symbol *Reln*) is contained in chromosome 5 and is spread over about 450 kilobases (kb) of genomic DNA, organized in 65 exons. The human RELN gene, which is located in chromosome 7, present a similar organization to murine gene. The promoter region contains two different transcription initiation sites and forms a CpG island instead of the consensus TATA box, with recognition sites for transcription factors such as Sp1, Ets-1, AP2, Pax6, Tbr1, CREB and NF-KB. In addition to regulation by transcription factors, epigenetic modulation regulates the activation of *Reln* by chromatin remodelling (Doehner & Knuesel, 2010) (Royaux *et al.*, 1997).

The *Reln* gene encodes for a 12-kb mRNA, with eight protein-coding region repeats. The transcribed sequence can present an alternative polyadenylation site and can be alternatively spliced in a transcript with an inclusion of a hexanucleotide. This micro-exon is present in the neuron mRNA but not in non-neuronal cells (Tissir & Goffinet, 2003).

The *reelin* mRNA is translated into a 3461 amino acid (aa) glycoprotein with a predicted molecular mass of 440 kilo Daltons (KDa), 386 KDa in its unglycosylated form. The full length protein is structured in eight repeats of 350-390 aa, each of which presents an epidermal growth factor (EGF)-like motif in the centre **(Figure I.3.1)**. The N-terminal (Nt) region can be glycosylated and contains the signal peptide for secretion followed by a small region similar to F-spondin and an epitope recognized by the CR-50 monoclonal antibody. Whereas at the C-terminus (Ct) there is a carboxyl terminal region (CTR), which is absent in the alternatively polyadenylated coding mRNA (Ranaivoson *et al.*, 2016)(Lee & D'Arcangelo, 2016)(Tissir & Goffinet, 2003) (Jossin *et al.*, 2003).

Once it is secreted, Reelin is anchored to the ECM, where it can be cleaved by various metalloproteases at two specific sites giving rise to a total of five different fragments of 320kDa, 240 kDa, 180kDa, 120 kDa and 100 kDa, present in both the developing and the adult brain. Although full length Reelin remains anchored to the ECM in the place where it is secreted, its proteolytic fragments may diffuse (Ranaivoson *et al.*, 2016). The Nt cleavage has been shown to be involved in Reelin multimerization. In specific, the presence of CR-50 epitope is required for the proper formation of the tertiary structure, consisting of disulfide-linked homodimers (Chai & Frotscher, 2016). The central Reelin fragment (composed of repeats 3 to 6) has a pivotal role, being necessary and sufficient to initiate the downstream singnaling and to rescue the *reeler* phenotype, caused by the loss of Reelin protein. The C-terminal fragment has been suggested to be necessary for protein secretion, folding and for signaling efficacy (Knuesel, 2010) .

Several Reelin-cleaving enzymes have been identified, such as the serine protease tissue plasminogen activator (tPA), the matrix metalloproteinase (MMP), the metalloproteinases meprin α and β and metalloproteinases with trombospondin motifs

(ADAMTS). The existence of diffusible fragments proves that Reelin processing could stimulate activity in targeted cells away from the site of secretion (Lussier *et al.*, 2016) (Wasser & Herz, 2017)(Lee & D'Arcangelo, 2016)(Lussier *et al.*, 2016).

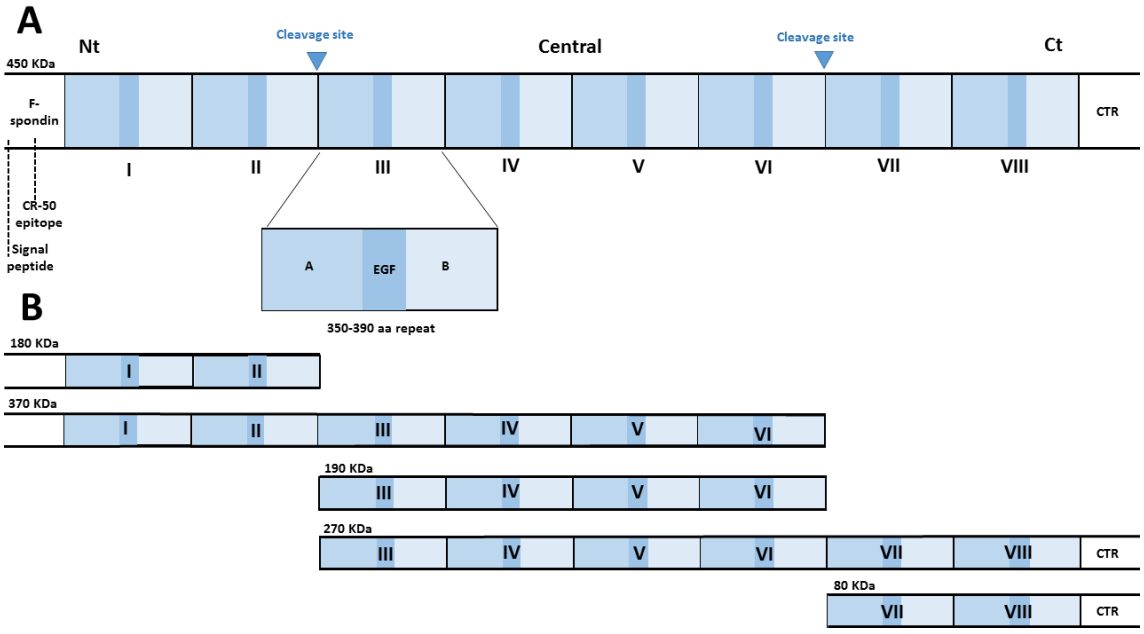

Figure I.3.1 | Domain organization and structural organization of the Reelin protein and its cleavage fragments. (A) The diagram represents the modular structure of the full length Reelin protein. Two cleavage sites (blue arrowheads) are represented on the top of the diagram, highlighting the N-terminal (Nt), Central and C-terminal (Ct) cleavage products. Each Reelin repeat (I-VIII) is composed by two subrepeats A,B separated by an epidermal growth factor (EGF)-like motif. The white box on the left side represents the N-terminal part of the protein, where the signal peptide, the F-spondin domain, and the CR-50 epitope are located. The white box on the right side dashes the C-terminus of the Reelin protein with the carboxyl terminal region (CTR). **(B)** Schematic representation of the five different proteolytic fragments cleaved, from 80 to 370 kDa in size. Adapted from: (Ranaivoson *et al.*, 2016).

3.2. The Reelin signalling pathway

It has been proposed that dimerization of Reelin protein is necessary for the clustering with its receptors, including the very low density lipoprotein receptor (VLDLR) and the apolipoprotein E receptor 2 (ApoER2, also called LRP8), and the transduction of intracellular signals. In the canonical signalling pathway, binding of homomeric Reelin to its two major receptors ApoER2 and VLDLR, triggers the dimerization of the receptors and tyrosine phosphorylation of cytoplasmatic adaptor protein disabled 1 (Dab1) **(Figure I.3.2.)** (Hiesberger *et al.*, 1999)(Trommsdorff *et al.*, 1999).

The *Dab1* gene is located in chromosome 1p32-p31 in mouse and presents a similar organization with the human gene. Either the inactivation or the spontaneous mutation of *Dab1* gene generate a *reeler*-like phenotype, scrambler and yotari mutants respectively. Dab1 protein binds to VLDLR and ApoER2 through its N-terminal region, and becomes phosphorylated in response to Reelin. Upon Dab1 phosphorylation by the Src-family kinases

(SFKs), Fyn and Src in tyrosine residues Y185, Y198, Y220 and Y232, additional non-receptor tyrosine kinases are recruited and activated, beginning the activation of a cytosolic kinase cascade. Phosphorylation of Dab1 in Y220 and Y232 promotes Dab1-Crk/CrkL interaction and C3 glomerulopathy (C3G) phosphorylation stimulating the activation of a Ras-releated protein 1, Rap1. Activation of Rap1 allows the control of neuronal adhesion molecules such as fibronectin, N-cadherin, Nectins and α5β1 integrins **(Figure I.3.2.** pathway 1**)**. In the same way, phospho-Dab1 in Y185 and Y198 induces the activation of PI3K, leading to two different pathways. Activation of the PI3K/Akt pathway promotes gene transcription and protein translation via the mammalian target of rampamycin (mTOR) **(Figure I.3.2.** pathway 2**)**. Reelin-mediated serine phosphorylation of GSK3β via Akt results in hyperphosphorylation of the microtubule-stabilizing protein, Tau. Phosphorylation on specific tyrosine residues of GSK3β induces phosphorylation of the microtubule-associated protein, MAP1B, and cytoplasmic linker-associated protein 2 (CLASP2), settling microtubule dynamics **(Figure I.3.2.** pathway 3**)**. In addition, Reelin/PI3K activation induces Cdc42 and Rac1 that regulate the actin cytoskeleton via LIM motif-containing protein kinase 1 (LIMK1) dependent inhibition of n-cofilin **(Figure I.3.2.** pathway 4**)**. Finally, phosphorylation of Dab1 also triggers the recruitment of Lis1, involved in regulating both, the actin and microtubule cytoskeleton dynamics, and the augmentation of calcium ions entry through NMDA receptors **(Figure I.3.2.** pathway 5**)** (Frotscher *et al.*, 2009)(Knuesel, 2010) (Ranaivoson *et al.*, 2016)(Jossin & Goffinet, 2007)(Lee & D'Arcangelo, 2016)(Ishii *et al.*, 2016)(Santana & Marzolo, 2017).

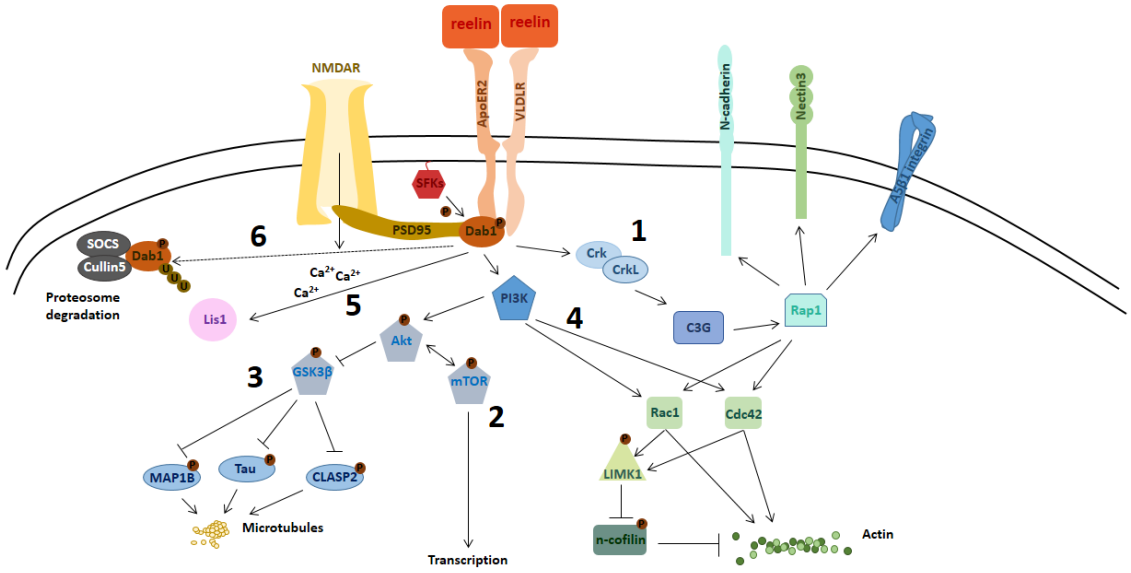

Figure I.3.2. | Reelin canonical signalling pathway. Binding of multimeric Reelin to its two major receptors ApoER2 and VLDLR triggers the intracellular clustering and phosphorylation of Dab1 (pDAb1) mediated by SFK. pDab1 further promotes the activation of other intracellular cascades. One is CrK/CrkL which in turn leads to the insertion of cell-cell adhesion proteins in the cell membrane by inducing Rap1. Notably, pDab1 also induces PI3K cascade activation driving different functions in the control of the actin and microtubules dynamics. pDab1 is finally down-regulated after ubiquitination by SOCS and Cullin5, limiting the duration of the Reelin-triggered signalling. Adapted from: (Santana & Marzolo, 2017)

Upon its binding, the activated Reelin signalling pathway is down-regulated by several mechanism that involves either phosphorylated Dab1 degradation or endocytosis of receptor complexes. Phosphorylated Dab1 (pDab1) is rapidly downregulated by polyubiquitination and proteasome-dependent degradation. The Cullin-5 (Cul5) component of ubiquitin E3 ligase complex as well as the suppressors of cytokine signalling (SOCS) proteins SOCS6 and SOCS7, are essential for pDab1 degradation **(Figure I.3.2.** pathway 6**)** (Simo & Cooper, 2013). Endocytosis of Reelin-receptor complex has also been suggested. Reelin and ApoER2 complexes are endocytosed after clustering and then translocated and degraded in lysosomes, whereas binding of Reelin to VLDLR directly induces the internalization of the complex (Chai & Frotscher, 2016).

The receptors ApoER2 and VLDLR are differentially expressed but structurally similar, with an extracellular domain, a unique transmembrane region and a cytoplasmic tail, where Dab1 binds. Binding of Reelin to ApoER2 is calcium dependent and can be inhibited by ApoE (Ranaivoson *et al.*, 2016)(Dlugosz & Nimpf, 2018). Furthermore, alternative splicing of ApoER2 can modify ApoER2 cleavage fragments affecting both the binding of Reelin with the receptor and the intracellular signaling pathway, including inhibition of Reelin-transcription (Wasser & Herz, 2017). Despite ApoER2 and VLDLR are the major Reelin receptors in the developing brain, other transmembrane proteins have been proposed to functions as Reelin receptors although only ApoER2 and VLDLR double-mutant mice show a *reeler* phenotype (Knuesel, 2010)(Lee & D'Arcangelo, 2016)(Wasser & Herz, 2017):

- β1-containing integrins: they are expressed during corticogenesis in layer I-V neurons and glial cells. Through its interaction with Reelin, β1 integrins regulate radial glia scaffold and the formation of the CRC layer (Chai & Frotscher, 2016).
- EphB tyrosine kinase receptor: through its interaction with the Nt region of Reelin, EphB activates a signalling cascade with important functions for the proper lamination of CA3 region of the hippocampus. In addition, the binding of EphB with its receptor, allows the activation of SFKs necessary for the phosphorylation of Dab1 (Senturk *et al.*, 2011).

3.3. Expression and function in brain development

Developmental expression of *reelin* transcripts is first detected at E10 in the telencephalon and the diencephalon, but later on Reelin is still expressed in other brain structures such as the cerebral cortex, the hippocampus, striatum, olfactory bulb and in discrete nuclei of the basal forebrain (Alcantara *et al.*, 1998)(Ikeda & Terashima, 1997). Reelin exerts different functions in the developing brain where it controls the correct development of layered structures, such as cortex, hippocampus and cerebellum but it is also relevant for axonal growth, dendritogenesis and synaptogenesis.

3.3.1 Reelin in the formation of the neocortex

Between E11-E12 *reelin* is predominantly expressed by CR cells from the PP **(Figure I.3.3.)**. At E14 when the PP has splitted into the MZ and the subplate layer and the CP has emerged, Reelin remains closely associated to the surface of the CRC located in the outermost part of the pia, the MZ (Hirota & Nakajima, 2017). This pattern of Reelin expression remains essentially the same by P0. During cortical development, Reelin signalling constitutes a key regulator to configure the inside-out gradient of the layered cortical structures.

In *reeler* mice, the early-born CP neurons fail to split the PP, suggesting that Reelin signalling is therefore necessary for PP splitting. In the first phase of neuron migration, future deeper layer neurons (layer VI neurons) exhibit multipolar morphology in the VZ and migrate in a RG-independent way, a process called somal translocation. At later stages, when the CP is developed, postmitotic neurons become bipolar within the IZ with a defined leading process and a trailing axon and start radial migration. The presence of Reelin and ApoER2 in the lower part of the IZ, suggests a role of Reelin in neuronal polarization and axon specification (Ranaivoson *et al.*, 2016)(Santana & Marzolo, 2017)(Chai & Frotscher, 2016) (Frotscher, 1998). Between the multiple changes that neurons undergo at this stage, Reelin controls multiple mechanisms. On the one hand, Dab1-Crk/CrkL-C3G-Rap1/Cdc42 pathway activation promotes early-born neuron polarization and splitting of the PP by somal translocation through their role in cytoskeleton dynamics. On the other hand, Reelin signaling pathway also controls the trafficking and the membrane localization of adhesion molecules such as N-cadherins. The plasma membrane localization of those proteins, which is controlled by Rap1 and its downstream effectors Cdc42 and Rac1, mediates the cellular interaction between the migrating neurons and the CRC. As a consequence of this interaction the anchoring of the leading processes is established promoting the polarization of postmitotic neurons (Franco *et al.*, 2011) . In addition, LIMK1 activation via PI3K promotes cofilin-mediated stabilization of the actin cytoskeleton which allows the stabilization of the leading process as well as their attachment to the MZ (Chai *et al.*, 2009)(Chai & Frotscher, 2016). Regarding cytoeskeletal dynamics, Reelin signaling pathway also regulates microtubules assembly and stabilization via PI3K/Akt/GSK3β activation that allows MAP1B phosphorylation (Santana & Marzolo, 2017). It has been proposed that ApoER2 is the main Reelin receptor implicated in this stage, since ApoER2 and not VLDLR is expressed in the lower IZ/SVZ (Sekine *et al.*, 2014)(Dlugosz & Nimpf, 2018).

Radial migration in *reeler* mice is also impaired (Boyle *et al.*, 2011). In the locomotion mode of migration, bipolar neurons existing in the IZ migrate through the CP towards the MZ using the RG fibers as a template. In *reeler* cortices RG cells are poorly packed and the RG scaffold fail to form (Forster *et al.*, 2002). Furthermore, during locomotion the surface expression of N-cadherin is required to establish RG-migrating neuron contacts (Santana & Marzolo, 2017) (Gil-Sanz *et al.*, 2013).

Finally, in the last step of cortical migration, migrating neurons extend their leading processes to reach just beneath the MZ. This process, called terminal translocation, also needs the detachment of migrating neurons from RG fibers (Franco & Muller, 2011). It has been proposed that similar mechanism between somal translocation and terminal translocation may

be involved in the Reelin-dependent regulation of these processes. Activation of Dab1-Crk/CrkL-C3G-Rap1 pathway promotes neuronal adhesion to the fribronectin localized in the extracellular matrix of the MZ via integrin α5β1 (Kawauchi *et al.*, 2010)(Sekine *et al.*, 2012)(Chai & Frotscher, 2016). In addition, Dab1-dependent activation of PI3K-Cdc42/LIMK-cofilin axis is also required for the stabilization of actin cytoskeleton in the leading process (Santana & Marzolo, 2017). Similarly, Rap1/N-cadherin pathway activates the homophilic interaction of N-cadherins between CRC and migrating neurons. In association with the cadherin system, interaction of Nectins 1/3 is also required for somal translocation. In the MZ, CRC express Nectin 1 while somal translocating neurons express Nectin 3. Therefore, Reelin signaling induces N-cadherines and Nectins adhesion by stabilizing both proteins at the cell surface of CRC and migrating neurons (Gil-Sanz *et al.*, 2013).

Furthermore, migration arrest seems to be also controlled by Reelin signalling. In the outermost part of the CP, VLDLR is the major Reelin receptor expressed, whereas ApoER2 is expressed more superficially, just beneath the MZ, and in the IZ. However, the specific contribution of both receptors in migration arrest is still unclear (Santana & Marzolo, 2017). Between the mechanisms that control stop migration, the Reeling-induced degradation of Dab1 via SOCS7-Cul5-Rbx2 has been suggested to be essential for rapidly downregulation of Dab1 signalling (Simo & Cooper, 2013) (Feng *et al.*, 2007). In addition, binding of Reelin with VLDLR induces their direct internalization and degradation very quickly resulting in a rapid decrease of extracellular Reelin that allows to stop migration (Chai & Frotscher, 2016).

Besides the well known role of Reelin in neuronal migration and cortical layer formation, Reelin has also been suggested to control neocortical neurogenesis. Earlier than in migrating neurons, Reelin enhances Notch signalling within RG progenitors that also express Reelin receptors. This, in turn, contributes to the maintenance of the progenitor pool. Furthermore, the disappearance of CRC at postnatal stages roughly coincides with the shift of NPCs from the neurogenic phase to astrogliogenesis in the neocortex (Lakoma *et al.*, 2011).

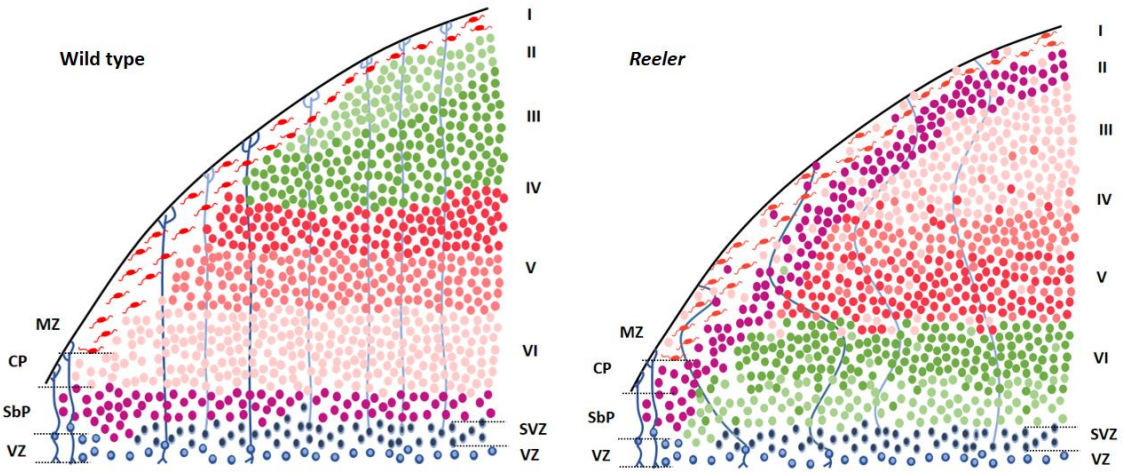

Figure I.3.3. | Reelin role in the development of layered neocortex. Left, normal cortical development. The first cohort of neurons (purple cells) born after asymmetric division of radial glia cells (blue cells), exit the ventricular zone (VZ) and form the preplate that is then subdivided

into the marginal zone (MZ) where Reelin-expressing Cajal-Retzius cells (red cells) are located and the subplate (SbP). The incorporation of a second cohort of cells (pink cells) gives rise to the cortical plate (CP). After that, neurons generated in the subventricular zone (SVZ) move through the CP towards the MZ. The colors of the six layers (I-VI) represent the inside-out pattern of cortical migration, with later born neurons (green cells) occupiying the upper layers and early born neurons (magenta cells) placed in the lower layers. **Right,** cortical development in *reeler* mice. In *reeler* cortices splitting of the PP does not occur properly and cortical migration becomes impaired, disrupting the typical pattern of layered cortex and sometimes inversing it to an outside-in architecture. Adapted from: (Curran & D'Arcangelo, 1998)

3.3.2. Reelin in the formation of the hippocampus

In the developing hippocampus *reelin* expression is primary detected at E12-E14 in a thick layer of cells in the outer MZ. Later on, between E15-E16 when the typical layering of future CA1 and the primordium of the DG are visible, Reelin-expressing CRC occupy the outer MZ (future stratum lacunosum moleculare). From E16 onwards, some Gad65/67 positive neurons also express Reelin in the prospective sr and so. At early postnatal stages, *reelin* expression is still visible in CRC from the molecular layer (ML)/slm, but the intensity and the number of CRC-expressing cells are diminished from P15 onward. Nevertheless, *reelin* expression persists from P21 to adult stages in double Reelin-Gad65/67-positive neurons distributed throughout the hippocampal layers and in some CRC (Alcantara *et al.*, 1998) (del Rio *et al.*, 2002)(Borrell *et al.*, 1999)(Abraham & Meyer, 2003).

In the *reeler* hippocampus, the normal neuronal organization in layers is severely disrupted **(Figure I.3.4.)**. Hippocampal pyramidal cells are misspositioned in a splitted layer and granule cells are scattered along the entire DG. Thus, Reelin signalling has a pivotal role during hippocampal development in the control of both pyramidal and granule hippocampal neurons migration and in the maturation and branching of the entorhinal afferents (Del Rio *et al.*, 1997) (Forster, Zhao, *et al.*, 2006).

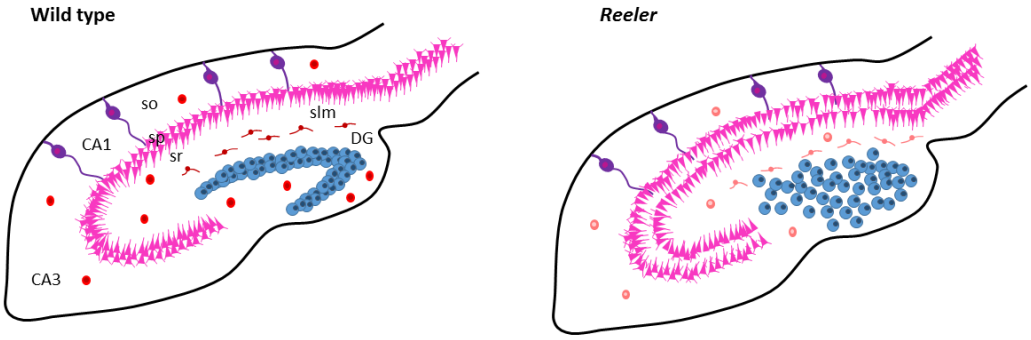

Figure I.3.4. | Reelin role in the formation of the hippocampus. Left, normal hippocampal structure. In wild type mice, Cajal-Retzius cells and GABAergic interneurons (red cells) express Reelin. The hippocampus of wild type mice exhibit a compact layer of pyramidal neurons (pink cells) in CA1 and CA3 as well as a defined dentate gyrus (DG). **Right,** hippocampus structure in *reeler* mice. In *reeler* hippocampus the stratum pyramidale (sp) appears

subdivided into two layers. Further, granule cells (blue cells) of the DG are dispersed arround the hilus. Adapted from: (Curran & D'Arcangelo, 1998).

3.3.3. Reelin in piryform and entorhinal cortices

In the piryform and entorhinal areas, *reelin* mRNA is detectable from E12 in CRC of the MZ. From E18 onwards, expression of *reelin* is also visible in layer II stellate neurons. These neurons that are known to project to the DG do not express any of the GABAergic interneuron markers, and their expression persists in the adult brain (Ray & Brecht, 2016) (Alcantara *et al.*, 1998).

The *reeler* mutant mice also exhibit alterations in the entorhinohippocampal afferents, including abnormal termination of the circuit as well as reduced axonal branching and aberrant synaptogenesis (Del Rio *et al.*, 1997) (Borrell *et al.*, 1999).

3.3.4. Reelin in the formation of the cerebellum

The first embryonic structure that gives rise to the formation of the cerebellum, in which *reelin* expression is observed is the rhombic lip, where granule cell precursors are born (Curran & D'Arcangelo, 1998). In the embryonic cerebellum Reelin starts to be expressed by deep nuclear neurons at E13.5 in the area near to the pial surface. From E14 to E18 Reelin is also expressed by granule cell precursors at the inner part of the EGL. At early postnatal stages, Reelin expression disappears from deep nuclear neurons, whereas is maintained by pre-migratory postmitotic granule cells in the developing EGL and by post-migratory granule neurons in the IGL (Miyata *et al.*, 1996)(D'Arcangelo & Curran, 1998) (Sotelo, 2004)(Nakamura *et al.*, 2016).

At E14.5 the Purkinje cell plate is present in a normal cerebella but not in the *reeler* cerebellum **(Figure I.3.5.)** (Miyata *et al.*, 2010). In the *reeler* mice Purkinje cells are abnormally positioned with less branched dendrites and there is a reduction in the number of both granule and Purkinje cells (Curran & D'Arcangelo, 1998) (Forster, Jossin, *et al.*, 2006). In addition, the size of the *reeler* cerebellum is severely diminished and abnormally foliated because of the reduction of PC and granule cell populations (Rahimi-Balaei *et al.*, 2018). Thus, Reelin seems to regulate the proper positioning of the Punkinje cells and the neural proliferation in the cerebellum (Cocito *et al.*, 2016).

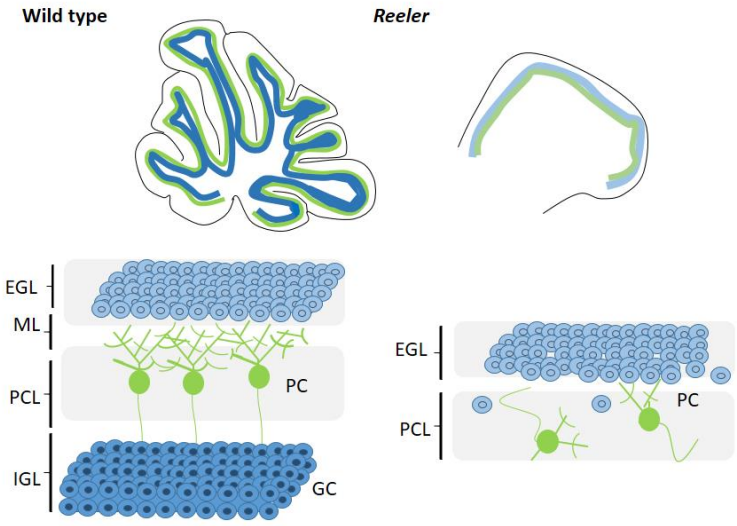

Figure I.3.5. | Reelin role in the development of the cerebellum. Left, normal cerebela development. At early embryonic stages granule cells (GC, light blue cells) migrate tangentially to form the external granule layer (EGL). Later on granule cells start to express Reelin at the time that Purkinje cells (PC, green cells) migrate radially from the ventricular zone to occupy the Purkinje cell layer (PCL) and develop their dendrites in the molecular layer (ML). Finally, granule cells leave the EGL and migrate inwardly towards the internal granule layer (IGL). **Right,** development of the cerebellum in *reeler* mice. In reeler cerebellum PC are ectopically placed and less branched. In addition, there is a reduction in the total number of PC and granule cells. Consequently, the *reeler* cerebellum is smaller and less foliated. Adapted from: (D'Arcangelo & Curran, 1998)

3.3.5. Reelin in dendritogenesis

Early postnatally, secreted Reelin has been shown to modulate axonal and dendritic outgrowth by controlling the stability of the cytoskeleton. Neurons from *reeler* mice exhibit reduced dendritic branching with fewer dendritic spines. Several Reelin-induced pathways may operate during dendritic development including ApoER2/Dab1/PI3K pathway which activates the RhoGTPase Cdc42 to enhance cortical neurite outgrowth and the PI3K/Akt pathway, required for the activation of mTOR **(Figure I.3.2.)** (Wasser & Herz, 2017). In addition, Reelin-signalling pathway also regulates microtubule and actin stability through the activation of Lis1 via VLDLR or by the inactivation of cofilin through LIMK1. In neurons close to the MZ, the expression of several microtubule-associated proteins such as end-binding protein 3 (EB3), Tau or CLASP2, is enriched in response to Reelin signalling (Senturk *et al.*, 2011)(Rio *et al.*, 1997). Furthermore, Reelin also modulates the number of dendritic spines and the molecular composition of synapsis since the *reeler* mice present lower spine density and composition. During development, the formation of hippocampal synapsis depends on NR2B subunit of NMDARs but as synapsis mature, the major component of NMDAR shift to NR2A subunits. This switch in addition to the insertion of AMPAR into synaptic membranes are regulated by Reelin signalling (Wasser & Herz, 2017).

3.4. Expression and function in the adult brain

In the adult brain the expression pattern of Reelin changes. Although the CRC population declines during the first postanatal weeks, a small number of CRC are still present in the marginal zone of the neocortex (defined as layer I), as well as in the slm of the adult hippocampus and in the outermost layer of the adult DG (Knuesel, 2010). Nevertheless, the main source of Reelin are GABAergic interneurons located in the neocortex and hippocampus and glutamatergic mitral cells in the cerebellum and layer II pyramidal cells in the piryform and entorhinal cortex (Knuesel, 2010)(Wasser & Herz, 2017)(Jossin & Goffinet, 2007). Despite this shift in the Reelin expression at adult stages, the main functions of Reelin in the adult brain through the activation of its signaling pathway are the control of the actin cytoeskeleton and microtubule dynamics pointed to the modulation of adult synaptic plasticity (Ishii *et al.*, 2016).

3.4.1. Reelin in adult synaptic plasticity

It is known that Reelin signalling is important for adult synaptic plasticity. First, Reelin signalling mediates tyrosine phosphorylation of the NMDA receptor subunits NR2A and NR2B, triggering an increase in the calcium influx in the postsynaptic area. The coupling of ApoER2 and phosphorylated Dab1-Src/Fyn complex to the NMDA receptor requires Dab1 binding site and a unique fifty-nine amino acid insert in the exon 19 of ApoER2 that interacts with PSD-95. Upon Reelin binding to ApoER2, Src is recruited via PSD95 allowing the interaction and the subsequent phosphorylation of NMDA receptor subunits, inducing LTP. Second, the consolidation of LTP requires Reelin-mediated translation in mTOR-dependent manner (Knuesel, 2010)(Wasser & Herz, 2017)(Dlugosz & Nimpf, 2018)(Santana & Marzolo, 2017). Moreover, Reelin can also modulate AMPA receptor-mediated responses. Through its interaction with ApoER2, the adapter protein GRIP1 binds to ephrinB2 and AMPARs in a complex, triggering the insertion of AMPARs in the synapse (Dlugosz & Nimpf, 2018). Furthermore, Reelin controls dendritic outgrowth and stabilization of dendrites, inducing release of neurotransmitters in the presynaptic compartment in an ApoER2/Dab1/PI3K-dependent manner, that requires the activation of mTOR (Ishii *et al.*, 2016)(Ferrer-Ferrer & Dityatev, 2018). Finally, changes in the adult levels of Reelin have also been implicated in the control of the shapes, sizes and types of dendritic spines, but not in the spine number, leading to bigger or smaller spines under excess or lack of Reelin signalling, respectively (Pujadas *et al.*, 2010)(Bosch *et al.*, 2016).

3.4.2. Reelin in adult neurogenesis

There is discussion as to whether Reelin has a role in adult neurogenesis itself, or if Reelin has an effect on migration, morphology and maturation of new-born adult neurons. Disturbed migration results in malpositioning of neurons that might be associated with severe dysfunction such as mental retardation and epilepsy. For instance, in mesial temporal lobe epilepsy (MTLE) a migration defect of the dentate granule cells is observed. In *reeler* mice, the

malpositioning of granule cells in the DG correlates with the extent of those effects present in MTLE patients. These morphological defects are suggested to be pro-epileptogenic (Korn *et al.*, 2016). However, since decreased levels of Reelin have been noticed in MTLE patients, it is difficult to clarify if Reelin deficiency causes granule cell dispersion which in turn leads to epilepsy or if epileptic seizures alter Reelin expression (Haas & Frotscher, 2010) (Gong *et al.*, 2007).

Decreased neurogenesis in the adult *reeler* DG as well as a shift towards glial fate of the newly generated cells have been confirmed, indicating a role of Reelin in the differentiation of precursor cells (Zhao *et al.*, 2007)(Brunne *et al.*, 2013). In addition, induced Reelin overexpression increases the rate of adult neurogenesis and causes abnormal cell migration and integration of the new-born granule cells (Pujadas *et al.*, 2010) as well as an accelerated dendritic maturation (Teixeira *et al.*, 2012).

Moreover, recent studies have shown that upon Reelin or Dab1 inactivation in adult mice, adult-generated granule cells migrate aberrantly and they present a defective integration and dendritic arborisation with basal dendrites misoriented through the hilus and ectopic synapses formed in the hilus (Haas & Frotscher, 2010)(Korn *et al.*, 2016). An increase in the number of glia was also observed after adult suppression of Reelin signalling pathway (Teixeira *et al.*, 2012).

On the other hand, neuroblasts born in the SVZ depend on Reelin for detaching from the tangentially oriented RMS and start radial migration in the olfactory bulb. In addition, in *reeler* mice neuroblasts appear clustered in the OB as a consequence of a failed switch to radial migration (Hack *et al.*, 2002).

3.5. Recent animal tools to study the role of Reelin pathway

3.5.1. Knock-in mouse with deletion of the Reelin CTR (ΔC-KI)

In this ΔC-KI mouse model, the carboxyl terminal region (CTR) of the Reelin gene was replaced with a FLAG epitope. The mouse was viable and unlike the *reeler* mouse, it did not exhibit ataxic behaviour. Although the gross structure of the brain seemed normal, the presence of a narrower MZ in the somatosensorial areas of the cortex was evident from early postanatal stages in these mice, indicating a role of Reelin CTR in the formation and maintenance of the MZ. Furthermore, the authors provided evidences that after Reelin CTR sequence deletion upper-layer neurons invaded the MZ, and presented apical processes that were misoriented or poorly branched. The hippocampal structure of these mice was also altered. The CA1 pyramidal cell layer was split into two layers and GCs of the DG were less densely packed (Kohno *et al.*, 2015). In addition, they found ectopic clusters of PCs in the lobules VI-VII of the postnatal cerebellum containing higher amount of Dab1 protein and VLDLR (Nakamura *et al.*, 2016). Finally, the behavioural characterization of these mice demonstrated that they were hyperactive and exhibited reduced anxiety-like and social

behaviours as well as impaired working memory, recapitulating some of the aspects of neuropsychiatric disorders (Sakai *et al.*, 2016).

3.5.2. Inducible conditional Reelin knockout (cKO) mouse

By using this inducible Reelin cKO mouse model, the effect of adult Reelin depletion was assessed in mice at two months old. After Reelin suppression, the authors described no alterations in the cortical layering as well as a normal cerebella and hippocampi. Furthermore, neurons from the cKO mice presented normal dendritic spine density and morphology, suggesting that disruption of Reelin signalling in the fully formed brain did not alter brain structures. However, these mice showed some mild behavioural alterations, including reduced anxiety, sensorimotor deficits and increased LTP, raising the possibility of synaptic alterations in the hippocampus of these mice (Lane-donovan *et al.*, 2015).

3.5.3. Inducible endothelial specific Dab1 loss-of-function mice (Dab1$^{i\Delta EC}$)

The induction of Dab1 deletion in endothelial cells in these mice both at embryonic (E10.5 to E12.5) and at early postanatal stages (from P1 to P3) impaired vascular growth as reflected by a reduction in vessel density, vessel length and reduced number of branch points, that were compensated at adult stages. The altered vascular morphology also correlates with defective migration of cortical neurons, when Dab1 was deleted at embryonic (E10.5 to E12.5) and perinatal stages. Specifically, embryonic deletion induced aberrant positioning of early- and late-born cortical neurons, whereas after perinatal deletion of Dab1 from endothelial cells a persistent invasion of layer I by later-born neurons was observed in Dab1$^{i\Delta EC}$ mice. In addition, a number of later-born neurons failed to migrate and remained below layer IV (Segarra *et al.*, 2018).

AIMS OF THE STUDY

The main goal of this study is to gain insight in the specific function of Reelin during brain development and in the adult brain. In particular the aim of this study has been to analyse the specific contribution of Reelin selectively expressed by Cajal-Retzius cells and by GABAergic interneurons and the effect of its deficiency during different developmental stages and in the adult brain. To this end, we established the following objectives:

1. **Role of Reelin expressed by Calretinin positive cells in corticogenesis and hippocampus formation.**
    1.1. Generation and validation of a constitutive Calretinin Reelin deficient mouse model.
    1.2. Analysis of Reelin deficiency from Calretinin positive cells in neuronal cortical distribution.
    1.3. Analysis of Reelin deficiency from Calretinin positive cells in the layering of the hippocampal structures.

2. **Role of Reelin expressed by GAD65 interneurons in corticogenesis and hippocampus formation.**
    2.1. Generation and validation of a constitutive GAD65 interneuron Reelin deficient mouse model.
    2.2. Analysis of Reelin deficiency from GAD65 interneurons in neuronal cortical distribution.
    2.3. Analysis of Reelin deficiency from GAD65 interneurons in the hippocampus cytoarchitecture.

3. **Analysis of the conditional loss of Reelin signaling in early postnatal development and adult stages in the cortex, hippocampus and cerebellum.**
    3.1. Generation and validation of an ubiquitous inducible conditional Reelin deficiency mouse model.
    3.2. Analysis of postnatal loss of Reelin signaling in neuronal cortical distribution.
    3.3. Analysis of Reelin depletion in adulthood in cortical plasticity.
    3.4. Analysis of the conditional loss of Reelin in the layering of hippocampal structures.
    3.5. Analysis of Reelin deficiency during adulthood in adult neurogenesis in the subgranular zona of the dentate gyrus.
    3.6. Analysis of adult conditional loss of Reelin in dendritic orientation and migration of adult-generated granule cells.

MATERIAL AND METHODS

1. Animals

1.1. Floxed Reelin (fR/fR) mice

The floxed fR/fR mice were obtained using a targeted plasmid (MluI-Eco47III) containing the first exon of the *Rln* gene flanked by two loxP sites accompanied from downstream and upstream genomic sequences for homologous recombination **(Figure MM.1.)**. After positive selection of genome recombination by Southern blotting, chimeric animals (containing Reelin floxed allele) were obtained after injection of ES targeted cells into C57Bl/6J blastocysts. These chimera animals were crossed with C57Bl/6J and the resultant offspring (heterozygous floxed Reelin mice, fR/wt) were backcrossed to obtain homozygous floxed Reelin mice (fR/fR) in a C57Bl/6J background.

Homozygous floxed Reelin mice (fR/fR), which have the exon 1 of the Reelin gene flanked by loxP sequences, were crossed with different Cre recombinase expressing mice in order to obtain double transgenic mice with conditional deletion of the Reelin gene, in a C57BL/6J background.

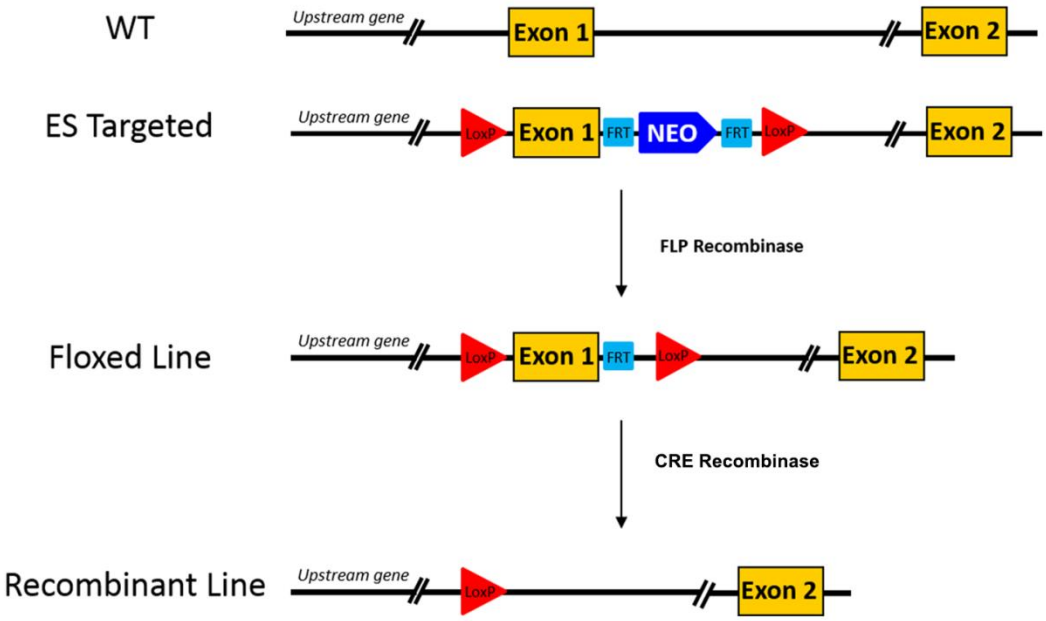

Figure MM.1. | Generation of the floxed Reelin mouse model. Schematic representation of the strategy used for the conditional targeting of the *Rln* gene. The scheme shows Reelin cDNA of wild-type (WT) allele, Reelin-Exon1-floxed allele in the targeting vector(top), Reelin-Exon1-floxed allele of conditional line and Reelin-Exon1-recombinant allele after Cre-mediated recombination.

1.2. CR line (CR fR/fR)

In order to obtain this colony, we crossed the fR/fR mice with a Cre line to specifically deplete Reelin in the Cajal-Retzius cells (Taniguchi *et al.*, 2011). In this case, Cre recombinase expression was under the control of the Calretinin promotor (*Calb2*$^{tm1(cre)Zjh}$/J, stock #010774, The Jackson Laboratory) and the resulting offspring was homozygous for floxed Reelin (fR/fR) and either had two copies of Cre (CR fR/fR), one copy (heterozygous) or none (fR/fR). For experimental procedures only homozygous of Cre (CR fR/fR) and the ones without Cre (fR/fR) were used, whereas the heterozygous were used as breeders. In this colony we expected Cre recombinase activity and deletion of the floxed sequence (Reelin exon 1) in Calretinin expressing cells, such as CR cells and Calretinin expressing interneurons of the brain.

1.3. Gad line (Gad fR/fR)

To obtain this colony, we crossed the fR/fR mice with a Cre line to specifically deplete Reelin in GABAergic interneurons (Taniguchi *et al.*, 2011). In this case, the Cre recombinase was under the control of the GAD2 (GAD65) promotor (*Gad2*$^{tm2(cre)Zjh}$/J, stock #010802, The Jackson Laboratory) and the resulting offspring was homozygous for floxed Reelin (fR/fR) and either had two copies of Cre (Gad fR/fR), one copy (heterozygous) or none (fR/fR). In this line only the Cre homozygous (Gad fR/fR) and the ones without Cre (fR/fR) were used for experimental purposes and the heterozygous were used for crossings. In this colony Cre recombinase activity is induced in GAD2 (or Gad65) expressing cells.

1.4. Cre fR/fR mice

Mice with a ubiquitous conditional deletion of reelin upon tamoxifen administration were obtained by crossing the homozygous floxed Reelin (fR/fR) mice with the hemizygous ubiquitous UbiCreER^{T2} line. The UbiCreER^{T2} line (B6.Cg-Tg(UBC-cre/ESR1)1Ejb/J, stock #008085, The Jackson Laboratory) expresses the Cre recombinase ubiquitously fused to the hormone-binding domain (HBD) of the mutated estrogen receptor (ER^{T2}) (Kristianto *et al.*, 2017) (Ruzankina *et al.*, 2007). Upon administration of the synthetic estrogen tamoxifen (TAM), Cre recombinase activity is induced and recombination results in the deletion of the floxed sequence (Reelin exon1) from virtually all tissues. After breeding the resulting offspring were homozygous for floxed Reelin (fR/fR), and either heterozygous for the UbiCreER^{T2} allele (Cre fR/fR mice), or wild-type for the UbiCreER^{T2} allele (fR/fR mice).

All mice were housed in groups in a 12h light/dark cycle with free access to water and food. All procedures were performed with mice from both genders according to the guidelines of the European Community Directive 2010/63/EU and were approved by the local ethics committee for Animal Experimentation of the University of Barcelona (CEEA, Barcelona, Spain).

2. PCR

Genomic DNA was extracted from a 1-3mm tail fragment by adding 50 mM sodium hydroxide. The tails were incubated at 100ºC for 15 minutes and then stored at until use. For mouse genotyping standard PCR amplification protocol was performed according to The Jackson Laboratory guidelines, using GoTaq® Green Master Mix (Promega, M712) and the primers described in **Table MM.2.1**.

PCR name	Primers sequence	PCR conditons	PCR products
CRE PCR	Mutant Forward: 5' GCG GTC TGG CAG TAA AAA CTA TC 3' Mutant Reverse: 3' GTG AAA CAG CAT TGC TGT CAC TT 5' Wild type Forward: 5' CTA GGC CAC AGA ATT GAA AGA TCT 3' Wild type Reverse: 3' GTA GGT GGA AAT TCT AGC ATC ATC C 5'	3 min 94ºC (30 sec at 94ºC 1 min at 51.7ºC 1 min at 72ºC) x35 cycles 2 min 72ºC 10 ºC	Wild type band: 324 bp CRE band: 100 bp
CR PCR	Common: 3' AGG TCT GGG AAG GAG TGT CA 5'; Mutant Forward: 3' CCA CTA GAT CGA ATT CCG AAG 5' Wild type Forward: 3' ACC TGG AGA TTG TGC TCT GC 5'	2 min 94ºC (20 sec at 94ºC 15sec at 65ºC 10 sec at 68ºC) x10 cycles (15 sec at 94ºC 15sec at 60ºC 10 sec at 72ºC) x28 cycles 2 min 72ºC 10 ºC	CR band: 175 bp Wild type band: 125 bp
GAD PCR	Common: 3' CAC CCC ACT GGT TTT GAT TT 5' Mutant Forward: 3' AAA GCA ATA GCA TCA CAA ATT TCA 5' Wild type Forward: 3' CTT CTT CCG CAT GGT CAT CT 5'		GAD band: 352 bp Wild type band: 250 bp
FLOX PCR	Common: 5' CACCGACCAAAGTGCTCCAATCTGTCG 3' Flox : 5' CGAGGTGCTCATTTCCCTGCACATTGC 3' '	2 min 94ºC (30 sec at 94ºC 30 sec at 55ºC 90 sec at 72ºC) x35 cycles 5 min 72ºC 10 ºC	Flox band: 613 bp :Wild type band 496 bp

Table MM.1 | Collection of primers used for Cre CR, GAD and FLOX PCRs, PCR conditions and expected PCR products.

3. Tamoxifen administration

3.1. Postnatal administration

To conditionally delete Reelin at early postnatal stages, pups received a daily intragastric injection of tamoxifen (TAM, Sigma-Aldrich, T5648-1G; 1 mg/ml dissolved in 2.5% EtOH/97.5% peanut oil) at 0.05 mg/pup/day for 3 consecutive days from P1 to P3. Mice were then sacrificed at different postnatal days ranging from P0 to P15.

3.2. Adult administration

To obtain temporally controlled ubiquitous Cre-mediated recombination in late postnatal (P20-30) and adult (>P45) Cre fR/fR mice, intraperitoneal TAM injections were administered for 3 consecutive days (30 mg/ml dissolved in 10% EtOH/90% sunflower oil) at 90 mg/Kg/day or 180mg/Kg/day, respectively. Unless otherwise stated, mice were then sacrificed at 3-4 months after TAM injection. Tamoxifen injections were performed at P30 for proliferation

analysis, >P45 for general histological characterization, and for the neurogenesis analysis; and 2, 3 or 8 weeks after RV-GFP injections for the new-born neurons morphology analysis.

4. Chemicals

Common chemicals and reagents were purchased from Sigma-Aldrich and Panreac. Specifically, ammonium persulfate (APS), Diaminobenzidine reagent (DAB), Hydrogen Peroxide (H_2O_2), 4,-6,-Diamino-2-phenylindole dihydrochloride (DAPI), Triton X-114, Eukitt mounting media, Nissl (Cresyl violet acetate and Thionine acetate salt), Hoechst 33342, 5-Bromo-2'deoxyuridine (BrdU, B5002), Tamoxifen (TAM), Sunflower oil and Peanut oil were purchase from Sigma-Aldrich. Paraformaldehyde, Ethanol and Gelatine were from Panreac. Mowiol 4-88 was from Calbiochem. BCA Protein Assay was from Thermo Fisher.

5. Antibodies

Commercial primary and secondary antibodies used for immunohistochemistry (IHC) and Western Blot (WB) detection are detailed in **Table MM.2.**

	Antibody	Reference	IHC Dilution	WB Dilution
Primary	Anti-Reelin (clone G10)	MAB5364, Millipore	1:500	1:4000
	Anti-Cux1	SC-13024, Santa Cruz Biotechnology	1:250	
	Anti-CTIP2	ab18465, Abcam	1:500	
	Anti-BrdU	OBT0030, Axyll	1:250	
	Anti-BrdU (clone BU1/75)	ab6326	1:250	
	Anti-Calretinin	7699/3H Swant Antibodies	1:1000	
	Anti-NeuN	MAB377B, Millipore	1:500	
	Anti-GAD65/67	AB1511, Chemicon International	1:1000	
	Anti-GFP (Chicken)	GFP 1020, Aves Lab	1:500	
	Anti-GFP (Rabbit)	A11122, Life Technologies	1:1000	
	Anti-Prox1	Kind gift from S. Pleasure, University of California, San Francisco	1:10000	
	Anti-GFAP	AB5840, Millipore	1:1000	
	Anti-Sox2	ab97959, Abcam	1:750	
	Anti-DCX	SC-8066, Santa Cruz Biotechnology// AB5910 Millipore	1:500	
	Anti Zic1/2	Kind gift of Dr. J. Aruga, RIKEN Brain Science Institute	1:500	
	Anti-β Tubulin	MMS-435P, Covance		1:10000
	Anti-Actin	MAB1501, Millipore		1:10000
	Anti-Dab1	U100P, ExAlpha		1:2000
	Anti-ApoER2 (clone 2561)	Kind gift of Dr. J. Herz, University of Texas Southwestern Medical Center, Dallas	1:500	
	Anti-VLDLR (clone 2897)	Kind gift of Dr. J. Herz, University of Texas Southwestern Medical Center, Dallas	1:500	
Secondary	F(ab')$_2$ fragment anti mouse IgG	Jackson ImmunoResearch	1:300	
	Alexa Fluor-488 goat anti-rat	A11006, Life technologies	1:500	
	Alexa Fluor-488 goat anti-mouse	A11029, Life technologies	1:500	
	Alexa Fluor-488 goat anti-rabbit	A11070, Life technologies	1:500	
	Alexa Fluor-568 goat anti-rabbit	A21069, Life technologies	1:500	
	Alexa Fluor-568 goat anti-mouse	A11031, Life technologies	1:500	
	Alexa Fluor-568 goat anti-rat	ab175476, Life technologies	1:500	
	Biotinylated goat anti-rat	BA-9400, Vector	1:200	
	Biotinylated horse anti-goat	BA-9500, Vector	1:200	
	Biotinylated goat anti-mouse	BA-9200, Vector	1:200	
	HRP-labeled secondary atibodies	DAKO		1:2000

Table MM.1.1 | Summary of primary and secondary antibodies used for IHC and WB.

6. Tissue processing and Immunohistochemistry

Embryonic tissue (E12, E16) was fixed by immersion in 4% Paraformaldehide (PFA) in 0.1 M phosphate buffer (PB) for 24h at 4ºC, cryoprotected with PBS-30% sucrose, frozen in 2-methylbutane at -40ºC to -50ºC, coronally sectioned on a cryostat (Leica CM1900) at 15 microns and collected on Superfrost Plus slides (Thermo Scientific). Tissue slides were kept at -20ºC until use. Early and late postnatal (P1 and P15) and adult mice were deeply anaesthetize with ketamine/xylacine at a lethal dose and transcardially perfused for 15-20 minutes with 0.1 M PB containing 4% PFA. After perfusion, the brain was quickly removed from the skull and post-fixed 24h at 4ºC. Afterwards, brains were dehydrated with PBS-30% sucrose, frozen, and coronally sliced on a freezing microtome (Leica SM2010R) at 30 (P15 and P30) or 50 microns (P1 and new-born neurons morphology study) and distributed in either 10 or 6 series, respectively. Tissue was kept in cryoprotective medium (334 mL glycerol 85%, 257 mL ethylene glycol 100x, 409 mL PBS 0.1 M) at -20ºC until use.

For immunodetection of antigens, brain sections were blocked for 2h at Room Temperature (RT) with 10% Normal Goat/Horse Serum (NGS or NHS), 0.2% gelatin, 0.3%/0.05% (adult/postnatal and embryonic tissue respectively) Triton-X100 and $F(ab')_2$ fragment anti-mouse unconjugated IgG (1:300 Jackson ImmunoResearch, 115-007-003) when needed. For BrdU, heat-mediated antigen retrieval was performed for 30 min at 45ºC with hydrochloric acid (HCl) 1M before the blocking. For CTIP2 detection, antigen retrieval was performed for 30min at 80ºC with citrate buffer (10mM Citric Acid, 0.05% Tween 20, pH 6.0).

Primary antibodies were incubated overnight at 4ºC (PBS containing 0.2% gelatine, 5% of NGS/NHS, 0.3%/0.05% Triton-X100, 0.02% Azide and primary antibodies at their respective concentration).

For IHC, inactivation of peroxidases was performed for 15 minutes at room temperature (RT) with PBS containing 3% hydrogen peroxide (H_2O_2) and 10% methanol before blocking. After primary antibody incubation, a sequential incubation with biotinylated secondary antibodies (1:200; 2h at RT) and streptavidin-HRP (1:400; 2h at RT) was performed in PBS containing 0.2% gelatine, 5% of NGS/NHS and 0.3%/0.05% Triton-X100. Bound antibodies were visualized using 3,3'-diaminobenzidine (DAB) and H_2O_2 reaction. The reaction was stopped with PB 0.1M, and when was needed, the slices were mounted on adhesive slides and left drying overnight at RT. Once dried, sections were dehydrated and mounted with Eukit® (UN1866). When needed, nuclei were counterstained with Nissl staining.

For immunofluorescence, sections were incubated for 2h at RT with Alexa Fluor secondary antibodies (1:500) in PBS containing 0.2% gelatine, 5% of NGS/NHS and 0.3%/0.05% Triton-X100 and then counterstained with Hoechst for nuclei detection. Postnanatal and adult sections were then mounted in Mowiol, and stored at −20°C. Embryonic sections were directly covered with coverslip mounting solution Mowiol and stored at −20°C.

7. Western Blot (WB)

Mice were sacrificed by decapitation and the brain was immediately removed from the skull. Then brains were dissected into two hemispheres and the cerebellum, frozen in liquid nitrogen and stored at -80ºC until use. For sample preparation, forebrains were homogenized in lysis buffer (Hepes 50mM pH 7.5, 150mM NaCl, 1.5mM MgCl2, 1mM EGTA, 10% glycerol, 1% TritonX-100) with protease and phosphatase inhibitors (Roche Complete Mini protease inhibitor cocktail, 10mM NaF, 200µM Na2H2P2O7, 10mM Na3VO4), using a Polytron homogenizer. Next, samples were sonicated (80%A, 15half cycles) and centrifuged at maximum speed for 20 minutes at 4ºC to remove insoluble debris. Supernatant was collected and stored at -20ºC until use. Protein concentration was estimated with BCA protein assay (Pierce, 23225) according to the manufacturer protocol. Around 40 µg of protein were prepared in Loading Buffer (0.5mM Tris-HCl pH 6.8, 2.15M β-mercaptoethanol, 10% SDS, 30% glycerol and 0.012% bromophenol blue). Samples were resolved by 6% SDS-polyacrylamide gels (1.5M Tris pH 8.8, 30% acrylamide/bis-acrylamide, 10% SDS, 10% ammonium persulfate, and N,N,N',N'-tetramethyl-ethylenadiamine) using an eletrophoresis apparatus (Bio-Rad) and transferred onto nitrocellulose membranes. Membranes were then blocked for 2h at RT in TBST (Tris 10mM pH7.4, NaCl 140mM, 0.1% Tween 20) containing 5% non-fat milk. Afterwards, membranes were incubated with the primary antibodies in TBST overnight at 4ºC. After incubation with secondary HRP-labeled antibodies for 1h at RT (1:2000, Pierce, 1858413 in TBST-5% non-fat milk), membranes were developed with the ECL system (GE healthcare, RPN2232). GelPro32 (Media Cybernetics) software was used for WB quantification.

8. BrdU Administration

BrdU was intraperitoneally administered at a dose of 50 mg/kg from a 5mg/mL stock prepared in PBS.

8.1. Embryonic administration

Pregnant females from timed mating crossings were given two pulses of BrdU (50mg/Kg; 2h interval between injections) at Embryonic (E) day 12 and 15.5 to label the lower and upper cortical layer cells, respectively. The day of the vaginal plug was considered as E0. The resulting offspring was sacrificed at postnatal day (P) 30 and tissue was collected for IHC as previously described in the methods section.

For cell birthdating analysis in Cre fR/fR mice, timed mating pregnant females were given 3 pulses of BrdU (50mg/Kg) at E15, E15.5 and E16, to ensure the labeling of upper cortical layer cells. Pups from the offspring were sacrificed after tamoxifen injections at P15 (when tamoxifen was injected at P1-P3) or P60 (tamoxifen injections at P20) and tissue was collected and processed for immunohistochemistry as previously described in the methods section. In addition, to prove that the miss-positioned cells present in layer I were not newly born after TMX inactivation, mice were injected with TAM for 3 consecutive days at P60, then injected with BrdU twice a day (6h interval) on days 4, 8 and 12 post-inactivation and sacrificed around P120.

8.2. Postnatal administration

Pups were injected with BrdU at P10 and P11 and were later sacrificed at P30 and tissue was collected for immunohistochemistry as previously described in the methods section.

8.3. Proliferation/Neurogenesis analysis

For proliferation analysis, 2 pulses of BrdU were administered with a 2 hour interval 2 weeks after tamoxifen administration. Mice were perfused 24 hours after injection and tissue was collected for immunohistochemistry as previously described in the methods section.

For neurogenesis analysis 2 pulses of BrdU were administered per day (with a 6 hour) 4, 8, and 12 days after tamoxifen injection. Mice were perfused 2 months after BrdU injection and tissue was collected for immunohistochemistry as previously described in the methods section.

9. Electroporation

Mouse embryos were electroporated *in utero* at E14 as previously described (Cardenas A. et al., 2018). Briefly, pregnant females were deeply anesthetized with isoflurane. The uterine horns were exposed and GFP (plasmid) under the control of CAG promotor was injected into the ventricular zone of the embryos using pulled glass micropipettes. Square electric pulses (28-35V, 50ms on – 950ms off, 5 pulses) were applied with an electric stimulator (Cuy21EDIT Bex C., LTD) using round electrodes (CUY650P5, Nepa Gene). At P1 pups were perfused with 4% PFA and the brain was quickly removed and post-fixed for 24h at 4ºC. The tissue was then cryoprotected with PBS-30% sucrose, frozen and sliced at 50 microns in a Leica cryostat. Slides were kept at -20ºC until use.

10. Generation of GFP-expressing retrovirus

Retrovirus (RVs) were produced by transient infection of 293T cells as previously described (Zhao et. all, 2006). Briefly, a total of 6 x 10^6 cells were seeded into 10 cm plates with 10mL of culture medium (DMEM, 10% FBS, non-essential amino acids, Na pyruvate, Penicillin, Streptomycin, Glutamine). A day later, cells were tranfected by adding a volume of 2mL of transfection mix: 10 µg of plasmid PSD95-GFP, 7.5 µg of plasmid pCLeco for Maloney virus, 2.5 µg of VSVg, 250 mM of CaCl2 in H_2O plus 1mL of 2X HBSS (50mM HEPES pH 7.5, 10mM KCl, 12mM Dextrose, 280 mM NaCl, 1.5 mM Na_2HPO_4 in H_2O) pH 7.05. 4 hours after transfection, cells were washed with PBS and replaced with 10 mL of culture medium. Three days after, cell culture containing virus was collected and concentrated by ultracentrifugation at 26000rmp at 4ºC to working titles of 1 x 10^7 – 1 x 10^8 pfu/mL.

11. Retroviral injection

For the new-born neurons morphology analysis, GFP-encoding retrovirus were injected in the DG of P30-35 mice as previously described (Teixeira *et al.*, 2012) (Praag *et al.*, 2002).

Briefly, mice were anaesthetized with ketamine/xylacine at a dose of 100µL/30g and placed on the stereotaxic device. The scalp was incised and small holes were drilled on the skull. The coordinates to target the DG were relative to bregma in the anteroposterior, lateral and dorsoventral planes as follows: -0.2, ±0.16, -0.22 (in mm). Each DG was injected with 1.5 µL of GFP-encoding RV solution at a rate of 12 µL/hour with a glass micropipette.The micropipettes were generated using a Puller (Flaming/Brown Micropippette Puller, Sutter instrument). After the injection, the micropipette was left in place for 5 additional minutes to avoid diffusion. The scalp was sutured and the animals were placed in the recovery cage until completely awaken before returned to their own cage. At different time points after surgery (2,3 or 8 weeks), Reelin supression was induced and 4 weeks after TAM injection animals were sacrificed and tissue was collected for immunohistochemistry as previously described in the methods section.

12. Image acquisition and data analysis

Unless otherwise stated, bright field and fluorescent images were acquired with an Olympus D72 camera attached to a Nikon's Eclipse E600 microscope. General image processing and quantification was done with FIJI (Image J, NIH-freelydownloadable at http://fiji.sc/Fiji) (Schindelin et al. 2012). Reelin bright field images were also acquired using a NanoZoomer 2.0-HT (Hamamatsu Photonics) and processed with NDP.view2. Image acquisition and quantifications were done blindly to the mice genotype for all the experiments.

12.1. Analysis of cortical distribution

To determine the layer distribution of cells in the cortex images from the Primary Somatosensory Barrel Field (SBF1) were taken using either a Leica TCS SP2 or Leica TCS SP5 Confocal Laser Scaning Microscope and the 10x, 20x and 40x oil-immersion objectives. For each mouse, at least 9 Regions of Interest (ROIs) comprehending the whole length of the cortex (strip from the upper edge of the marginal zone to the corpus callosum) were defined using the maximum intensity Z-projection of the acquired confocal images. Those cortical strips were then divided in 10 identical bins using a macro created in Image J (FIJI) and the number of cells in each bin was manually quantified. The mean number of cells in each bin was calculated for each animal and expressed as a percentage of the total number of cells *per* strip. For the BrdU counts, images were acquired with a Nikon's Eclipse E600 microscope and processed and quantified as described above.

To obtain the profile plots, representative images were selected of each genotype and the Plot profile tool of Image J was used to generate them.

12.2. Analysis of hippocampal width

With the aim of determine the thickness of the layered hippocampal structures CA1 and DG, images were acquired with a Nikon's Eclipse E600 microscope. The total width of each

hippocampus was determined by the mean of 10 differents measures, covering the entire structure. At least 3 images were measured *per* animal. Representative images were taken with either a Nikon E600 microscope or a Olympus D72 camera.

12.3. Analysis of hippocampus cell dispersion

In order to determine the cell dispersion in the hippocampus, the distribution of BrdU positive cells in the granular cell layer of the dentate gyrus (DG; BrdU at E12 and E15.5) and the CA1 (BrdU at E15.5 and p10-11) was analyzed. The cell layers were virtually subdivided in three (upper, medial and inner layer) and the number of BrdU positive cells in each position was counted. In the DG, the number of BrdU positive cells located in the hilus was also counted.

12.4. Analysis of proliferation

BrdU+ cells were quantified live with an Olypmus CX31 microscope and the 40x objective. For each mouse, the total number of BrdU positive cells was measured in at least 3 DG in the infrapyramidal blade, the suprapyramidal blade and the hilus separately. The mean number of BrdU+ cells in each DG was normalized by the total length of the DG and calculated for each animal. Representative images were taken with a Nikon E600 microscope and an Olympus D72 camera.

12.5. Analysis of DG cell dispersion

To analyse the DG cell dispersion and cell miss-location, Prox 1 (granule cell layer marker) images were acquired with a Leica TCS SP2 Confocal Laser Scanning Microscope. For each mouse 5-7 DG where analysed using the maximum intensity Z-projection of the acquired confocal images to delineate the upper and lower blades of the DG. The area of the blades of the DG as well as the number of cells located outside the blades (in the hilus and the molecular layer) were counted.

12.6. Analysis of immature neurons

To analyse the number of immature neurons, the number of doublecortin (DCX) positve cells were quantified live with an Olypmus CX31 microscope and the 40x objective. The total number of DCX positive cells was manually quantified in the supra and infra granule cell layers as well as in the hilus separately in at least 3 DG *per* animal. The mean number of DCX+ cells in each DG was normalized by the total length of the DG and calculated for each animal. Representative images were taken with a Nikon E600 microscope and Olympus D72 camera.

12.7. Analysis of mature neurons

To unravel the total number of mature neurons fluorescence images were acquired using a Leica TCS SP5 confocal microscope and the 40x magnification. Using the ImageJ software, the number and location of double labelled cells (BrdU+/NeuN+) was also analysed in at least 3 DG *per* animal. Migration of the newly generated neurons in the DG was also analysed by measuring the distance migrated from the SGZ.

12.8. Analysis of new-born neurons morphology

Images collected using a Leica TCS SP5 confocal microscope and the 20x magnification were analysed using the ImageJ software. The total number of apical and basal dendrites of at least 20 GFP labelled new-born neurons *per* animal was counted. Only neurons with clearly visible dendritic tree were taken into account. Location of the new-born neurons in the DG was also analysed by measuring the distance migrated from the SGZ.

12.9. Misslocated Purkinje cells

To determine the layer distribution of Purkinje cells in the cerebellum, images were taken using a Leica TCS SP2 Confocal Laser Scanning Microscope. For each mouse 3-4 cerebellums were analysed using the maximum intensity Z-projection of the acquired confocal images. For the analysis, first the Zic1/2 staining (granular cells) was used to delineate the limit between the granular and molecular layers. Next, the number of Purkinje cells somas (Calbindin+) was counted distinguishing between the ones properly positioned, that formed a 20µm width monolayer between de granule and the molecular layers, and the miss-positioned ones that were clearly outside the monolayer. The number of correct and miss-positioned cells was calculated as a percentage of the total number of cells counted.

13. Statistical Analysis

All statistical analysis were performed using GraphPad Prism 6.0 Software. Data was analyzed using either two-tailed unpaired t-test or two-way ANOVA with multiple comparison post-hoc tests. All the data is presented as mean $\pm$ sem (standard error of the mean) and sample size is detailed in each figure. Statistical significance was set at $p<0.05$. All the quantifications were performed blindly.

RESULTS

1. Role of Reelin expressed by Calretinin positive cells in corticogenesis and hippocampus formation.

1.1. Generation and validation of a constitutive Cajal-Retzius Reelin deficient mouse model.

To determine the role of Reelin expressed by CRC in corticogenesis and hippocampus formation, we generated the CR fR/fR line by crossing the floxed Reelin mice (fR/fR) with Calb2-Cre mice, expressing Cre recombinase constitutively under the control of the Calretinin promoter. In this colony we expected to supress Reelin in Calretinin expressing cells such as CRC and some Calretinin positive interneurons.

The general appearance of mice deficient for Reelin from Calretinin positive cells (CR fR/fR) was normal, they were viable, did not exhibit cerebellar ataxia and motor problems and no significant differences were found in the body weight of P30 mice (males and females) between controls fR/fR (15,74g ± 0,8363) and CR fR/fR mice (17,38g ± 0,7952). Data represents mean ± s.e.m, Unpaired two-tailed Student's t-test (t= 1.364 df= 10 p= 0.2025, n.s. n=7 fR/fR and 5 CR fR/fR).

In order to analyse the disappearance of Reelin from Calretinin positive cells, we first compared the general pattern of expression of Reelin protein in P30 controls (fR/fR) and CR fR/fR mice **(Figure R.1.1)**. At this age, secreted Reelin protein is broadly expressed throughout the brain mainly by cortical and hippocampal GABAergic interneurons (Alcantara *et al.*, 1998). Immunohistochemistry against Reelin in P30 mice confirmed generally unaltered Reelin distribution in control fR/fR and CR fR/fR brains, with a strong signal detected in layer II of the piriform and enthorinal cortical areas **(**Arrowheads **Figure R.1.1.a)**. However, a more detailed analysis revealed a slightly lower density of Reelin expressing cells in the hippocampus of CR fR/fR compared to control mice, including the so and slm **(Figure R.1.1.b** and **Figure R.1.1.c** left**).** In the neocortex, a shift upward in the distribution of layer V-VI Reelin expressing cells was observed in CR fR/fR mice compared to fR/fR mice, suggesting an altered distribution of Reelin-expressing cells **(Figure R.1.1.b** and **Figure R.1.1.c** center**)**. On the other hand, histological analysis of the cerebellar cortices demonstrated that both CR fR/fR and controls mice has a highly foliated cerebellum without any apparent structural malformation **(Figure R.1.1.b** and **Figure R.1.1.c** right**)**. In addition, a decrease in the levels of Reelin signaling in CR fR/fR mice was observed in other brains regions including the olfactory area, the lateral septum, the caudate-putamen septum and the nucleus accumbens.

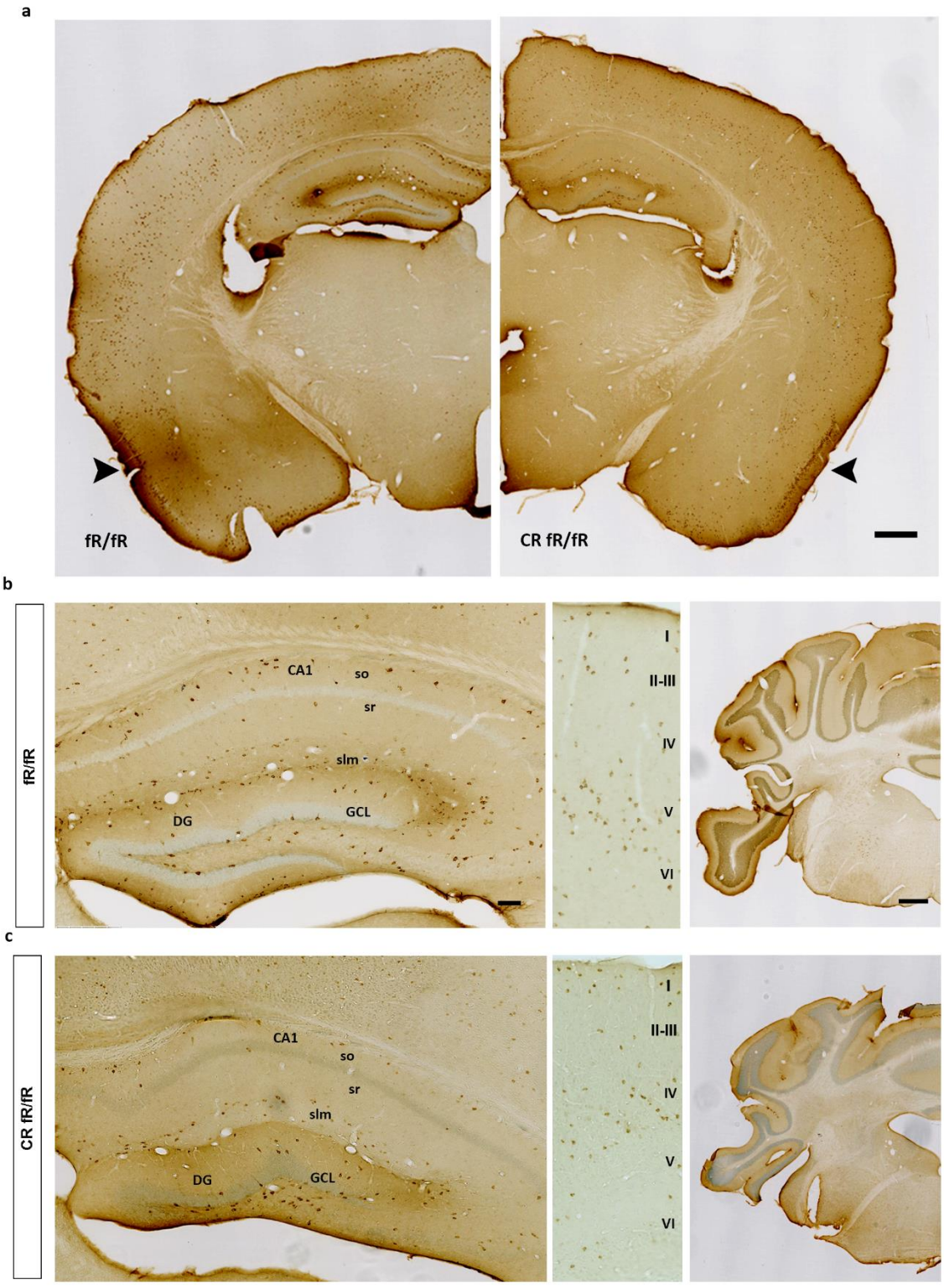

Figure R.1.1. | Pattern of expression of Reelin protein in CR fR/fR mice. **a-c**, Immunohistochemical detection of Reelin protein in coronal sections of P30 mice. **a**, Representative photomicrograph showing Reelin cortical distribution in the whole brain (Scale bar= 500 µm) in the presence (fR/fR, left) and absence of Reelin from Calretinin+ cells (CR fR/fR, right). Arrowheads pointed to layer II piriform cortex. **b**, **c**, Representative images of Reelin immunostaining in control animals (b) and in CR fR/fR mice (c), in the hippocampus (left, scale bar= 250 µm), in the primary somatosensory cortex (center, scale bar=), and in the cerebellum (right, scale bar=500 µm). CA1, Cornus Ammonis 1; so, stratum oriens; sr,

stratum radiatum; slm, stratum lacunosum moleculare; DG, Dentate gyrus; GCL, granule cell layer; I, Cortical Layer I, II-III, Layers II-III; IV, Layer IV; V, Layer V; VI, and Layer VI.

To further characterize Reelin protein levels in our model, a timecourse experiment was conducted on dissected forebrain lysates (including cortex and hippocampus) at E16, P1 and P30. Protein extracts were prepared and equal amounts of total protein were analyzed by Western blotting with antibodies against Reelin, using tubulin as a loading control. Blots showed a general decrease in Reelin levels in the full-length form (410 KDa bands) and its cleavage products (320 KDa and 180KDa bands) in CR fR/fR when compared to fR/fR mice at all the stages analysed **(Figure R.1.2.a**, **Figure R.1.2.b** and **Figure R.1.2.c)**.

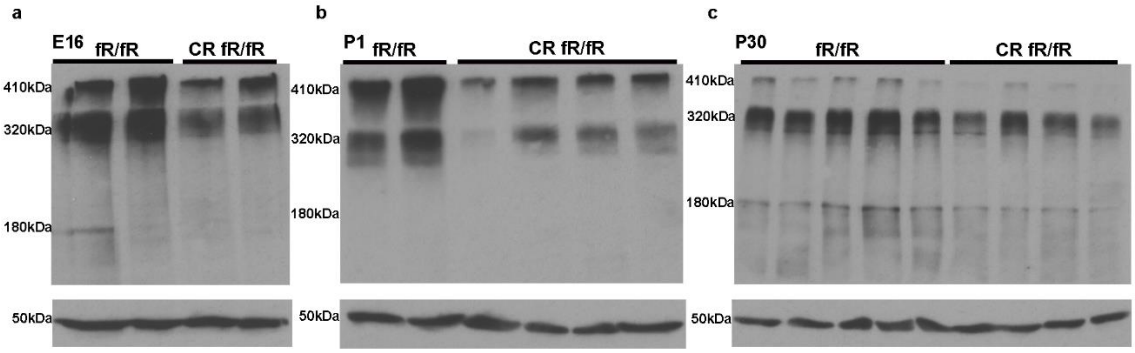

Figure R.1.2. | Reelin protein levels in CR fR/fR mice. a-c. Western Blot analysis of extracts from cerebral cortex and hippocampus showing the levels of Reelin protein (top) in controls fR/fR and CR fR/fR mice at E16 (a), P1 (b) and P30 (c). Expression of β-tubulin was used as loading control (bottom).

To decipher if Reelin has effectively disappeared from Calretinin positive cells in cortical regions, double immunofluorescence of Reelin and Calretinin was performed at E12, E16, P1 and P30 stages and colocalization was analysed **(Figure R.1.3.** and **Figure R.1.4.).** Calretinin has been widely used as a marker of CRC in the developing neocortex (Ha *et al.*, 2017). At E12 when the PP is already formed, postmitotic neurons start to migrate arranged in the CP that will divide the ancient PP into a superficial layer, the MZ and an inner layer, the SP (Santana & Marzolo, 2017). From this moment, CRC on the MZ start to synthesize and secrete the extracellular matrix protein Reelin (Alcantara *et al.*, 1998). Analysis of cortical regions in E12 mice demonstrated a expression of Reelin in Calretinin positive cells in control fR/fR but not in CR fR/fR mice **(Figure R.1.3.a)**. At E16, control fR/fR mice also exhibited normal Reelin expression in CRC in the MZ, whereas none of the CRC identified by Calretinin staining dysplayed Reelin staining in CR fR/fR mice **(Figure R.1.3.b)**.

In the first postnatal week, CRC start to disappear by apoptosis, giving way to a cell devoid layer I in the neocortex (Soriano & Del Rio, 2005). At P1, Reelin-expressing CRC were still visible in control fR/fR mice, but not in CR fR/fR mice **(Figure R.1.3.c).**

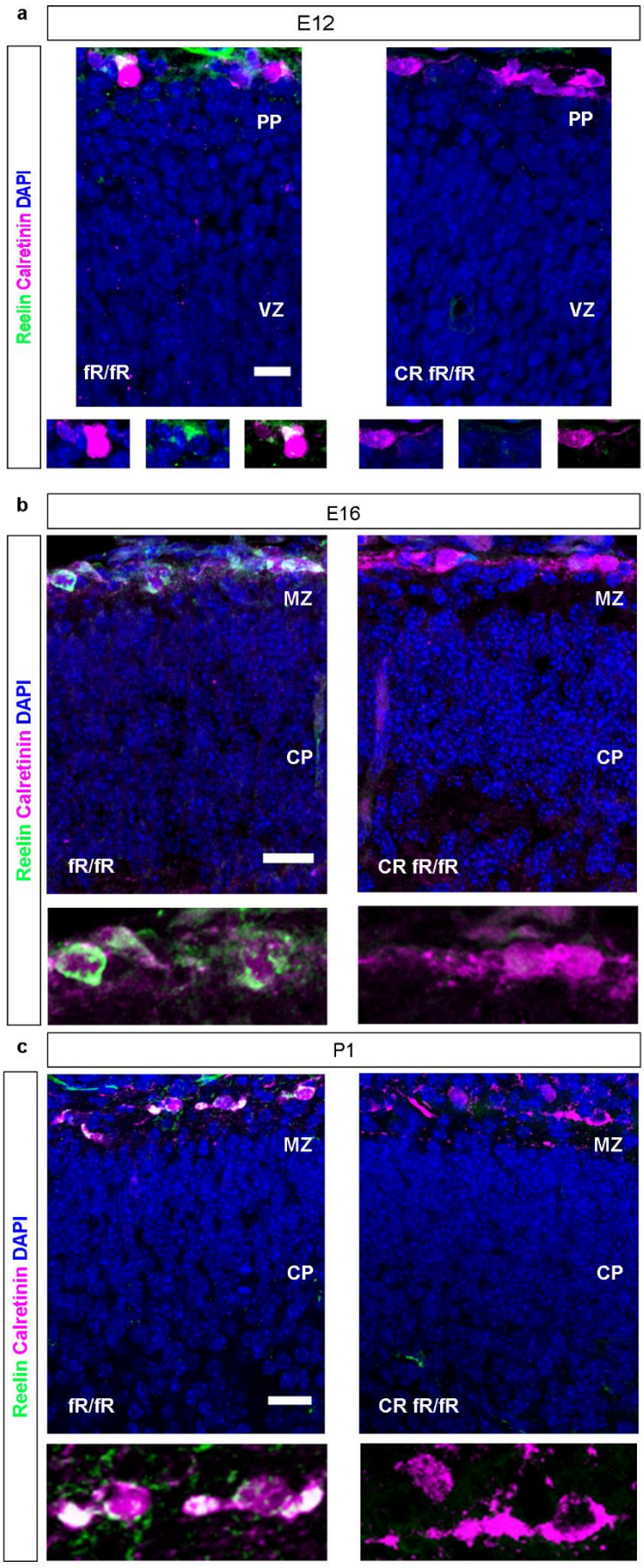

Figure R.1.3. | Reelin expression in Calretinin positive cells in the developing cortex. a, b, c, Double IHC of Reelin+ (green) and Calretinin+ cells (magenta) at E12 (**a**, scale bar=15µm), E16 (**b**, scale bar=20µm) and P1 (**d,** scale bar=20 µm) in the presence (fR/fR, left) and absence (CR fR/fR, right) of Reelin from Calretinin positive cells. Magnification of Marginal Zone (MZ) cells (**a**, **b, c** bottom). PP, Preplate; VZ, Ventricular zone; CP, Cortical Plate.

By the time that CRC undergo programmed cell death, Reelin begins to be expressed by GABAergic interneurons, including some Calretinin positive interneurons that are widely distributed throughout the cortex (Soriano & Del Rio, 2005)(Alcantara *et al.*, 1998). Despetite the presence of Reelin expressing cells in CR fR/fR cortices, analysis of Reelin-Calretinin double labelled interneurons were detected in control fR/fR mice, but not in CR fR/fR mice confirming the selective supression of Reelin only in Calretinin positive cells in these mice **(Figure R.1.4.)**. No major differences in the density of Reelin positive cells were observed between both groups.

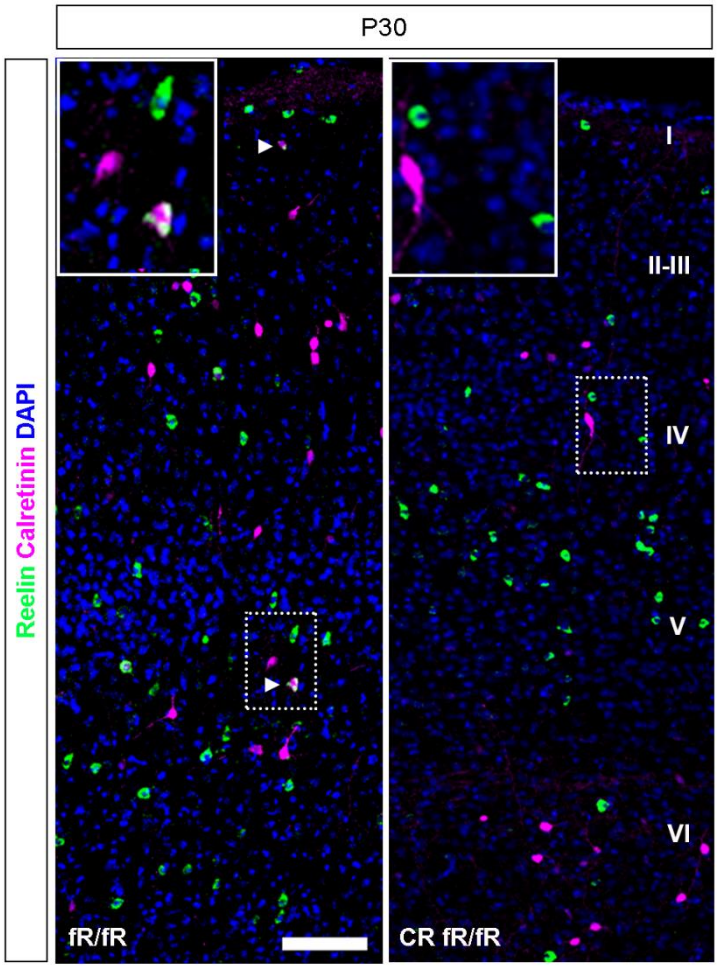

Figure R.1.4. | Reelin expression in Calretinin positive cells in the adult primary somatosensory cortex. Double IHC of Reelin+ (green) and Calretinin+ cells (magenta) at P30 in the presence (fR/fR, left) and absence (CR fR/fR, right) of Reelin from Calretinin positive cells. ▷ double labelled cells, scale bar=100 µm. Magnifications at the top of each image. I, Cortical Layer I; II-III, Layers II-III; IV, Layer IV; V, Layer V; VI, Layer VI.

In addition to the study of Reelin expression in Calretinin positive cells during corticogenesis, analysis of Reelin-expressing Calretinin positive cells during the formation of the hippocampus was performed at different stages **(Figure R.1.5)**. At P1, the majority of hippocampal CRC in control fR/fR pups, identified by Calretinin-immunostining, co-expressed Reelin **(Figure R.1.5.a**, left**)**. These Reelin-expressing CRC were densely packed at the ML and slm, in close proximity to the hippocampal fissure. In addition, there were some Reelin-/Calretinin+ neurons, mainly in the hilus, corresponding to immature granule cells and other cell types. In CR fR/fR pups, hippocampal CRC completely lacked Reelin expression. In fact, the

dense band of Reelin+/Calretinin+ cells seen at the ML/slm interphase in control mice was almost completely disappeared in CR fR/fR mice **(Figure R.1.5.a**, right**)**. Even though, there were Reelin-positive neurons remaining near the hippocampal fissure and into the hilus, likely corresponding to Calretinin- GABAergic interneurons. An interesting feature seen at these stages was that the characteristic, highly laminated distribution of CRC in the hippocampus (with a marked enlargement at the CA3 region) was severely disrupted in CR fR/fR mice, in which CRC were less homogeneously distributed, sometimes forming ectopic mases at the GCL/hilus. These findings suggest that the lack of Reelin in Calretinin positive cells could alter the lamination pattern of CRC in the hippocampus.

At later stages, from P15 onward, the remnants of hippocampal CRC in the hippocampal fissure still express Reelin, although, the major source of Reelin protein comes from GABAergic interneurons distributed throughout the hippocampal layers (Alcantara *et al.*, 1998). The analysis of P30 hippocampus showed that whereas some Reelin+/Calretinin+ cells were still present in the hippocampal fisure, in the supra and infra molecular layer **(Figure R.1.5.b, left)** as well as in the CA region **(Figure R.1.5.c, left)** of control fR/fR mice, no co-localization was observed in CR fR/fR hippocampus **(Figure R.1.5.b** and **Figure R.1.5.c**, right**)**. In addition, Reelin protein was also expressed by a large number of Calretinin- neurons in different layers of the hippocampus in both control and CR fR/fR mice, corresponding mainly to Calretinin- GABAergic interneurons. Furthermore, in CR fR/fR mice, Calretinin positive granule neurons failed to form a compact granular layer in the inner part of the pyramidal blades and some of them were misslocated, invading either the hilus or the granular layer and showing a less packed structure **(Figure R.1.5.b)**.

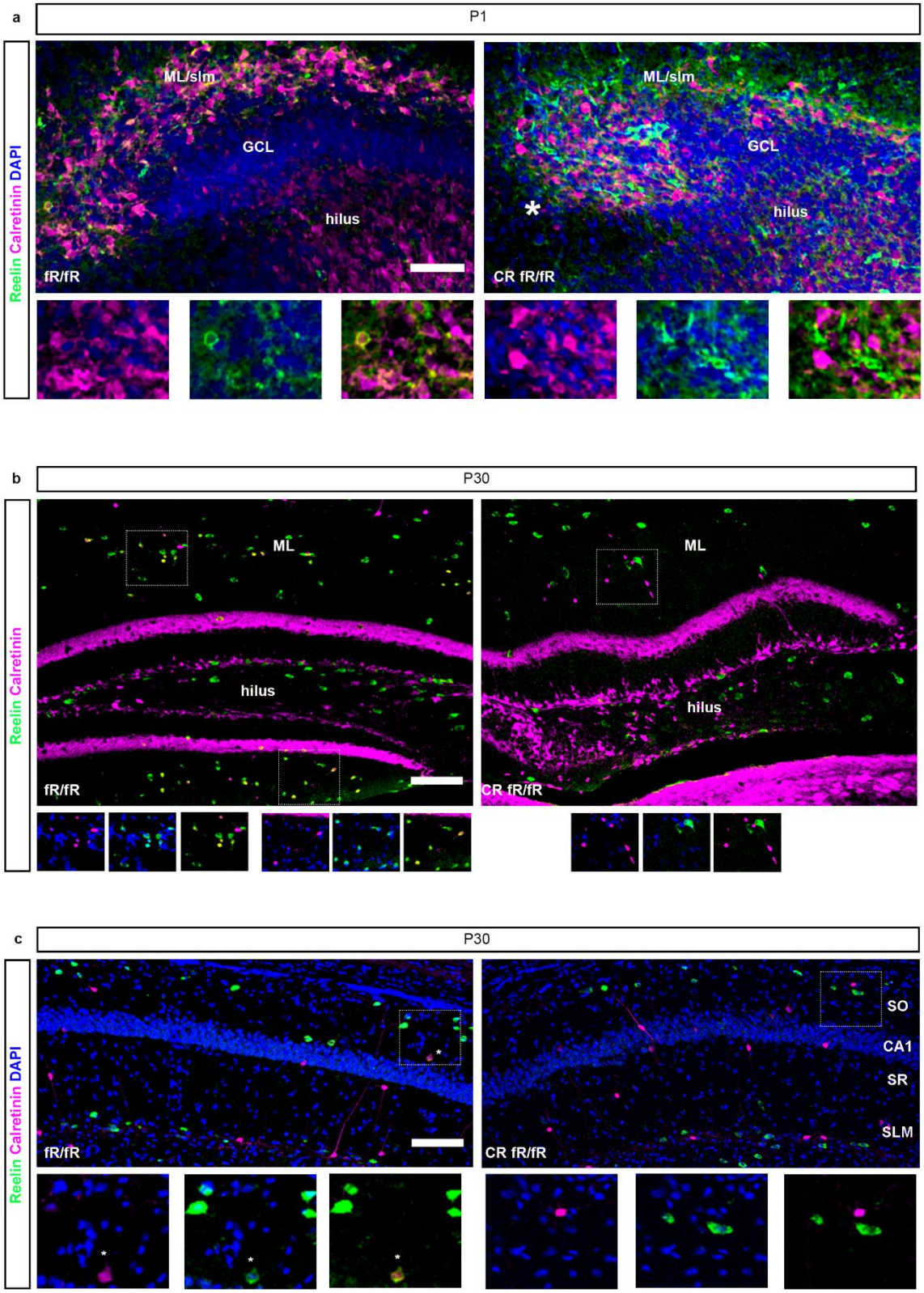

Figure R.1.5. | Reelin expression during hippocampus formation. **a-c**, Hippocampus double IHC of Reelin+ (green) and Calretinin+ cells (magenta) at P1 (**a**, * pointed to CA3 region, scale bar= 50µm) and P30 (**b,** Dentate Gyrus; **c,** Cornus Ammonis, * double labelled cells; scale bar= 100µm) in the presence (fR/fR, left) and absence of Reelin from Calretinin+ cells (CR fR/fR, right). Magnifications at the bottom of each image. ML, molecular layer; slm, stratum lacunosum moleculare; GCL, granule cell layer; so, stratum oriens; sr, stratum radiatum.

1.2. Reelin deficiency in Calretinin positive cells alters cortical distribution without *reeler*-like layering inversion.

After PP splitting, early-born neurons start radial migration towards their final position in the lower part of the developing cortex. From this moment on, younger neurons must bypass the deeper layers of early-generated neurons to more superficial ones. At this stage, Reelin signaling has been shown to be essential for the proper layering of the cortex (Hirota & Nakajima, 2017).

Taking advantage of the CR fR/fR model, we analysed the specific contribution of Reelin expressed by Calretinin positive cells in the layering of the cortex, centered upon the primary somatosensory cortex (S1BF) due to its easy identification. For this purprose we performed immunostainings against layer specific markers at different developmental stages. First, CTIP2 immunostaining was performed in order to label early-born neocortical neurons, mainly layer IV to VI of the adult cortex. Second, we used Cux1 antibody as a marker of cortical upper layers neurons. Cux1 is an homeobox transcription factor, and its expression pattern has been shown to define the layers II-III and IV in the adult mouse cerebral cortex (Nieto et. All, 2004) (Molyneaux et al., 2007).

At E16, the majority of early generated neurons reach their final position in the lower part of the CP, while late-generated neurons, destined to upper layers, are still migrating (Zhou *et al.*, 2007). At this time, the control fR/fR embryos analyzed presented two different well defined layers at the neocortex, with CTIP2 neurons highly agrupated at the bottom part of the CP, and Cux1 neurons occupying mainly the upper part of the CP, just under the MZ. Some Cux1 positive neurons were present in the IZ, presumably because they were still migrating **(Figure R.1.6.a).** In contrast, in CR fR/fR embryos layers were not as defined as in controls. Cux1 neurons were widely distributed through all the cortical layers, even invading the MZ. In addition to Cux1 positive cells, CTIP2 labeled neurons showed a different distribution compared to control littermates and were concentrated into the upper part of the CP **(Figure R.1.6.b).** Nonetheless, the cortical distribution of CR fR/fR mice was different from the inverted layering present in *reeler* mice, suggesting that some of the late-born neurons were able to migrate past layers of earlier-born neurons and that preplate splitting might happen normally in CR fR/fR mice.

The analysis of cortex lamination at P1 demonstrated that the altered phenotype still persisted in CR fR/fR mice at this stage. In control fR/fR mice, Cux1 positive cells were placed just below the MZ, in the upper part of the CP **(Figure R.1.6.c)**. Conversely, in CR fR/fR mice a number of Cux1 neurons failed to migrate and remained into the IZ of the neocortex, displaying a marked disorganization of the upper neocortical neurons throughout the cortex **(Figure R.1.6.d** and **Figure R.1.6.f)**. In addition, although invasion of MZ was no longer visible at this stage, an upward shift of Cux1+ neurons was observed in the upper part of the neocortex. Quantification of Cux1 positive neurons in layers II-III was not posibble due to the high density of cells accumulated. Therefore, we plotted the mean Cux1 intensity in the area between the MZ and the layer IV. In CR fR/fR the profile showed a narrowed curve in the area between layers II-III compared to controls, as well as a peak on Cux1 intensity in the lower part

of the cortex **(Figure R.1.6.e)**. Analysis of early-born neurons distribution at this point also evidenced an altered location of those cells in CR fR/fR mice. Whereas in control fR/fR mice CTIP2 neurons were located at the bottom half of the CP **(Figure R.1.6.c)**, in CR fR/fR mice lower layer neurons were mainly present in the lower part of the CP, but some of them remained accumulated below CP, in close proximity to the IZ **(Figure R.1.6.d** and **Figure R.1.6.g)**.

Thus, these findings point to a role of Reelin expressed by CRC in the distribution of cortical neurons, however the lack of layer inversion suggested the these effects are independent of preplate splitting.

The main lamination defects observed in CR fR/fR mice at embryonic and early postanatal stages were also present at P30 in the somatosensory cortices **(Figure R.1.7)**. To sum, both in control fR/fR and in CR fR/fR mice, two well differenciated bands of Cux1 and CTIP2 neurons were observed. However, subsets of Cux1 positive cells undermigrated and formed ectopic intermittent clusters in deeper layers matching areas devoid of CTIP2 positive cells in CR fR/fR mice. The observed ectopic masses of Cux1+ neurons were particulary frequent in the region of the somatosensory cortex where barrel columns are formed **(Figure R.1.7.a** and **Figure R.1.7.b)**. Secondly, analysis of early-born neurons distribution using CTIP2 antibody evidenced an upward shift in the cortical distribution of lower layer neurons in CR fR/fR compared to fR/fR controls **(Figure R.1.7.c)**.

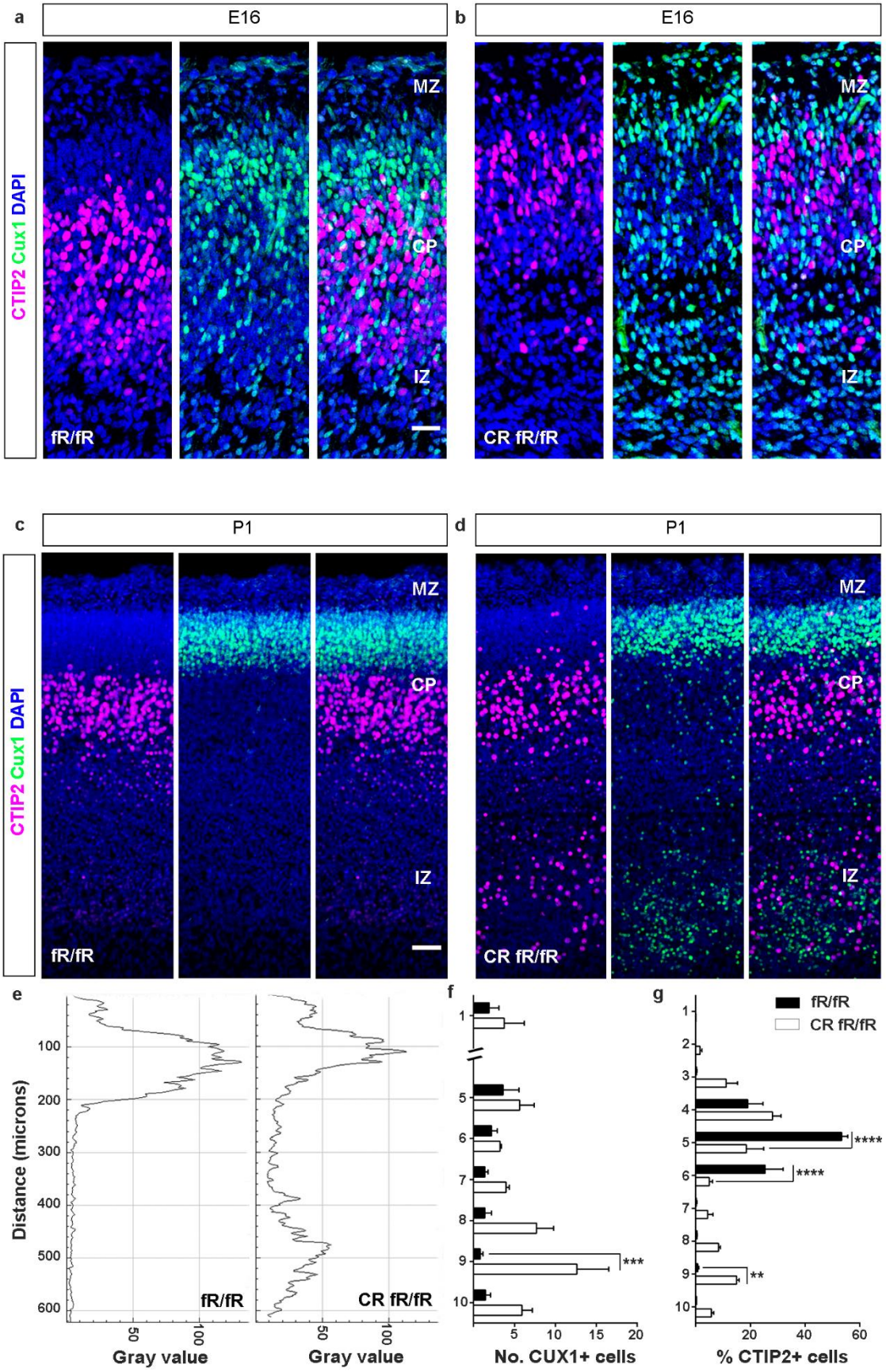
a
E16
b
E16
CTIP2 Cux1 DAPI
MZ
CP
IZ
fR/fR
CR fR/fR
c
P1
d
P1
e
Distance (microns)
100
200
300
400
500
600
fR/fR
CR fR/fR
50
100
Gray value
f
1
5
6
7
8
9
10
5
10
15
20
No. CUX1+ cells
***
g
fR/fR
CR fR/fR
1
2
3
4
5
6
7
8
9
10
****
****
**
20
40
60
% CTIP2+ cells

Figure R.1.6. | Cortical layer distribution at E16 and P1 in the absence of Reelin from Cajal-Retzius cells. a-d, Representative confocal images depicting the cortical distribution of Cux1+ (green, upper layers) and CTIP2+ cells (magenta, lower layers) at E16 (**a-b,** scale bar= 25µm) and P1 (**c-d**, scale bar= 50µm) in the presence (fR/fR; **a, c**) and absence (CR fR/fR; **b, d**) of Reelin from Cajal-Retzius cells. **e**, Representative profile of Cux1 intensity (Gray value) over distance (from MZ to VI) in P1 control (left) and Reelin deficient (right) mice. **f**, Quantification of the number of Cux1+ cells *per* bin at P1. Since the region between the MZ and the CP (corresponding to bins 2 to 4) at this particular stage was too densely populated to be counted, only bins 1 and 5 to 10 were counted and represented as absolute number of cells/bin (data represents mean ± s.e.m; Bin x Genotype Interaction $F(6, 28)= 2.648$ $p=0.0367$; Two-way ANOVA with Bonferroni post hoc test; $^{***}P < 0.001$, n= 3 mice per genotype). **g**, Quantification of the percentage of CTIP2+ cells *per* bin at P1 (data represents mean ± s.e.m; Bin x Genotype Interaction $F(9, 40)= 15.54$ $p<0.0001$; Two-way ANOVA with Bonferroni post hoc test; $^{**}P < 0.01$, $^{****}P < 0.0001$, n= 3 mice per genotype) .MZ, Marginal Zone; CP, Cortical Plate; IZ, Inner Zone; VI, Layer VI.

To further characterize the origen of the cortical misspositioning, birth-dating experiments using 5-bromodeoxyuridine (BrdU) pulses were performed. BrdU, is a synthetic nucleoside, analogue of thymidine, that is incorporated in the newly formed DNA chain in dividing cells, and thus allows the observation of the migratory behaviour of newly born neurons at the time of injection. Embryos were labeled with BrdU at E12 or E15.5 and analyzed at P30. As expected, in control fR/fR mice these BrdU pulses labelled different neuronal populations that were segregated in layers V-VI and II-III, respectively. In contrast, in CR fR/fR mice, the distribution of E12 born neurons was wider compared to controls **(Figure R.1.7.d** and **Figure R.1.7.e).** In the case of BrdU+ neurons injected at E15.5, later born neurons of CR fR/fR brains appeared distributed into two differentiated bands corresponding to layers II-III and layers VI-V **(Figure R.1.7.f** and **Figure R.1.7.g)**. These results that were in line with the observations from immunostainings against layer specific markers, demonstrated a role of Reelin expressed by Calretinin positive cells in migration itself, more than a switch in the type of transcription factor expressed by these cells.

All together, these findings suggest that the lack of Reelin in Calretinin positive cells leads to a permanent dispersion and misspositioning of cortical neurons in which the most prominent characteristic was the presence of a large number of late-generated neurons (CUX1 positive cells) in deeper cortical layers that were unable to migrate in a inside-out manner. In addition, the data shows a transient aberrant distribution of CUX1+ neurons in layer I at E16 which is corrected at later stages when Reelin protein starts to by expressed by GABAergic interneurons.

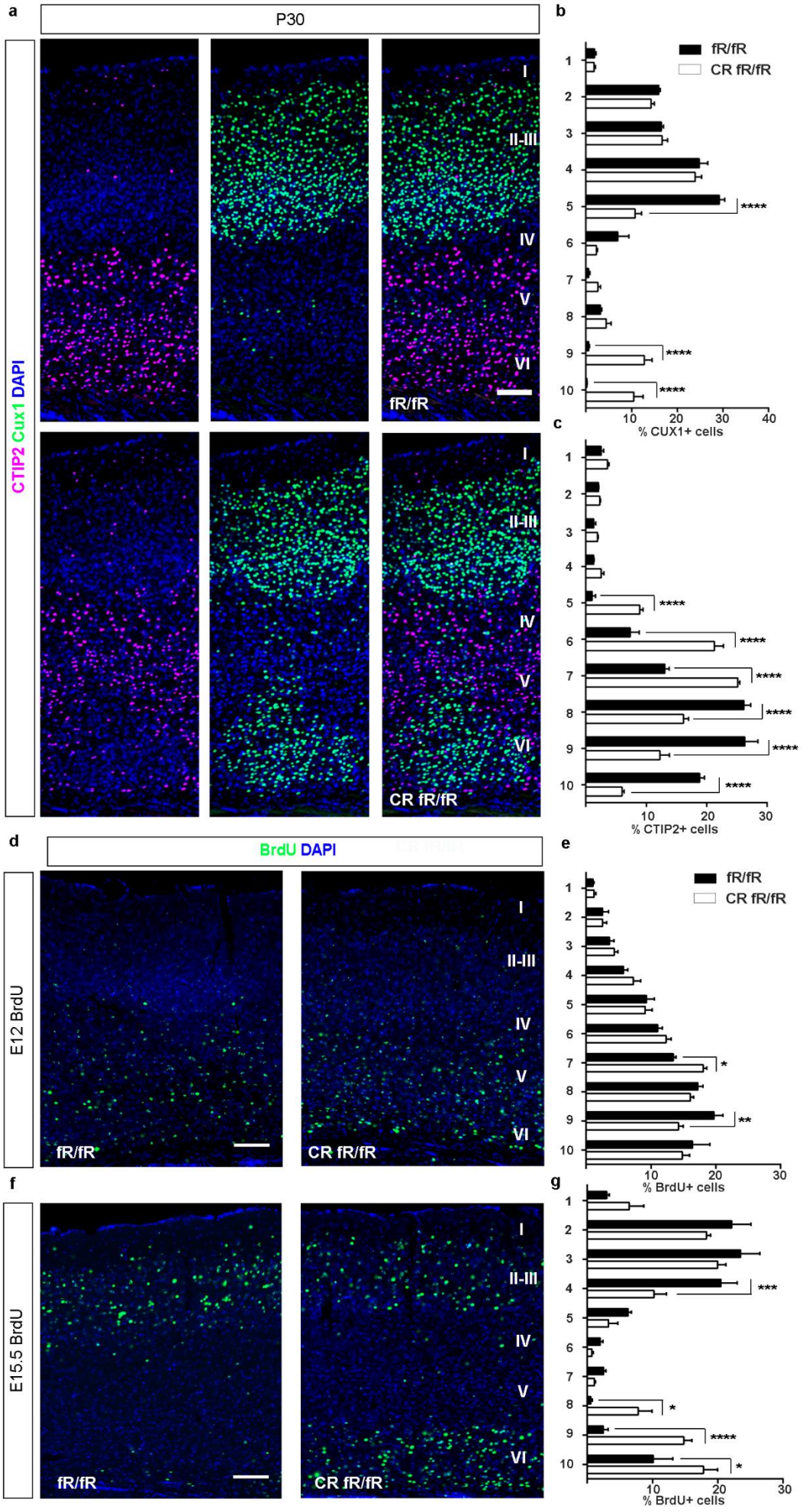
a
P30
CTIP2 Cux1 DAPI
I
II-III
IV
V
VI
fR/fR
CR fR/fR
b
fR/fR
CR fR/fR
% CUX1+ cells
c
% CTIP2+ cells
d
BrdU DAPI
E12 BrdU
e
% BrdU+ cells
f
E15.5 BrdU
g
% BrdU+ cells

Figure R.1.7. | Cortical layer distribution at P30 in the absence of Reelin from Calretinin positive cells. **a**, Representative confocal images at p30 illustrating the cortical distribution of Cux1+ (green, upper layers) and CTIP2+ cells (magenta, lower layers) in control (top) and Calretinin-Reelin deficient mice (bottom). Scale bar= 100 µm. **b**, Quantification of the percentage of Cux1+ cells *per* bin at P30 (data represents mean ± s.e.m; Bin x Genotype Interaction F(9, 50)= 26.54 p<0.0001; Two-way ANOVA with Bonferroni post hoc test; ****$P < 0.0001$, fR/fR n= 4 and CR fR/fR n=3). **c**, Quantification of the percentage of CTIP2+ cells *per* bin at P30 (data represents mean ± s.e.m; Bin x Genotype Interaction F(9, 40)= 59.49 p<0.0001; Two-way ANOVA with Bonferroni post hoc test; ****$P < 0.0001$, n= 3 mice per genotype). **d,f**, BrdU immunohistochemistry (IHC) of p30 mice injected with BrdU at E12 (**d**) and E15.5 (**f**). Scale bar= 100µm. **e, g**, Quantification of the percentage of BrdU+ cells *per* bin in mice injected either at E12 (**e**, data represents mean ± s.e.m; Bin x Genotype Interaction F(9, 40)= 3.338 p=0.0039; Two-way ANOVA with Bonferroni post hoc test; *$P < 0.05$, **$P < 0.01$, n= 3 mice per genotype) or E15.5 (**g**, data represents mean ± s.e.m; Bin x Genotype Interaction F(9, 60)= 8.059 p<0.0001; Two-way ANOVA with Bonferroni post hoc test; *$P < 0.05$, ***$P < 0.001$, ****$P < 0.0001$, n= 4 mice per genotype). Cortical Layer I (I), Layers II-III (II-III), Layer IV (IV), Layer V (V) and Layer VI (VI).

In order to confirm that the migration effects observed were independent of the thickness and total number of cells in the region analyzed, we compared the mean of these variables between control fR/fR and CR fR/fR mice, and no statisticaly significant differences were found between both genotypes in any of the anaylisis performed **(Table R.2.1.)**.

		fR/fR	CR fR/fR
a	**Number of CTIP2 cells at P1**	40,47 ± 3,72	56,81 ± 4,37
	Width (µm)	528,07 ± 55,31	699,9 ± 129,01
b	**Number of CTIP2 cells at P30**	77,94 ± 7,099	64,96 ± 1,988
	Width (µm)	1183 ± 63,72	1163 ± 81,62
c	**Number of Cux1 cells at P30**	127,7 ± 4,785	138,6 ± 8,727
	Width (µm)	1156 ± 44,56	1061 ± 10,22
d	**Number of E12 BrdU cells**	54,00 ± 7,314	62,73 ± 8,801
	Width (µm)	1007 ± 74,40	1089 ± 54,35
e	**Number of E15.5 BrdU cells**	31,33 ± 3,520	34,29 ± 4,695
	Width (µm)	985,4 ± 22,75	1079 ± 42,02

Table R.1.1. | Mean of the number of cells and width of the cortical region of interest (ROI) measured for each group of experiments. a-e, Quantification of average number of Cux1 and CTIP2 neurons and cortical thickness in the presence (fR/fR; left) and absence (CR fR/fR; right) of Reelin from calretinin positive cells. Data represents mean ± s.e.m, Unpaired two-tailed Student's t-test. **a**, for cell number (t= 5.113 df= 4 p= 0.0069, **$P < 0.01$ n=3 fR/fR and 3 CR fR/fR) and for width (t= 2.154 df= 4 p= 0.0975, n.s. n=3 fR/fR and 3 CR fR/fR). **b**, for cell number (t= 1.516 df= 5 p= 0.1900, n.s. n=4 fR/fR and 3 CR fR/fR) and for width (t= 0.1918 df= 5 p= 0.8554, n.s. n=4 fR/fR and 3 CR fR/fR). **c**, for cell number (t= 1.181 df= 5 p= 0.2909, n=4 fR/fR and 3 CR fR/fR) and for width (t= 1.777 df= 5 p= 0.1356, n.s. n=4 fR/fR and 3 CR fR/fR). **d**, for cell number (t= 0.5044 df= 6 p= 0.6319, n.s. n=4 fR/fR and 4 CR fR/fR) and for width (t= 0.8928 df= 4 p= 0.4224, n.s. n=3 fR/fR and 3 CR fR/fR). **e.** for cell number (t= 0.1918 df= 5 p= 0.8554, n.s. n=4 fR/fR and 3 CR fR/fR) and for width (t= 1.969 df= 6 p= 0.0965, n.s. n=4 fR/fR and 4 CR fR/fR).

1.3. Reelin expressed by Calretinin positive cells is necessary for correct neuronal migration and dendritic development of cortical neurons.

In addition to the analysis of cortical lamination we performed *in utero* electroporations (IUE) on E14 embryos and analyzed the brains at P1 **(Figure R.1.8)**. Since the GFP-expressing plasmid was introduced into the lateral ventricle, we expected to label cells born at the same time. The E14 is the time when cortical neurons destined to occupy future layer II-III are born in the adult cortex (Cooper, 2008).

In control fR/fR mice, GFP-labeled somas were located into the upper part of the CP (future II-III layers) and the leading processes of GFP-labeled neurons were properly oriented toward the MZ **(Figure R.1.8.a** left, and **Figure R.1.8.b** left panels**)**. In CR fR/fR mice, however, IUE revealed a wider distribution of GFP-labeled somas though all the layers of the cortex. Additionally, we found an increased number of GFP-labeled neuons in the lower cortical layers **(Figure R.1.a** center and right**)**. General defects in dendritic orientation were also observed in CR fR/fR mice. The marked cells displayed missaligned leading processes, with dendrites that failed to reach the MZ **(Figure R.1.8.c** top**)**. In addition, undermigrated GFP neurons also showed aberrant orientation of their apical dendrites **(Figure R.1.8.c** bottom**)**.

Therefore, the results suggest that Reelin expressed by CRC is necessary not only for the the proper layering of the cortex, but also for the correct dendritic growth and orientation of cortical neurons.

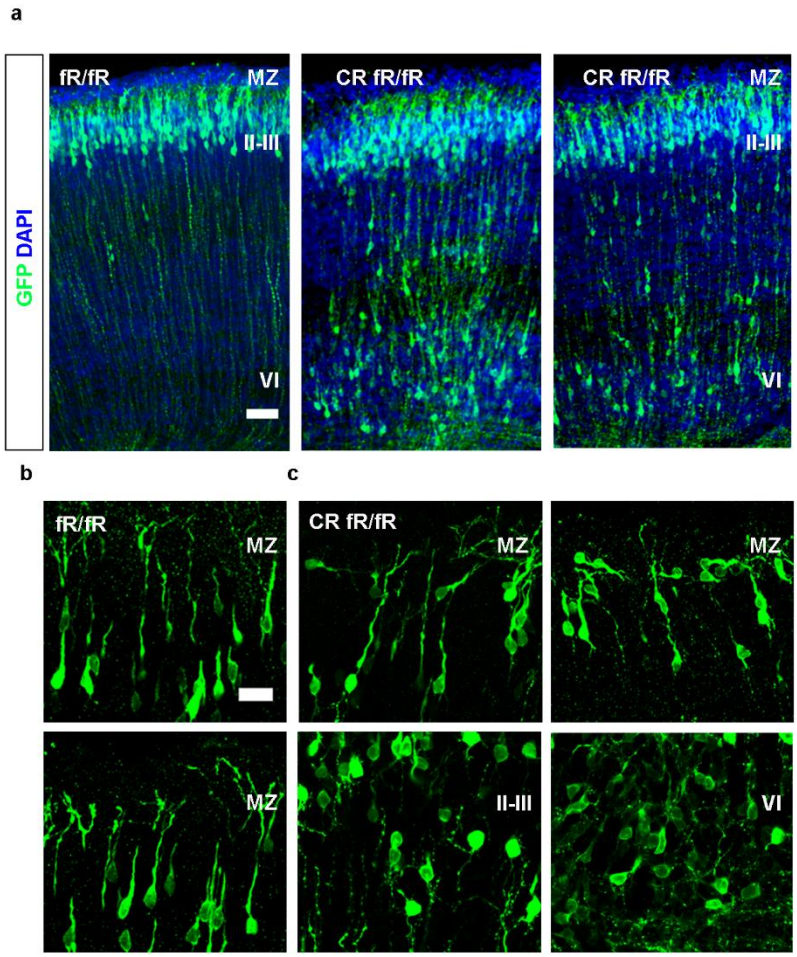

Figure R.1.8. | Positioning of Layer II-III cortical cells in the absence of Reelin from Calretinin positive cells. **a-c**, GFP-Immunostaining of mice electroporated in utero at E14 and sacrificed at P1 (fR/fR n=4 and CR fR/fR n=3). **a**, Representative confocal images of the full-length cortex in control (left) and Cajal-Retzius Reelin deficient mice (right). Scale bar=50µm. **b-c**, Representative confocal images of cortical MZ in control mice (**b**) and MZ (top center and right, bottom left), layers II-III (bottom center) and layer VI (bottom right) in Cajal-Retzius Reelin deficient mice (**c**). Scale bar=20 µm. Marginal Zone (MZ), Layers II-III (II-III) and Layer VI (VI).

1.4. Reelin expressed by Calretinin positive cells is necessary for the correct formation of the hippocampal structures.

First, we started analyzing the general structure of the hippocampus by using immunofluorescent detection of CTIP2 neurons to label pyramidal neurons of the Cornus Ammonis and Prox1 as a marker of granule cells in the DG **(Figure R.1.9)**. At E16, pyramidal neurons that will form the Ammon's horn of the hippocampus are migrating at the same time that start becoming arranged in a compact pyramidal layer. The formation of the granular cell layers of the DG is known to occur during postnatal stages, being the entire structure recognizable by P15 (Khalaf-Nazzal & Francis, 2013).

Whereas no effects were found in CR fR/fR hippocampus at E16 **(Figure R.1.9.a)**, with the main subdivisions being recognizable, some structural differences were observed at P1 **(Figure R.1.9.b)**. Regarding the CA1 pyramidal layer, CTIP2 labeling confirmed the presence of a thicker CA1 in CR fR/fR mice, with some pyramidal neurons ectopically placed in so and others dispersed in the sr, conferring a rugose aspect to the surface of the pyramidal cell layer **(Figure R.1.9.b**, top**)**. In the case of the emerging granular cell layer, in control fR/fR mice, granular cells labeled with Prox1 antibody appeared migrating in the process of compactation into blades. Prox1 is a marker of a large number of cells in the developing DG, including

progenitor cells in the hilus and both immature and mature granule neurons. Conversely, in CR fR/fR mice such distribution was clearly disorganized, with granular cells homogenously distributed along the entire hilus and others ectopically placed in the slm **(Figure R.1.9.b**, bottom**)**. At later stages (P30), the migration abnormalities were even more evident in CR fR/fR mice and the infrapyramidal blade (ipb) of the DG, including both the granular cell layer and the molecular layer, was either not well developed or absent in some cases **(Figure R.1.9.c** and **Figure R.1.10.a)**. In addition, in CR fR/fR mice, the suprapyramidal blade (spb) displayed irregular boundaries and an uneven border between the granule cell layer and the molecular layer **(Figure R.1.9.c)**.

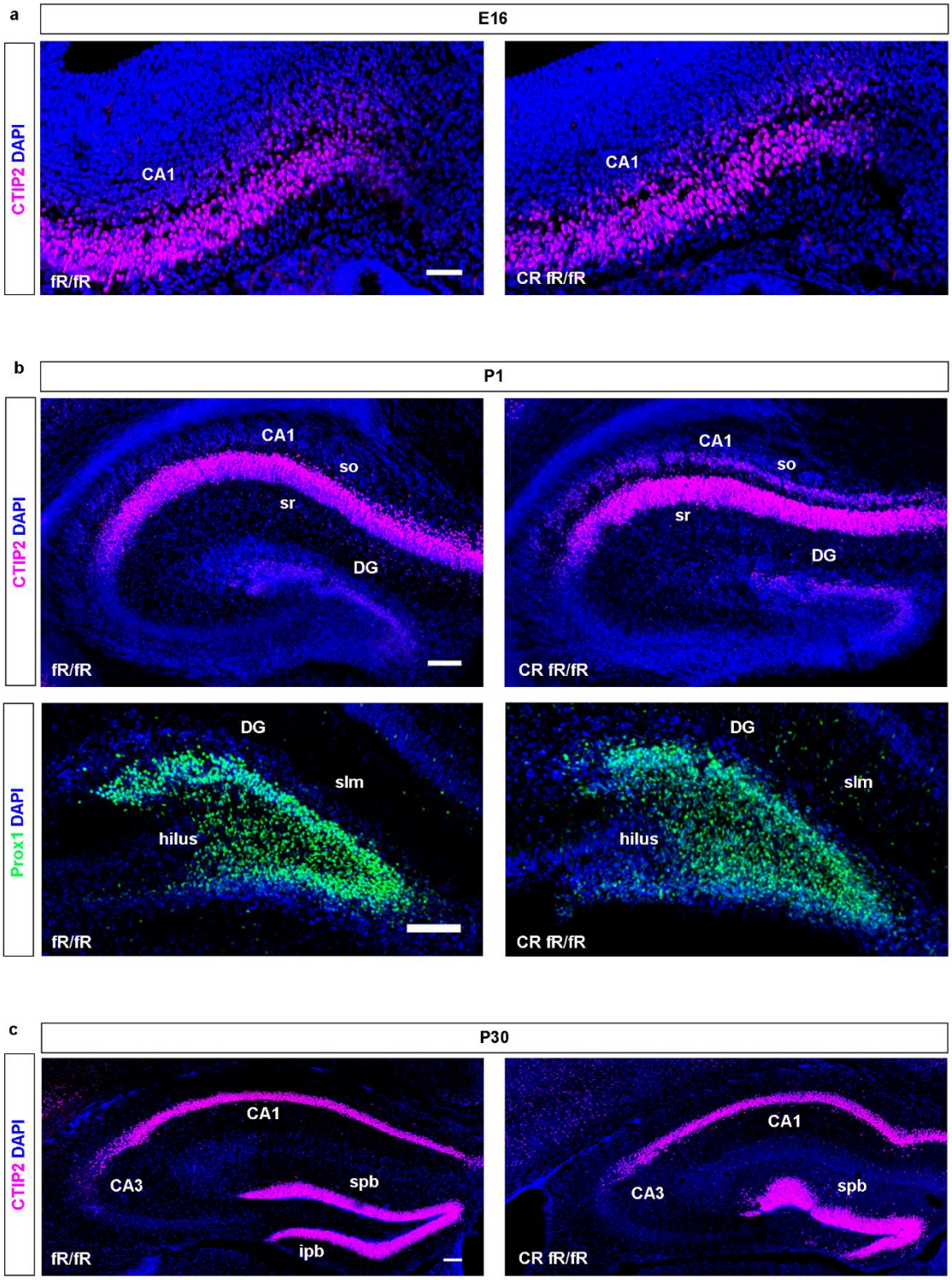

Figure R.1.9. | Hippocampal cytoarchitecture in the absence of Reelin from Calretinin positive cells. a-c, Representative confocal images of the hippocampus at E16 (**a**, CTIP2, scale bar=50µm), P1 (**b,** top CTIP2 and bottom Prox1, scale bar=100µm) and P30 (**c**, CTIP2, scale bar=100µm) in the presence (fR/fR; left) and absence (CR fR/fR; right) of Reelin from Calretinin+ cells. CA1, Cornus Ammonis 1; CA3, Cornus Ammonis 3; so, stratum oriens; sr, stratum radiatum; DG, Dentate gyrus; slm, stratum lacunosum moleculare; spb, suprapyramidal blade; ipb, infrapyramidal blade.

We analyzed the frequency of infrapyramidal blade phenotypes and we found that around 67% of CR fR/fR mice anaylzed completely lacked the IPB, 11% of the cases showed a small proportion (<20%) of IPB developed and in 22% of the cases the IPB was present in a major proportion (>20%) **(Figure R.1.9.a)**.

To further characterize the disorganized phenotype of CR fR/fR, we measured the width of the suprapyramidal blade (present in all the cases) and the CA1 region and a statistically significant increase in the width was observed from both regions in comparison to control fR/fR mice **(Figure R.1.9.c)**. This was particularly evident in the DG which exhibited regions in which the GCL clearly expanded to the ML with numerous ectopic GCs **(Figure R.1.9.b)**.

Analysis of cellular dispersion was performed in more detail by the examination of the diposition of BrdU positive cells within the CA1 and the SPB of the DG layers. Embryos were labeled with BrdU at E12 and E15.5 and analyzed at P30. Pups were injected with two pulses of BrdU at P10 and P11 and also analyzed at P30. On the one hand, BrdU positive neurons labeled at postanatal stages that were mainly present in the lower part of the GCL in control animals, showed a wider disposition in CR fR/fR mice, and a statistically significant decrease in the number of BrdU positive neurons was observed in the inner part of the GCL in these animals with a tendency to accumulate in other layers, especially in the hilus **(Figure R.1.9.d)**. Furthermore, analysis of BrdU injections at E15.5 showed that whereas in control fR/fR mice labeled GCs where mainly accumulated in the ourtermost part of the GCL, in CR fR/fR some BrdU+ cells failed to migrate and remained accumulated in the inner part of the GCL **(Figure R.1.9.e)**. On the other hand, as occurs in the *reeler* hippocampus, a less confined CA1 was also observed in mice deficient for Reelin from Calretinin positive cells. Whereas E12 BrdU labeled neurons were mainly placed within the pyramidal layer in the area nearby to the sr in both genotypes **(Figure R.1.9.g)**, BrdU positive neurons labelled at E15.5 displayed an altered disposition in CR fR/fR mice**.** In fR/fR controls these E15.5 labeled neurons were positioned in the outermost part of the pyramidal layer, in contact with the so, whereas in CR fR/fR a number of cells were unable to migrate through the upper parte of the CA1, and remained in a lower position **(Figure R.19.f)**.

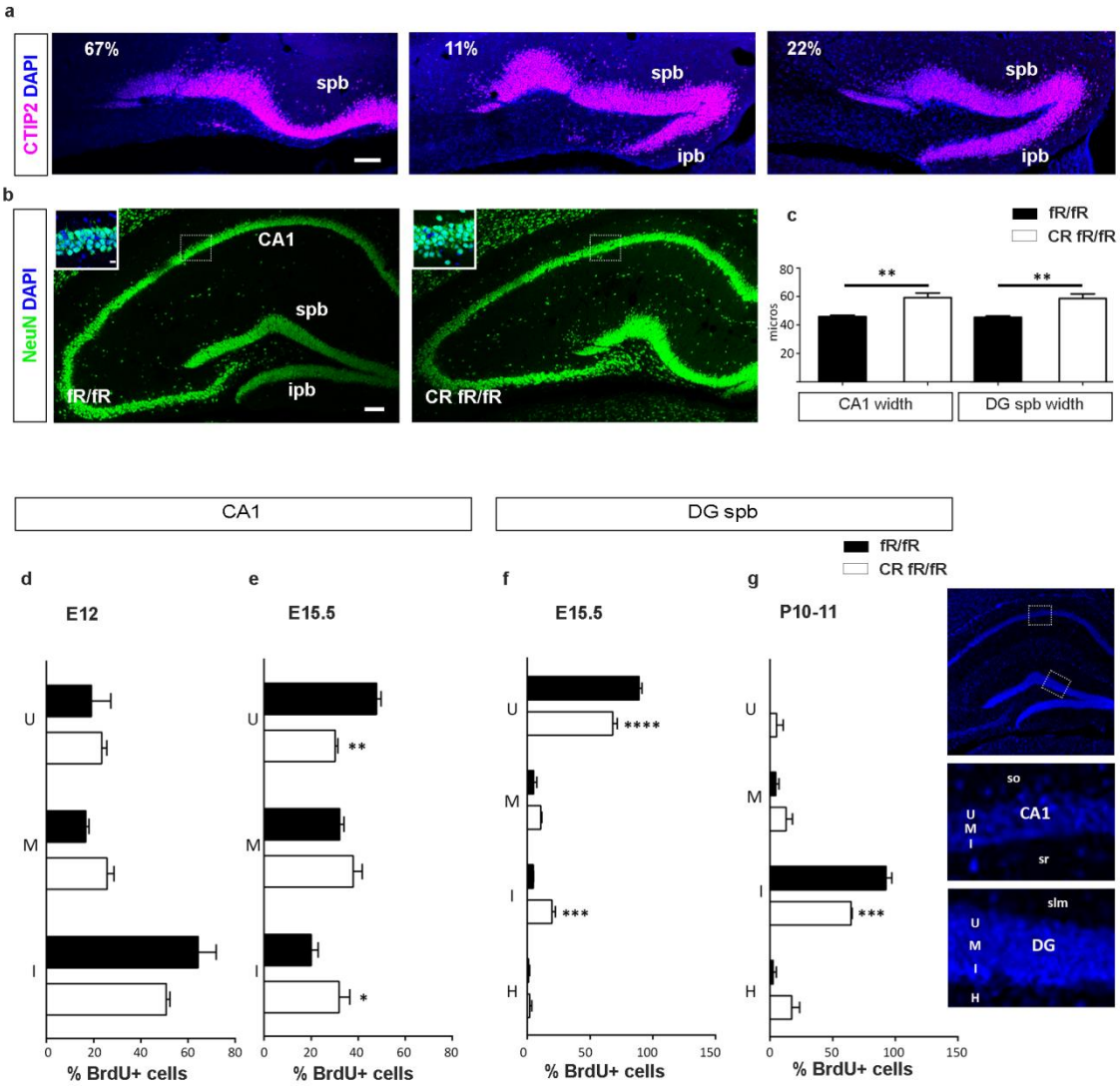

Figure R.1.10. | Hippocampus cell distribution and DG phenotype range in the absence of Reelin from Calretinin positive cells. a, Range of infrapyramidal blade (ipb) phenotypes in the absence of Reelin from Calretinin+ cells: absence of ipb (left, 67%), < 20% ipb (center, 11%) and >20% ipb (right, 22%) present. Scale bar=100µm. **b**, Representative confocal images of the hippocampus at P30 with NeuN in the presence (fR/fR; left) and absence (CR fR/fR; right) of Reelin from Calretinin+ cells Scale bar=100µm. Magnifications of CA1 region at the bottom of each image. Scale bar= 10µm **c**, Quantification of the mean width of CA1 (**left,** data represents mean ± s.e.m, Unpaired two-tailed Student's t-test; t= 4.695 df= 5 p= 0.0054; $^{**}P < 0.01$, n=4 fR/fR and 3 CR fR/fR) or spb of DG (**right**, data represents mean ± s.e.m, Unpaired two-tailed Student's t-test; t= 5.164 df= 5 p= 0.0036; $^{**}P < 0.01$, n=4 fR/fR and 5 Gad fR/fR).). **d-e**, Analysis of BrdU positive cells dispersion in the CA1 of mice injected with BrdU at E12(**d**, data represents mean ± s.e.m; Layer F(2, 12)= 36.77 p<0.0001; Two-way ANOVA with Bonferroni post hoc test; n.s. n= 3 mice per genotype) or E15.5 (**e**, data represents mean ± s.e.m; Layer x Genotype Interaction F(2, 12)= 13.88 p=0.0008; Two-way ANOVA with Bonferroni post hoc test; $^{*}P < 0.05$, $^{**}P < 0.01$, n= 3 mice per genotype). **f-g**, Analysis of BrdU positive cells dispersion in the suprapyramidal blade (spb) of the DG of mice injected with BrdU at E15.5 (**f**, data represents mean ± s.e.m; Layer x Genotype Interaction F(3, 16)= 23.85 p<0.0001; Two-way ANOVA with Bonferroni post hoc test; $^{***}P < 0.001$, $^{****}P < 0.0001$ n= 3 mice per

genotypeDG) or p10-11 (**g**, data represents mean ± s.e.m; Layer x Genotype Interaction F(3, 16)= 11.36 p=0.0003; Two-way ANOVA with Bonferroni post hoc test; ***$P < 0.001$, n= 3 mice per genotype). Dentate gyrus; spb, Suprapyramidal blade; CA1, Cornus Ammonis 1; U, Upper layer; M, Medial layer; I, Inner layer; H, Hilus.

2. Role of Reelin expressed by GABAergic interneurons in corticogenesis and hippocampus formation.

2.1. Generation and validation of a constitutive GABAergic interneuron Reelin deficient mouse model.

To unravel the function of Reelin selectively expressed by GABAergic interneurons in early postnatal and adult development, we crossed the Gad2-Cre micewith the fR/fR mice in order to obtain the Gad fR/fR mice in which the constitutive expression of the Cre recombinase is controled by GAD2 promoter. The survival of Gad fR/fR mice was normal, they presented a similar body weight (15,86g ± 0,5550) compared to their control littermates (14,98g ± 0,7757) and no apparent motor abnormal behaviours were found in these mice. Data represents mean ± s.e.m of P30 mice body weight measurements, Unpaired two-tailed Student's t-test (t= 0.9498 df= 25 p= 0.3513, n.s. n=16 fR/fR and 11 Gad fR/fR).

To address whether disappearance of Reelin from GABAergic interneurons occurs effectively in Gad fR/fR mice, we performed an immunohistochemical assay to asses the Reelin expression pattern in adult controls (fR/fR) and in Gad fR/fR mice **(Figure R.2.1)**. Histological analysis of immunoreactivity on P30 mice revealed virtually no Reelin expression through the cortical layers in Gad fR/fR mice **(Figure R.2.1.a** right and **Figure R.2.1.c** center), with the exception of layer II stellate neurons in the entorhinal and piriform cortices **(**Arrowheads **Figure R.2.1.a)**. Conversely, Reelin protein was roughly expressed in all the cortical areas in fR/fR mice **(Figure R.2.1.a** left and **Figure R.2.1.b** center). In the hippocampus of fR/fR mice, immunohistochemistry against Reelin confirmed unaltered Reelin expression in the so, sr and in the ML/slm, but also in the hilus of the DG **(Figure R.2.1.b** left**)**. By contrast, in Gad fR/fR mice, only a population of cells in the in the area of slm surrounding the fissure and in the lower ML of the DG exhibited Reelin signal, matching with areas where Calretinin positive cells are placed. These cells would correspond mainly with some Reelin expressing CRC that remain in the area surrounding the fissure and Calretinin positive interneurons in the infra ML **(Figure R.2.1.c** left and magnifications**)**. Regarding the cerebellum, histological analysis did not reveal detectable defects in the foliation pattern of Gad fR/fR. Specifically, a well-formed Purkinje plate as well as a normal thickness of the molecular and granule cell layers were found in mutant mice **(Figure R.2.1.b** and **Figure R.2.1.c** right**)**.

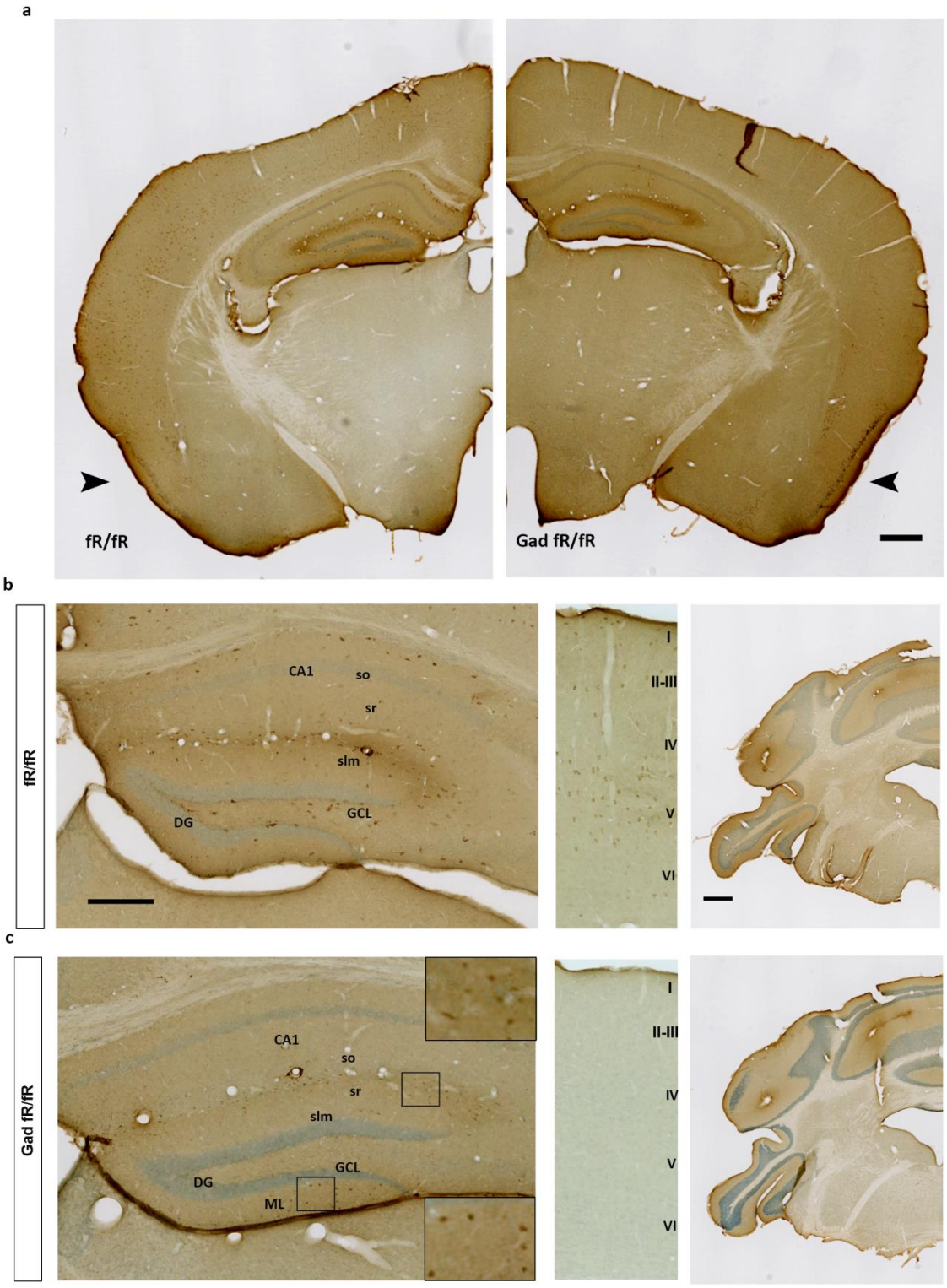

Figure R.2.1. | Pattern of expression of Reelin protein in Gad fR/fR mice. **a-c**, Immunohistochemical detection of Reelin protein in coronal sections of P30 mice. **a**, Representative photomicrograph showing Reelin cortical distribution in the whole brain (Scale bar= 500 µm) in the presence (fR/fR, left) and absence of Reelin from Gad65 positive cells (Gad fR/fR, right). Arrowheads pointed to layer II piriform cortex. **b**, **c**, Representative images of Reelin immunostaining in controls animals (b) and in Gad fR/fR mice (c), in the hippocampus (left, scale bar= 250 µm), in the primary somatosensory cortex and in the cerebellum (right, scale bar=500 µm). CA1, Cornus Amonis 1; so, stratum oriens; sr,

stratum radiatum; slm, stratum lacunosum moleculare; DG, Dentate girus; GCL, granule cell layer; I, Cortical Layer I, II-III, Layers II-III; IV, Layer IV; V, Layer V; VI, and Layer VI.

In order to compare Reelin expression levels between control fR/fR and Gad fR/fR mice, dissected protein extracts (including cortex and hippocampus) from E16 embryos, P1 pups and P30 mice, were prepared. Levels of protein were determined by Western blot against Reelin protein using tubulin as loading control. Whereas very similar levels of Reelin protein were observed at E16 **(Figure R.2.2.a)**, a substantial decrease in Reelin levels was detectable at P1 **(Figure R.2.2.b)** and a remarkable reduction was visible in the P30 blot of Gad fR/fR mice **(Figure R.2.2.c)**.

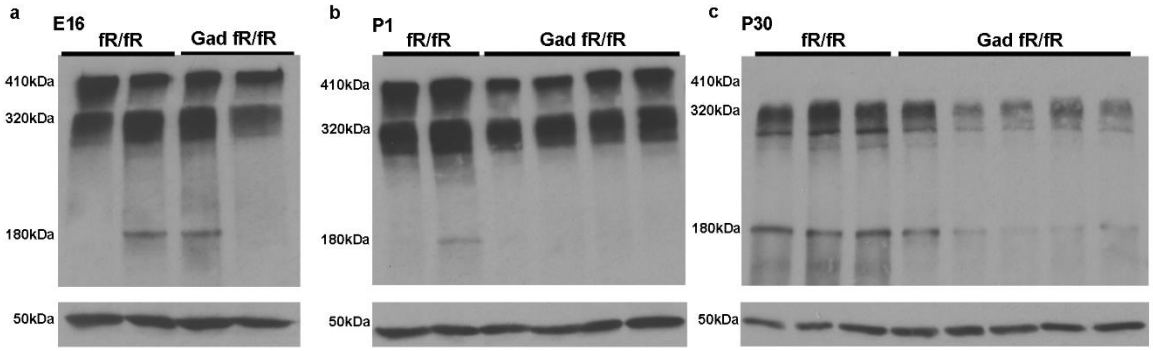

Figure R.2.2. | Reelin protein levels in Gad fR/fR mice. a-c. Western Blot analysis of extracts from cerebral cortex and hippocampus showing the levels of Reelin protein (top) in controls fR/fR and Gad fR/fR mice at E16 (a), P1 (b) and P30 (c). Expression of β-tubulin was used as loading control.

In order to confirm that Reelin specifically disappeared from GABAergic interneurons, we conducted a time course immunohistochemistry experiment with mice sacrificed at E16, P1 and P30 **(Figure R.2.3.)**. First, we analysed the pattern of expression of Reelin in Calretinin positive CRC, since they are the first population of Reelin expressing cells in the MZ of the developing neocortex. At E16, double immunofluorescence of Reelin and Calretinin showed no differences in the pattern of Reelin expressing CRC between controls fR/fR and Gad fR/fR mice **(Figure R.2.3.a)**. At P1, Reelin-expressing CRC population starts to decline in the MZ of the neocortex, at the time that Reelin expression switches to interneuron populations. Analysis of Reelin expression at this time demonstrated that despite Reelin-expressing cells were still visible in both control fR/fR and Gad fR/fR mice in the CRC of the MZ, no other areas of the neocortex displayed Reelin staining in Gad fR/fR mice. Conversely, in controls fR/fR mice, Reelin staning was also visible through the CP **(Figue R.2.3.b)**. Finally, we performed double immunofluorescence against Reelin and Gad65/67 antibody in P30 mice, in order to label the major population of Reelin expressing GABAergic interneurons. Whereas double labelled interneurons were detected in control fR/fR mice, none of Gad65/67 positive interneurons coexpressed Reelin in Gad fR/fR mice, confirming the selective supression of Reelin in Gad65 positive interneurons in Gad fR/fR mice **(Figure R.2.3.c)**.

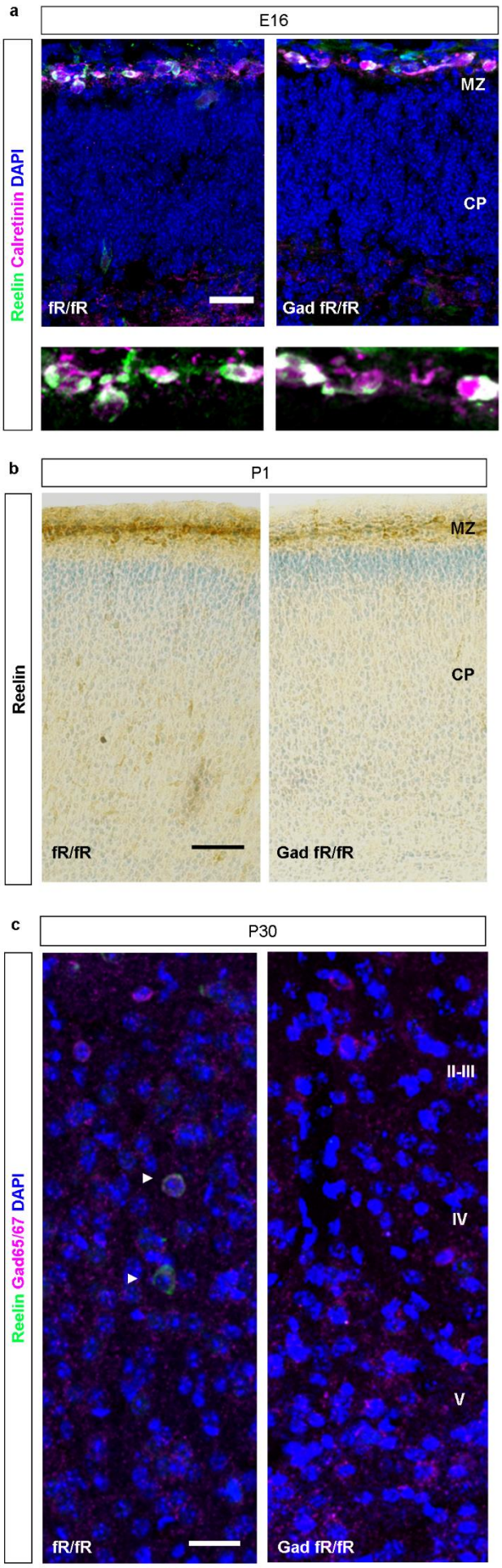

Figure R.2.3. | Reelin expression analysis in the primary somatosensoy cortex. a, Double IHC of Reelin+ (green) and Calretinin+ cells (magenta) at E16 and magnification of Marginal Zone (MZ) cells at the bottom. Scale bar=25µm. **b**, Representative photomicrograph showing Reelin cortical distribution at P1 (b, scale bar= 80µm) in controls (left) and GAD65-Reelin deficient mice (right). **c**, Double IHC of Reelin+ (green) and GAD65/67+ cells (magenta) at P30. Scale bar: 25µm . ▷ Double labelled cells. CP, cortical plate; II-III, Layers II-III; IV, Layer IV; V, Layer V.

Next, we analysed the pattern of Reelin expression during the formation of the hippocampus in controls fR/fR and mutant Gad fR/fR mice at P1 and P30 **(Figure R.2.4.)**. At P1, the majority of hippocampal Reelin protein comes from CRC. As corfirmed with Reelin immunohistochemistry, Reelin-expressing cells were densely packed in a band arround the ML and slm of the developing hippocampus, in close proximity to the hippocampal fissure both in control and Gad fR/fR mice **(Figure R.2.4.a)**.

At P30 stages, when hippocampal Reelin is mainly expressed by GABAergic interneurons, double immunodetection against Reelin and Gad65/67 demonstrated that whereas some Reelin-Gad65/67 double positive cells were found in the SGZ and ML of the DG in control fR/fR mice, no colocalization was observed in Gad fR/fR hippocampus. However, in addition to Gad65/67 interneurons, some other neurons, such as some Calretinin positive CRC cells also express Reelin in the adult hippocampus. In fact, in both fR/fR and Gad fR/fR mice, some Reelin positive-Gad65/67 negative cells were observed in different layers of the infra ML of the hippocampus **(Figure R.2.4.b)**.

Thus, these observations indicate that Gad fR/fR mice is a good model to further assess the contribution of Reelin expressed specifically by Gad65 interneurons in the cytoarchitecture of the brain.

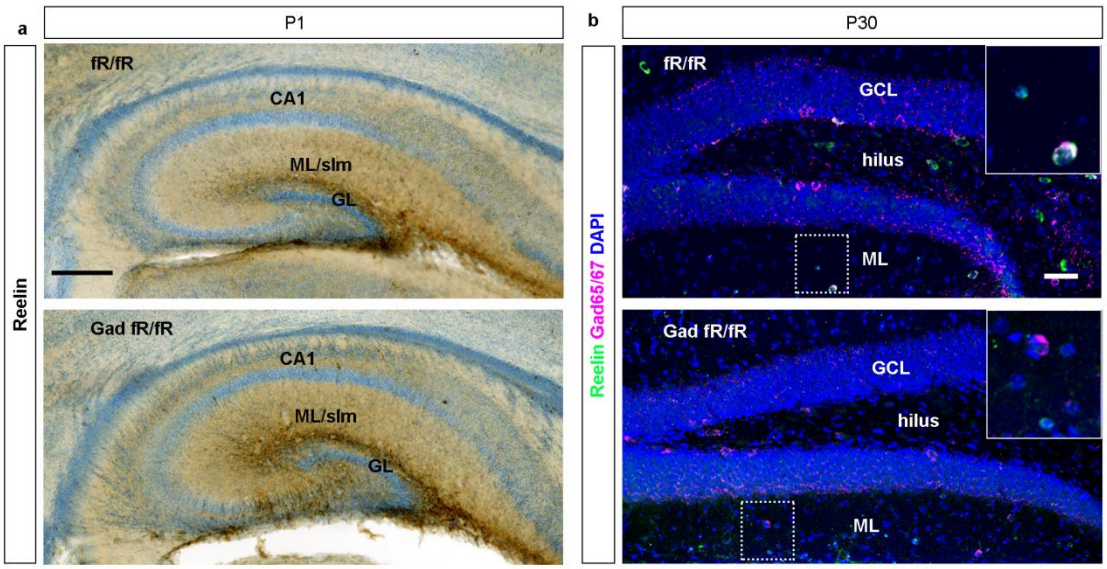

Figure R.2.4. | Reelin expression analysis in the hippocampus in the absence of Reelin from GAD65+ cells. a, Representative photomicrograph depicting Reelin expression pattern in the Hippocampus at P1 in the presence (fR/fR, top) and absence of Reelin from GAD65+ cells (Gad fR/fR, bottom). Scale Bar= 200µm. **b**, Double IHC of Reelin+ (green) and GAD65/67+ cells (magenta) at P30 in control (top) and Reelin deficient mice (bottom). Scale bar=100µm. Magnifications at the right side of each image. CA1, Cornus Ammonis 1; ML, molecular layer; slm, stratum lacunosum moleculare; GLC, granule cell layer.

2.2. Inactivation of Reelin in GAD65 interneurons leads to permanent invasion of cortical layer I.

In the cortex, pyramidal neurons of the upper layers complete their migration during the first days after birth, at the time that Reelin starts to be mainly expressed by GABAergic interneurons (Alcantara et al., 1998) (Tissir & Goffinet, 2003) (Sekine, Kubo, & Nakajima, 2014). By using the Gad fR/fR mouse model we intended to decipher the specific role of Reelin-expressing Gad65 interneurons in the final phase of cortical migration and in the maintenance of cortical layering in adult stages. In order to evaluate the morphological features in the cortical lamination after inactivation of Reelin in Gad65 interneurons, layer marker analysis was performed focusing on primary somatosensorial cortex at different stages, using Cux1 and CTIP2, markers for upper and deeper layer neurons, respectively **(Figure R.2.5.)**.

In contrast to the CR fR/fR mice, the analysis of cortex lamination at E16 did not show any difference between fR/fR and Gad fR/fR mice **(Figure R.2.5.a).** Cux1 and CTIP2 markers revealed two differenciated bands of staining in both genotypes with a layer of Cux1 positive cells formed on top of the CTIP2 positive layer. This pattern of lamination was also found in P1 brains of controls and Gad fR/fR mice, suggesting that later born neurons were able to bypass layers of the earlier born neurons in a normal fashion **(Figure R.2.5.c)**. Nevertheless, an upward shift of Cux1 labeled neurons was found in close proximity to MZ in Gad fR/fR mice, displaying a dense packed band in the upper boundary of the layers that they normally are destined to. The representation of the profile of Cux1 intensity over distance confirmed the observations from the histological analysis, and the peak of the intensity curve appeared displaced to an upper position in Gad fR/fR compared to control mice **(Figure R.2.5.b)**. Furthermore, quantification of Cux1 (excluding layer II-III) **(Figure R.2.5.d)** and CTIP2 positive neurons **(Figure R.2.5.e)** along the cortex at P1 did not show any difference in the cortical distribution between both genotypes.

However, analysis of the cortical distribution at later stages, from P15 onward, showed a remarkable invasion of Cux1 labeled neurons in cortical layer I, which is usually a cell sparse layer, in Gad fR/fR mice **(Figure R.2.5.i)**. Moreover, analysis of cortical distribution at P30 showed a number of undermigrated Cux1 positive cells in the lowest cortical layer as well as a striking overmigration of upper layer neurons in the layer I of the cortex. In addition, a reduced number of Cux1 positive cells was found between layers III-IV in Gad fR/fR mice **(Figure R.2.5.f** and **Figure R.2.5.g)**. Regarding the observations of lower layer labelled cells (CTIP2 positive neurons), a slight upward shift of early generated neurons was observed in the in Gad fR/fR mice, possibly due to the presence of Cux1+ cells in the lowest layer of the cortex **(Figure R.2.5.h)**.

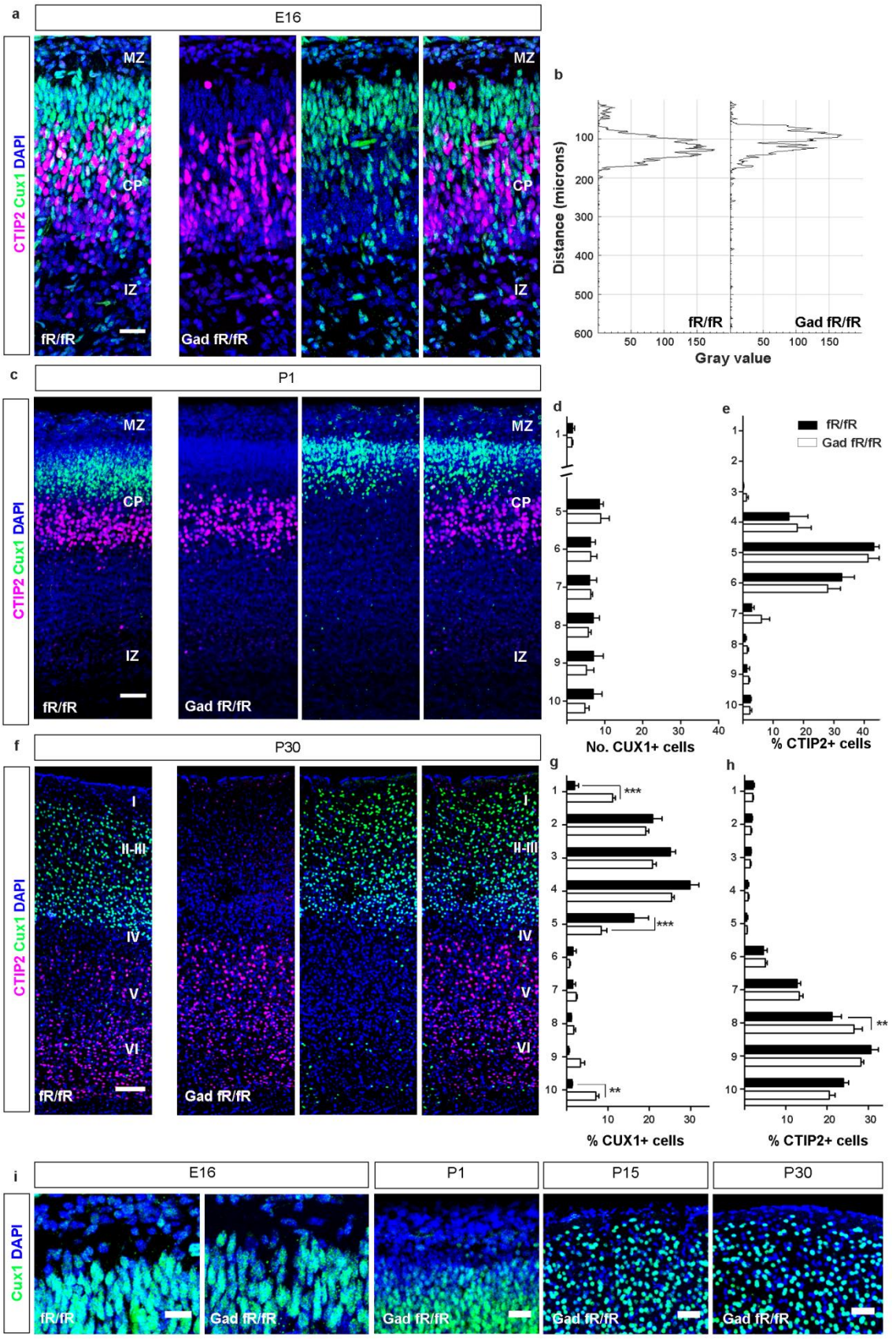

Figure R.2.5. | Distribution of cortical cells in the absence of Reelin from GAD65+ cells. a, c, f, Representative confocal images showing the cortical distribution of Cux1+ (green, upper layers) and CTIP2+ cells (magenta, lower layers) in control (fR/fR, left) and GAD65-Reelin deficient mice (Gad fR/fR, right) at E16 (**a**, scale bar= 25µm), P1 (**c**, scale bar= 50µm) and

P30 (**f**, scale bar= 100µm). **b**, Representative profile of Cux1 intensity (Gray value) over distance (from MZ to VI) in P1 control (left) and Reelin deficient (right) mice. **d,** Quantification of the number of Cux1+ cells *per* bin at P1. Since the region between the MZ and the CP (corresponding to bins 2 to 4) at this particular stage was too densely populated to be counted, only bins 1 and 5 to 10 were counted and represented as absolute number of cells/bin (data represents mean ± s.e.m; Bin F(6, 28)= 3.818 p=0.0066; Two-way ANOVA with Bonferroni post hoc test; n.s. (non-significant), n= 3 mice per genotype). **g**, Quantification of the percentage of Cux1+ cells *per* bin at P30 (data represents mean ± s.e.m; Bin x Genotype Interaction F(9, 50)=9.559; Two-way ANOVA with Bonferroni post hoc test; $^{**}P < 0.01$,$^{***}P < 0.001$, $^{****}P < 0.0001$, fR/fR n= 3 and Gad fR/fR n=4). **e, h**, Quantification of the percentage of CTIP2+ cells *per* bin at P1 (**e**, data represents mean ± s.e.m; Bin F(9, 40)= 72.99 p<0.0001; Two-way ANOVA with Bonferroni post hoc test; n.s., n= 3 mice per genotype) and P30 (**h**, data represents mean ± s.e.m; Bin x Genotype Interaction F(9, 70)= 2.717 p=0.0089; Two-way ANOVA with Bonferroni post hoc test; $^{**}P < 0.01$, fR/fR n= 4 and Gad fR/fR n=5). **i**, Cux1 IHC illustrating the time course of Layer I invasion in the absence of Reelin from GAD65 interneurons. Scale bar=15 µm for E16, 25 µm for P1, 50 µm for P15 and P30. MZ, Marginal Zone; CP, Cortical Plate; IZ, Inner Zone; I, Cortical Layer; II-III, Layers II-III; IV, Layer IV; V, Layer V and VI, Layer VI.

In order to investigate the lamination defects in more detail we conducted birth-dating studies by injecting BrdU to pregnant females at E12 or E15.5 and analyzed the resulting offspring at P30 **(Figure R.2.6)**. As expected, E12 labelled cells were placed in the deepest part of the cortex (mainly layers V-VI) and no differences in BrdU distribution could be observed between both genotypes **(Figure R.2.6.a** and **Figure R.2.6.b)**. However, in line with the observed results of Cux1+ cells distribution, E15.5 BrdU labeled cells destined to occupy upper layer neurons, were found in the lower cortical layers of the cortex, arranged in a clearly band, in Gad fR/fR mice. Furthermore, a more detailed analysis of the layer VI neurons showed double labeling of BrdU/Cux1 of these undermigrated cells **(Figure R.2.6.e)**. In addition, some E15.5-born neurons were also ectopically positioned in the layer I and an upward shift of the layer II-IV was also confirmed in Gad fR/fR mice **(Figure R.2.6.c** and **Figure R.2.6.d)**.

Thus, these findings suggested a role of Reelin specifically expressed by Gad65 interneurons as a stop signal for late born neurons in layer I of the cortex.

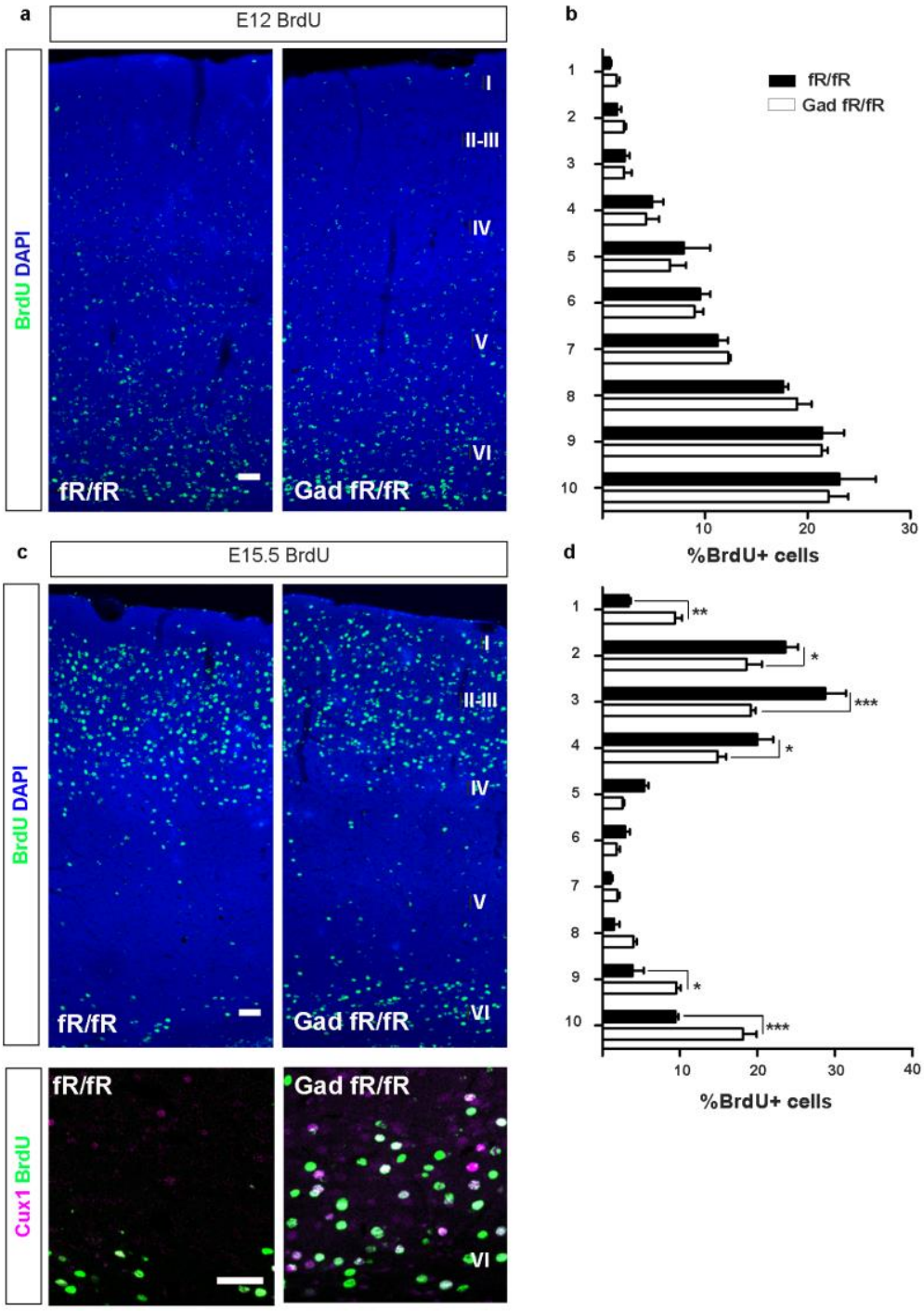

Figure R.2.6. | Positioning of cortical cells in the absence of Reelin from GAD65+ interneurons. a, c, BrdU immunohistochemistry (IHC) of p30 mice injected with BrdU at E12 (**a**) and E15.5 (**c**). Scale bar=50 µm. **b, d**, Quantification of the percentage of BrdU+ cells *per* bin in mice injected either at E12 (**b**, data represents mean ± s.e.m; Bin F(9, 40)= 68.56 p<0.0001; Two-way ANOVA with Bonferroni post hoc test; n.s., n= 3 mice per genotype) or E15.5 (**d**, data represents mean ± s.e.m; Bin x Genotype Interaction F(9, 50)= 12.54 p<0.0001; Two-way ANOVA with Bonferroni post hoc test; **P* < 0.05, ***P* < 0.01, ****P* < 0.001, fR/fR n= 3 and Gad fR/fR n=4). **e**, Double IHC of BrdU+ (green) and Cux1+ cells (magenta) of P30 mice injected at E15.5. Scale bar=50µm. I, Cortical Layer; II-III, Layers II-III; IV, Layer IV; V, Layer V and VI, Layer VI.

The effects observed were independent of the total number of cells or the cortex width in the region analyzed, since these variables do not present statically significant differences between control fR/fR and Gad fR/fR mice **(Table R.2.1)**.

		fR/fR	Gad fR/fR
a	**Number of CTIP2 cells at P1**	45,58 ± 3,496	51,71 ± 4,135
	Width (µm)	544,5 ± 38,76	547,5 ± 19,36
b	**Number of CTIP2 cells at P30**	78,33 ± 3,378	83,38 ± 6,414
	Width (µm)	1108 ± 42,11	1206 ± 52,02
c	**Number of Cux1 cells at P30**	79,67 ± 3,676	89,31 ± 8,806
	Width (µm)	1001 ± 55,09	1076 ± 70,93
d	**Number of E12 BrdU cells**	63,56 ± 15,47	52,04 ± 3,981
	Width (µm)	908,2 ± 12,70	964,1 ± 56,05
e	**Number of E15.5 BrdU cells**	47,31 ± 2,898	49,89 ± 4,929
	Width (µm)	1068 ± 68,41	1110 ± 42,89

Table R.2.1. | Mean of the number of cells and width (in microns) of the cortical region of interest (ROI) measured for each group of experiments. a-e, Quantification of average number of Cux1 and CTIP2 neurons and cortical thickness in the presence (fR/fR; left) and absence (Gad fR/fR; right) of Reelin from GAD65+ interneurons. Data represents mean ± s.e.m, Unpaired two-tailed Student's t-test. **a**, for cell number (t= 1.132 df= 4 p= 0.3209, n=3 fR/fR and 3 Gad fR/fR) and for width (t= 0.6863 df= 4 p= 0.9486, n=3 fR/fR and 3 Gad fR/fR). **b**, for cell number (t= 0.6422 df= 7 p= 0.5412, n=4 fR/fR and 5 Gad fR/fR) and for width (t= 1.409 df= 7 p= 0.2017, n=4 fR/fR and 5 Gad fR/fR). **c**, for cell number (t= 0.8879 df= 5 p= 0.4152, n=3 fR/fR and 4 Gad fR/fR) and for width (t= 0.7850 df= 5 p= 0.4680, n=3 fR/fR and 4 Gad fR/fR). **d**, for cell number (t= 0.7214 df= 4 p= 0.5106, n=3 fR/fR and 3 Gad fR/fR) and for width (t= 0.9721 df= 4 p= 0.3860, n=3 fR/fR and 3 Gad fR/fR). **e**, for cell number (t= 0.4090 df= 5 p= 0.6995, n=3 fR/fR and 4 Gad fR/fR) and for width (t= 0.5450 df= 5 p= 0.6092, n=3 fR/fR and 4 Gad fR/fR).

2.3. Inactivation of Reelin in GAD65 interneurons does not alter the hippocampus cytoarchitecture.

In contrast to the major defects observed in CR fR/fR mice, no effects where found in the analysis of the general structure and layering of Gad fR/fR hippocampus at postnatal and adult stages **(Figure R.2.7.)**. At P1, the gross analysis of the hippocampal structure did not revealed major alterations neither in the hippocampus proper (as revealed CTIP2 labeled pyramidal cells) nor in the emerging DG in both genotypes. Using Prox1 as a granule cell layer marker we observed that in both cases, granule neurons appeared migrating from the hilus towards the supra and infra-pyramidal blades, where they start to arrange in well delineated layers **(Figure R.2.7.a)**. At later stages (P30), the general appearance of the hippocampus including the granule cell layer and the piramidal layer, remained similar between control fR/fR and Gad fR/fR mice **(Figure R.2.7.b)**. In addition, using CTIP2 as a marker for pyramidal and dentate granule neurons, no differences in the average thickness of CA1 and the spb of the DG were found in the hippocampus, suggesting no evident cell dispersion in the absence of Reelin from Gad65 interneurons **(Figure R.2.7.c** and **Figure R.2.7.d)**. Furthermore, the analysis of

celullar dispersion performed by the analysis of the diposition of BrdU labeled cells within the CA1 and the SPB of the DG layers revealed no altered distribution of those cells in Gad fR/fR mice **(Figure R.2.7.e**, **Figure R.2.7.f**, **Figure R.2.7.g** and **Figure R.2.7.h)**.

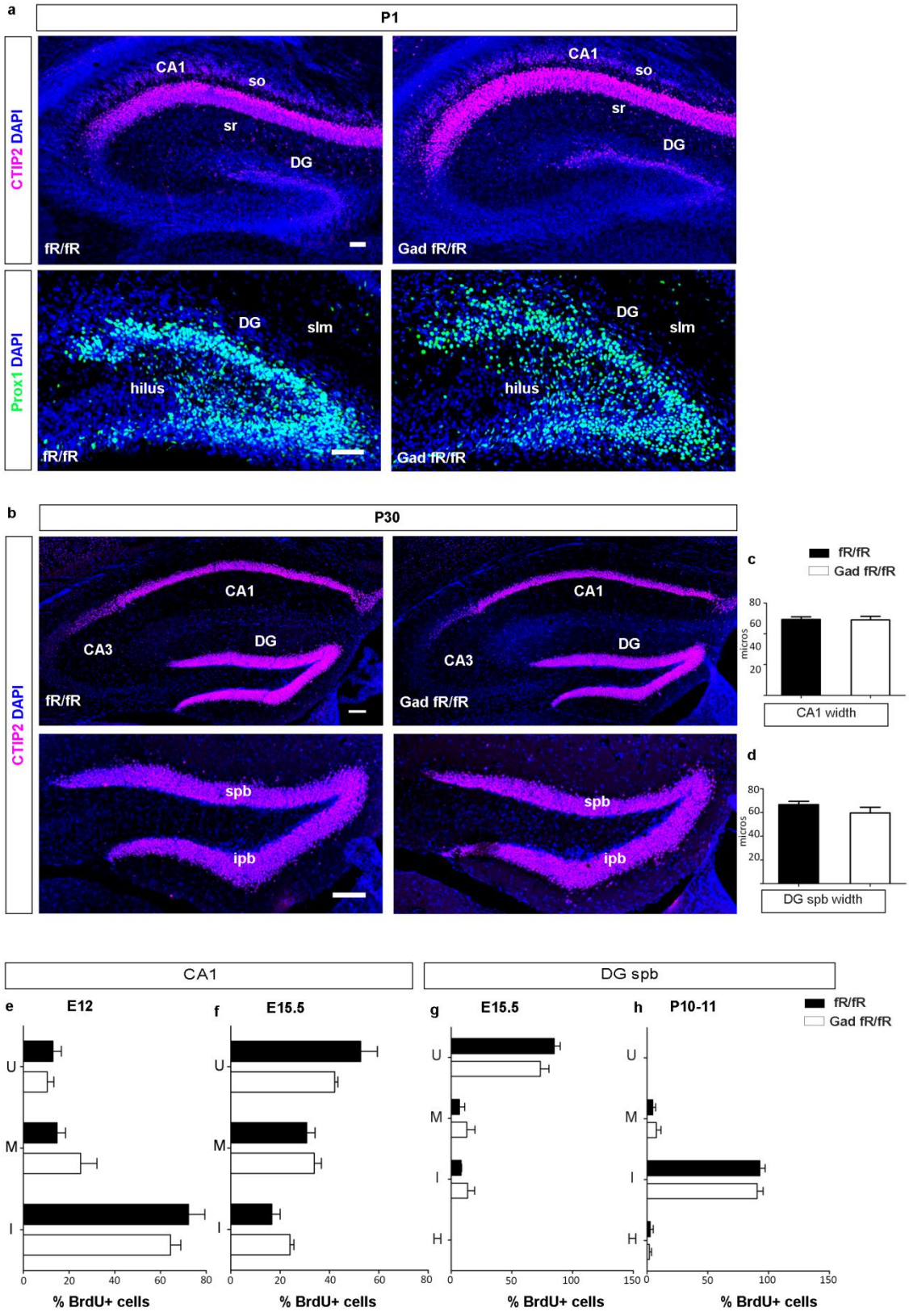

Figure R.2.7. | Hippocampal cytoarchitecture and cell distribution in the absence of Reelin from GAD65+ interneurons. a-b, Representative confocal images of the hippocampus at P1 (**a,** top CTIP2 and bottom Prox1) and P30 (**b**, CTIP2) in the presence (fR/fR; left) and absence (Gad fR/fR; right) of Reelin from GAD65+ interneurons. Scale bar=50 µm. **c-d**, Quantification of average thickness of CA1 (**c**, data represents mean ± s.e.m, Unpaired two-tailed Student's t-test; t= 0.1069 df= 7 p= 0.9178, n=4 fR/fR and 5 Gad fR/fR) or spb

of DG (**d**, data represents mean ± s.e.m, Unpaired two-tailed Student's t-test; t= 1.175 df= 7 p= 0.2785, n=4 fR/fR and 5 Gad fR/fR). **e-f**, Analysis of BrdU positive cells dispersion in the CA1 of mice injected with BrdU at E12 (**e**, data represents mean ± s.e.m; Layer F(2, 12)= 1.686 p=0.2262; Two-way ANOVA with Bonferroni post hoc test; n.s. n= 3 mice per genotype) or E15.5 (**f**, data represents mean ± s.e.m; Layer x Genotype Interaction F(2, 12)= 3.237 p=0.0751; Two-way ANOVA with Bonferroni post hoc test; n.s. n= 3 mice per genotype). **g-h**, Analysis of BrdU positive cells dispersion in the suprapyramidal blade (spb) of the DG of mice injected with BrdU at E15.5 (**g**, data represents mean ± s.e.m; Layer x Genotype Interaction F(3, 16)= 1.552 p=0.2399; Two-way ANOVA with Bonferroni post hoc test; n.s. n= 3 mice per genotype) or P10-11 (**h**, data represents mean ± s.e.m; Layer x Genotype Interaction F(3, 16)= 0.2468 p=0.8624; Two-way ANOVA with Bonferroni post hoc test; n.s. n= 3 mice per genotype) or CA1, Cornus Ammonis 1; CA3, Cornus Ammonis 3; so, stratum oriens; sr, stratum radiatum; DG, Dentate gyrus; slm, stratum lacunosum moleculare; spb, suprapyramidal blade; ipb, infrapyramidal blade.

3. Analysis of the conditional loss of Reelin signaling in early postnatal development and adult stages in the cortex, hippocampus and cerebellum.

3.1. Generation and validation of an ubiquitous conditional Reelin deficiency mouse model.

To bypass the deleterious consequences of embryonic absence of Reelin in the developing *reeler* brain (D'Arcangelo & Curran, 1998), we generated an inducible conditional Reelin knockout mouse (Cre fR/fR). Once obtained the homozygosity for the loxP sites (fR/fR), we crossed with a heterozygous inducible Cre recombinase-expressing line, Ubi-CreERT2 line. These mice ubiquitously express a fusion protein composed of Cre recombinase and a mutated form of the estrogen receptor (Cre-ERT2). After tamoxifen administration, nuclear Cre recombinase activity is induced and knockout of the Reelin is obtained.

With the purpose of finding out how long does it take for Reelin to effectively disappear from the induced knockouts, we conducted a timecourse experiment. For postnatal inactivation, pups were injected with tamoxifen for 3 consecutive days from postnatal day 1 to day 3. Mice were then sacrificed on different postnatal days after tamoxifen administration and Western blots (WBs) were performed on forebrain lysates against Reelin and its most immediate downstream effector, Dab1 **(Figure R.3.1.a)**. After the first injection, a decrease in Reelin level was confirmed by the gradual disappearance of Reelin specific bands at 370 and 180KDa in Cre fR/fR brains which completely disappeared by P6. In addition, a relative increase in Dab1 expression was seen in Cre fR/fR mice noticeable since P3, which is consistent with the higher Dab1 expression described in the *reeler* mouse model. Reelin-induced phosphorylation of Dab1 triggers its degradation, and thus loss of Reelin protein results in higher Dab1 protein levels and corroborates that the Reelin inactivation is effective. In order to visualize the brain-wide loss of Reelin, an immunohistochemistry detection of Reelin was performed on P15 Cre fR/fR mice after postnatal induced depletion. Analysis of brain sections confirmed unaltered Reelin expression in control brains and the complete disappearance of Reelin signal in Cre fR/fR mice in the neocortex and hippocampus **(Figure R.3.1.b)** but also in other brain regions including the olfactory bulb and the cerebellum.

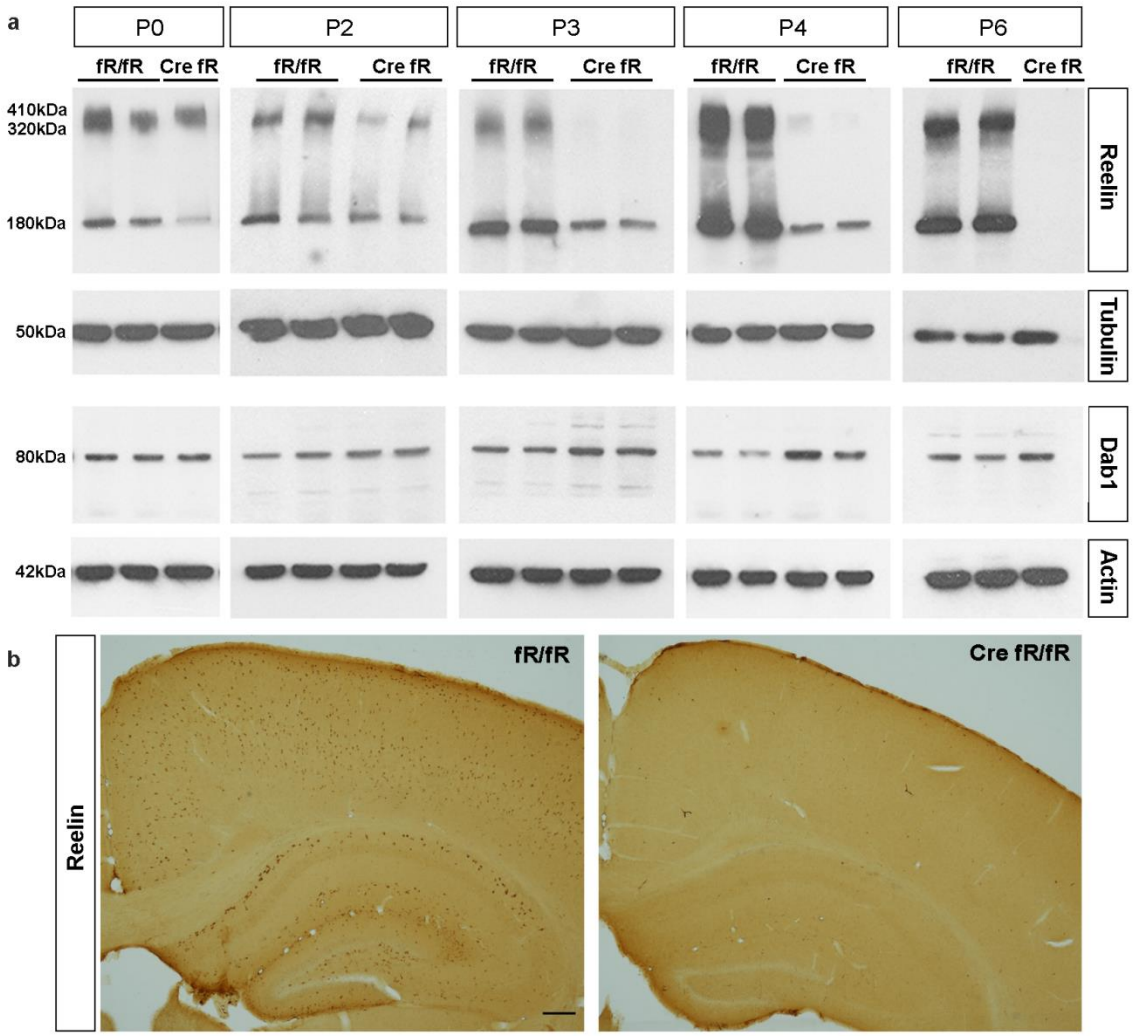

Figure R.3.1. | Generation and validation of conditional Reelin deficient mouse model. a. Western Blot analysis of brain extracts (excluding cerebellum) against Reelin and Dab1 protein at different time-points before (P0), during (P2-P3) and after (P4, P6) TMX administration to P1-3 pups in controls fR/fR and Cre fR/fR mice. Expression of β-tubulin was used as loading control in Reelin blots and actin levels in Dab1 blots. **b**. Representative IHC against Reelin in P15 control (fR/fR, left) and Reelin deficient mice (Cre fR/fR, right). Scale bar= 200 µm.

In order to determine the specific functions of Reelin protein in adult brain after normal development, we induced Cre recombinase activity by tamoxifen administration in 2 months old mice. Adult inactivation was induced by three daily consecutive injections of tamoxifen in adult Cre fR/fR mice that were then sacrificed 3-4 months after inactivation. To confirm that we were effectively disrupting Reelin signaling in Cre fR/fR mice quantitative Western blotting analysis was performed using forebrain lysates of adult mice **(Figure R.3.2.b)**. Quantifications demonstrated a statistically significant reduction in Reelin protein levels together with an increase in Dab1 abundance in Cre fR/fR compared to control mice. Conversely, no differences in the amount of the major Reelin receptors, ApoER2 and VLDLR, were observed between both genotypes. In addition, the immunohistochemistry detection against Reelin on adult mice brain sections confirmed unaltered Reelin expression in control brains (fR/fR) and the lack of Reelin in knockout mice brains (Cre fR/fR) after tamoxifen injection **(Figure R.3.2.a).**

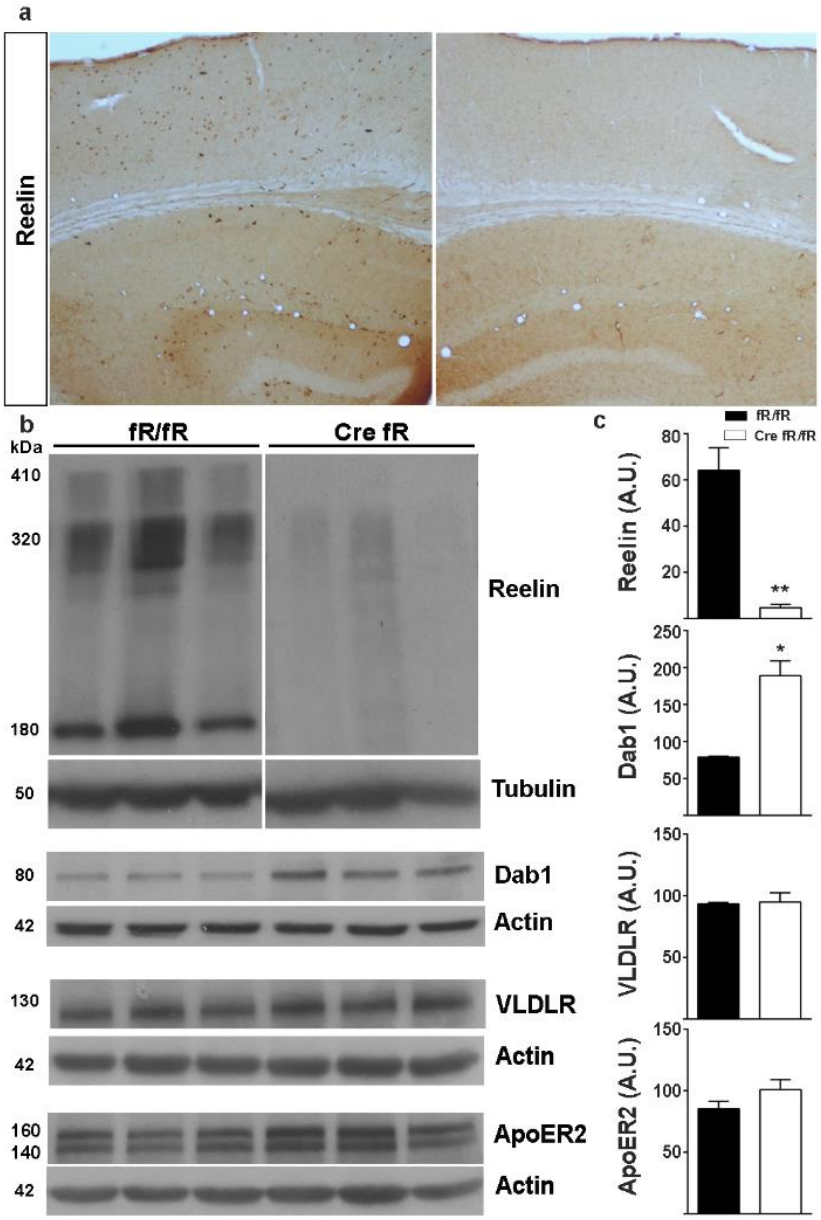

Figure R.3.2. | Reelin depletion during adulthood. a, Representative IHC against Reelin in adult control (fR/fR, left) and Reelin deficient mice (Cre fR/fR, right).**b**, Total brain homogenate Western Blot (excluding cerebellum) against Reelin,Dab1, VLDLR and ApoER2. **c**, Western blot quantifications for Reelin, Dab1, VLDLR and ApoER2. Data represents mean ± s.e.m and was analyzed using unpaired two-tailed Student's t-test with Welch correction (Reelin, t=6.020 df=3.137 p= 0.0081; Dab1, t=5.395 df=2.007 p=0.0325;* $P < 0.05$. ** $P < 0.01$, 3-4 animals per genotype).

3.2. Postnatal loss of Reelin signaling alters cortical upper-layer neuron positioning.

In the neocortex, late born pyramidal neurons destined to the upper layers complete their radial migration during the first postnatal days (Tissir & Goffinet, 2003). Taking advantage of the conditional deficient Reelin mice we intended to broaden the current understanding of Reelin role in the final phase of migration avoiding the deleterious consequences of altered neuronal arrangement of *reeler* mice during development.

In order to explore if the postnatal loss of Reelin could alter cortical layering distribution, a series of different immunodetections on brain sections were performed in the primary somatosensory cortex (S1BF) of control fR/fR and Reelin deficient Cre fR/fR mice sacrificed at P15 **(Figure R.3.3)**. First, we assessed the generic disposition of neurons by NeuN (a pan-neuronal nuclear marker) staining on coronal cortical sections. NeuN staining showed a massive invasion of cortical layer I by neuronal nuclei in Cre fR/fR compared to control littermates, which is one of the hallmarks of the *reeler* phenotype **(Figure R.3.3.a)**. So as to understand the origin of these ectopic nuclei, we analysed the distribution of postmitotic neurons using different layer-specific markers.

First, we used an anti-Cux1 antibody as a marker for upper layer neurons. Unlike *reeler* cortices in which invading layer I neurons are mainly layer VI neurons, analysis of the distribution pattern of Cux1-positive cells demonstrated that after postanatal Reelin suppression, upper layer neurons overmigrate into the layer I of the cortex in the Cre fR/fR mice compared to fR/fR controls **(Figure R.3.3.b** and **Figure R..3.d)**. These observations were confirmed after quantification of the percentage of Cux1 cells along the cortex, showing a statistically significant increase in cell percentage in the 1st bin, corresponding approximately to layer I, and a decrease in the 5th bin in Cre fR/fR, compared to control mice, suggesting an upward shift of the layer II-IV neurons **(Figure R.1.3.c)**. The aberrant presence of neurons in layer I of Cre fR/fR mice was visible throughout the cortex but often uneven, with a much bigger dispersion of Cux1-positive neurons in the cingulate cortex **(Figure R.1.3.h)**.

Secondly, we analyzed the deeper-layer neurons distribution using anti-Tbr1 and anti-CTIP2 antibodies. Tbr1 is a transcription factor expressed in some cortical neurons of layers II-III and mostly in layers V-VI, while CTIP2 is a typical marker of early-born neocortical neurons, mainly layer IV to VI. When deeper-layer neuronal distribution was explored using CTIP2 and Trb1 no apparent differences were found between Cre fR/fR and fR/fR control mice **(Figure R.3.3.e** and **Figure R.3.3.f).** In addition, quantitative analysis of the dispersion of Tbr1-positive neurons did not show any differences between both genotypes **(Figure R.3.3.g)**.

Thus, postnatal depletion of Reelin in the neocortex leads to an excessive migration of upper-layer neurons that complete migration during this period, but not the older neurons that are already established in the deeper layers. Since deeper layer neurons undergo migration much earlier during embryonic development, it might be that once they are established they are not affected by postnatal lack of Reelin signaling.

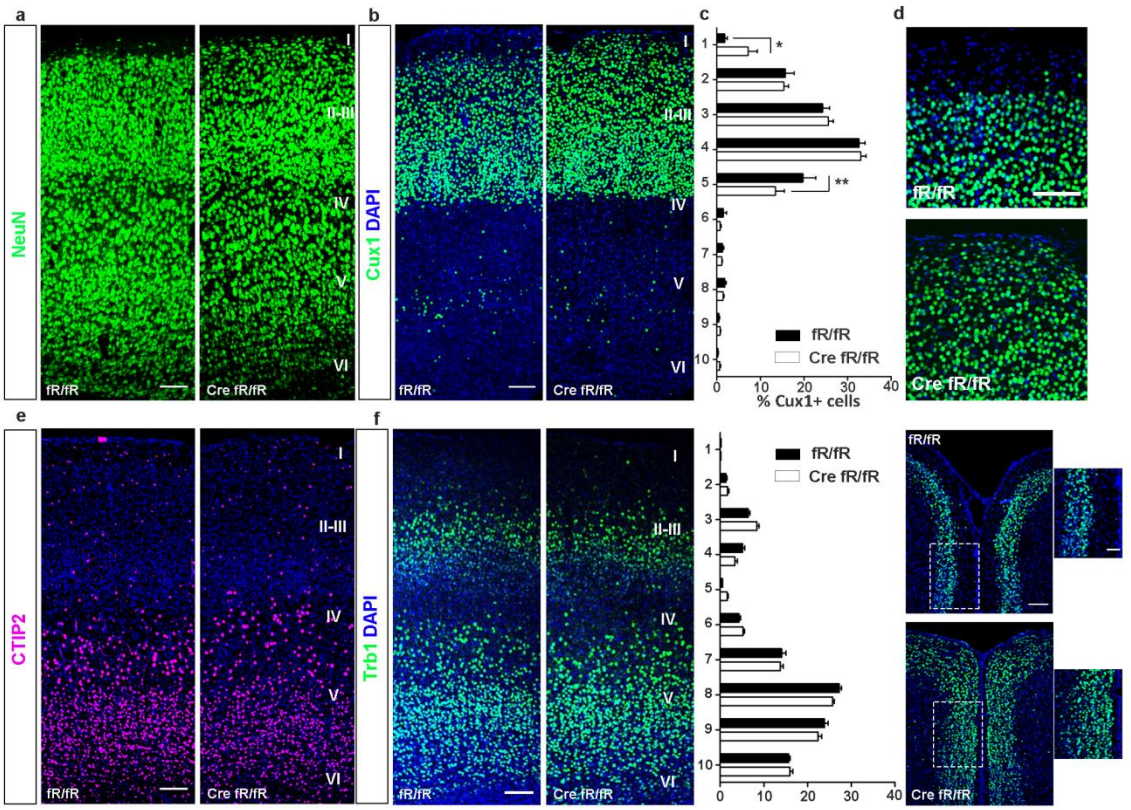

Figure R.3.3. | Reelin removal at early postnatal stages critically affects the distribution of cortical cells in the primary somatosensorial cortex. a-b, Representative confocal images depicting the cortical distribution of NeuN+ (**a**, all neurons, scale bar=100 µm) and Cux1+ cells (**b**, green, upper layers, scale bar=100 µm) at P15 in the presence (fR/fR; right) and absence (Cre fR/fR; left) of Reelin from early postnatal stages. **c**, Quantification of the percentage of Cux1+ cells *per* bin (data represents mean ± s.e.m; Bin x Genotype Interaction F(9, 100)= 2.579 p=0.0103; Two-way ANOVA with Bonferroni post hoc test; **P* < 0.05, ***P* < 0.01, n= 6 mice per genotype). **d**, Higher magnifications of IHC of Cux1+ cells (green) showing neuronal nuclei invasion of Layer I in control (fR/fR, top) and Reelin deficient mice (Cre fR/fR, bottom) at P15 Scale bar=100 µm. **e**, Representative photomicrograph showing CTIP2 (green, lower layers) cortical distribution at P15 in control (fR/fR, left) and Reelin deficient mice (Cre fR/fR, right) Scale bar=100 µm. **f**, IHC of Tbr1+ cells (green) at p15 in control (fR/fR, left) and Reelin deficient mice (Cre fR/fR, right) Scale bar=100 µm. **g**, Quantification of the percentage of Tbr1+ cells *per* bin (data represents mean ± s.e.m; Bin x Genotype Interaction n.s. n= 4 mice per genotype). **h**, Representative confocal images of the cingulate cortex immunostained with Cux1 (green) in control (fR/fR, top) and Reelin deficient mice (Cre fR/fR, bottom) at P15. Scale bar = 100 µm low magnification image and 50 µm high magnification image. I, Cortical Layer; II-III, Layers II-III; IV, Layer IV; V, Layer V and VI, Layer VI.

3.3. Reelin depletion in adult brains reveals a novel function of Reelin as a stop signal for cortical neurons.

To get insight into how the disruption of the Reelin signaling pathway could regulate structural plasticity during adulthood, we evaluated sections of adult Cre fR/fR mice for altered cytoarchitecture. Analysis of cortical lamination, centered in the primary somatosensory cortex, revealed the ectopic invasion of NeuN+ neurons **(Figure R.3.4.a)** in the layer I of the cortex in the Cre fR/fR mice.

To determine the identity of these neurons and further characterise the overall organization of cortical neurons in adult deficient mice, sections were stained with layer-specific markers for upper and lower layer neurons. In line with the results observed at P15, postmitotic neurons that distinctively invaded layer I, were Cux1+ neurons. In addition, an upward shift of the layer II-IV neurons was also detected **(Figure R.3.4.c** and **Figure R.3.4.d)**. In contrast to the observed phenotype at P15, the presence of neurons in layer I of Cre fR/fR mice was often uneven, forming large intermittent clusters of cells that conferred a rugose aspect to the surface of the cortex. Nevertheles, conversely to the examination conducted in P15 mice, the altered phenotype of late-born cortical neurons in layer I after adult depletion of Reelin, was not homogeneous throughout the cortex, but was particularly frequent in the somatosensorial and cingulate cortices **(Figure R.3.4.b)**. Examination of lower layer cortical neurons revealed no major differences in the distribution of CTIP2+ labeled cells between Cre fR/fR and control mice, however, a slight upward shift of CTIP2+ cells was confirmed in layer V in Cre fR/fR mice **(Figure R.3.4.e** and **Figure R.3.4.f)**.

To further confirm the defects in cortex lamination and to decipher the origen of misslocated neurons in layer I, we performed birth-dating experiments. BrdU injections were performed in time-mating controlled pregnant females from E14.5 to E15.5, in order to ensure the proper labeling of upper layer cortical cells. Effect of Reelin depletion was assessed in early postnatal (when tamoxifen was injected at P1-P3) and in later postnatal (in the case of tamoxifen injections at P20) stages and the resulting offspring was then sacrificed at P15 and P60 respectively. Analysis of cell distribution revealed the presence of double labeled Cux1+/BrdU+ cells in layer I in Cre fR/fR mice after supression of Reelin at early postnatal **(Figure R.3.4.g)** and adult stages **(Figure R.3.4.h)** confirming that these ectopic neurons corresponded to layer II-III neurons, supporting the embryonic origen of ectopic migrated neurons. In addition, experiments depleting Reelin at adult stages and birth-dating BrdU for several days after Reelin removal demonstrated that neurons invading layer I were not new born neurons **(Figure R.3.4.i)**.

Therefore, all these results suggest that Reelin signaling is essential to maintain the cortical cytoarchitecture during all phases of neuronal migration, including late migratory processes in the cortex, but also to ensure the structural plasticity on adult brain.

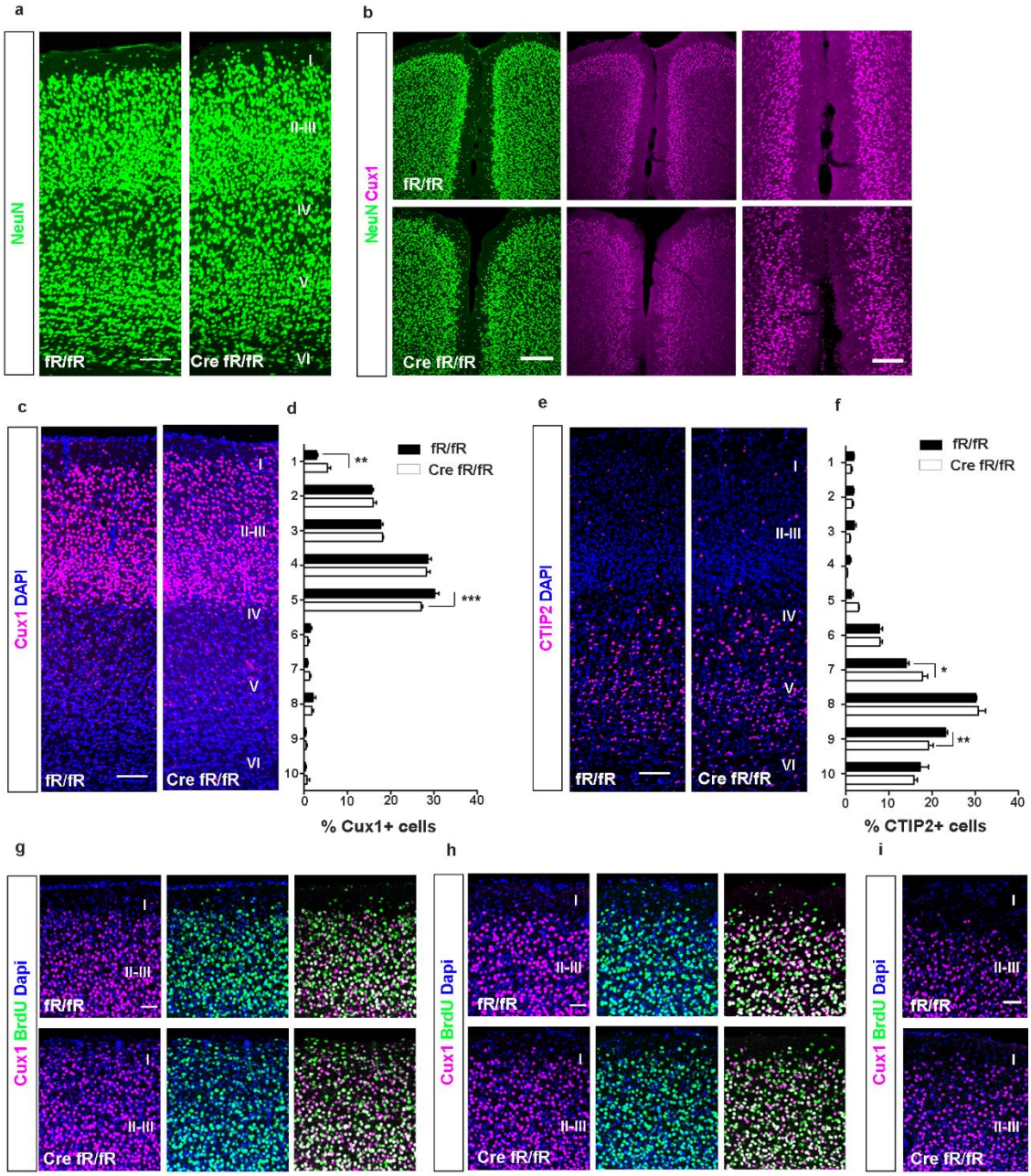

Figure R.3.4. | Reelin depletion at adult stages alters the distribution of cortical cells in the primary somatosensorial cortex. a, Representative adult mice confocal images illustrating the cortical distribution of NeuN+ green, all neurons) in control (fR/fR, left) and Reelin deficient mice (Cre fR/fR, right). Scale bar= 100 µm. **b**, Detail of the cingulate cortex stained with NeuN (green) and Cux1 (magenta) in the presence (fR/fR, top) and absence of Reelin (Cre fR/fR, bottom). Scale bar= 200 µm low magnification and 100 µm high magnification. **c**,Representative confocal images depicting the cortical distribution of Cux1+ (magenta, upper neurons) in the presence (fR/fR; right) and absence (Cre fR/fR; left) of Reelin. Scale bar=100 µm. **d**, Quantification of the percentage of Cux1+ cells *per* bin (data represents mean ± s.e.m; Bin x Genotype Interaction F(9, 80)= 3.569 p=0.0009; Two-way ANOVA with Bonferroni post hoc test; $^{**}P < 0.01$; $^{***}P < 0.001$, fR/fR n= 5 and Cre fR/fR n=5). **e**, Representative photomicrograph showing CTIP2 (green, lower layers) cortical distribution in control (fR/fR, left) and Reelin deficient mice (Cre fR/fR, right) Scale bar=100 µm. **f**, Quantification of the percentage of CTIP2+ cells *per* bin (data represents mean ± s.e.m; Bin x Genotype Interaction F(9, 80)= 3.569 p=0.0009; Two-way ANOVA with Bonferroni post hoc test; $^{*}P < 0.05$; $^{**}P < 0.01$, fR/fR n= 5 and Cre fR/fR n=5). **g,**

Representative confocal images of P15 mice showing the cortical distribution of Cux1+ (magenta, upper layers, left), BrdU+ cells (green, cells born between E14.5 and E15.5, center) and the merge of CUX1 and BrdU (right) in control (fR/fR, top) and early postnatal (TMX p1-p3) Reelin deficient mice (Cre fR/fR, bottom). Scale bar=50. **h**, Representative confocal images of P60 mice illustrating the cortical distribution of Cux1+ (magenta, upper layers, left), BrdU+ cells (green, cells born between E14.5 and E15.5, center) and the merge of CUX1 and BrdU (right) in control (fR/fR, top) and late postnatal (TMX p20-p30) Reelin deficient mice (Cre fR/fR, bottom). Scale bar=50 µm. **i**, Double IHC of BrdU (green) and Cux1 (magenta) of adult depleted Reelin mice injected with BrdU after Reelin removal. Scale bar=50 µm. I, Cortical Layer; II-III, Layers II-III; IV, Layer IV; V, Layer V and VI, Layer VI.

The effect on cell distribution is independent of the total number of cells or the cortex width, since these variables do not present statistically significant differences between genotypes **(Table R.3.1)**.

		fR/fR	Cre fR/fR
a	**Number of Cux1 cells at P15**	190,9 ± 16,15	227,9 ± 28,16
	Width (µm)	1156 ± 37,59	1247 ± 33,52
b	**Number of Cux1 cells adult**	125,7 ± 5,726	133,7 ± 4,436
	Width (µm)	1113 ± 25,12	1136 ± 23,26
c	**Number of CTIP2 cells adult**	50,92 ± 3,632	53,24 ± 3,685
	Width (µm)	1038 ± 25,36	1103 ± 31,82

Table R.3.1. | Mean of the number of cells and width (in microns) of the cortical region of interest (ROI) measured for each group of experiments. a-e, Quantification of the average number of neurons and cortical thickness in control (fR/fR; left) and Reelin deficient mice (Cre fR/fR; right). Data represents mean ± s.e.m, Unpaired two-tailed Student's t-test. **a**, for cell number (t= 1.139 df= 10 p= 0.2814, n.s. n=6 fR/fR and 6 Cre fR/fR) and for width (t= 1.799 df= 10 p= 0.1022, n.s. n=6 fR/fR and 6 Cre fR/fR). **b**, for cell number (t= 1.105 df= 8 p= 0.3015, n.s. n=5 fR/fR and 5 Cre fR/fR) and for width (t= 0.6746 df= 8 p= 0.5189, n.s. n=5 fR/fR and 5 Cre fR/fR). **c**, for cell number (t= 0.4428 df= 7 p= 0.6713, n.s. n=4 fR/fR and 5 Cre fR/fR) and for width (t= 1.545 df= 7 p= 0.1662, n.s. n=4 fR/fR and 5 Cre fR/fR).

3.4. Conditional loss of Reelin causes structural alterations in the hippocampus.

We next analyzed the contribution of postnatal Reelin signaling to the formation of the hippocampus. First, we started analyzing the general structure of the hippocampus by using immunofluorescent detection of NeuN neurons **(Figure R.3.5.a**, top pannels**)**. Whereas no effects were found in fR/fR hippocampus, with the main subdivisions being recognizable, NeuN staining reveals major alterations in the hippocampal morphology of Cre fR/fR mice resembling those observed in the *reeler* mice. The confined pyramidal layer of the Cornus Ammonis was clearly disorganizated in Cre fR/fR mice, with some pyramidal neurons ectopically placed in so and sr. In addition, a remarkable presence of ectopic small islands of NeuN neurons in the white matter, the region that separates the cortex and the hippocampus, were observed in Cre fR/fR hippocampus. Another striking alteration was observed in the emerging granular cell layer of Cre fR/fR mice. Analysis of granule cells by Calbindin (Calb) immunostaining showed that in Cre fR/fR mice, granule cells fail to form a well delineated infra- and supra-pyramidal blades and granular cells appeared homogenously distributed along the entire hilus **(Figure R.3.5.a**, bottom pannels**)**. The observed disorganized hippocampus resembles to *reeler*-like phenotype and is consistent with the late development of this particular structure.

To analyze whether Reelin signaling plays a role during adulthood in the maintenance of hippocampal laminated structures, adult mice were sacrificed 3-4 months after tamoxifen injection. No major lamination defects were observed in a gross analysis of the hippocampus morphology, neither in the CA1 pyramidal layer nor in the DG **(Figure R.3.5.b)**. In the case of the GCL, granular cells labeled with Prox1 antibody appeared to be packed in blades **(Figure R.3.5.c)** with a total area similar between control fR/fR and Cre fR/fR mice (143394 ± 13475 vs 143010 ± 6346; Data represents mean ± s.e.m, Unpaired two-tailed Student's t-test p=0.9803 t=0.02577 df= 6, n=4 *per* genotype). However, a significant increase in the number of Prox1 positive cells appeared ectopically located in the hilus, specially in the lower half of the hilus in Cre fR/fR mice **(Figure R.3.5.d)**.

These results suggest a role of Reelin in granule cell migration and DG layering maintenance.

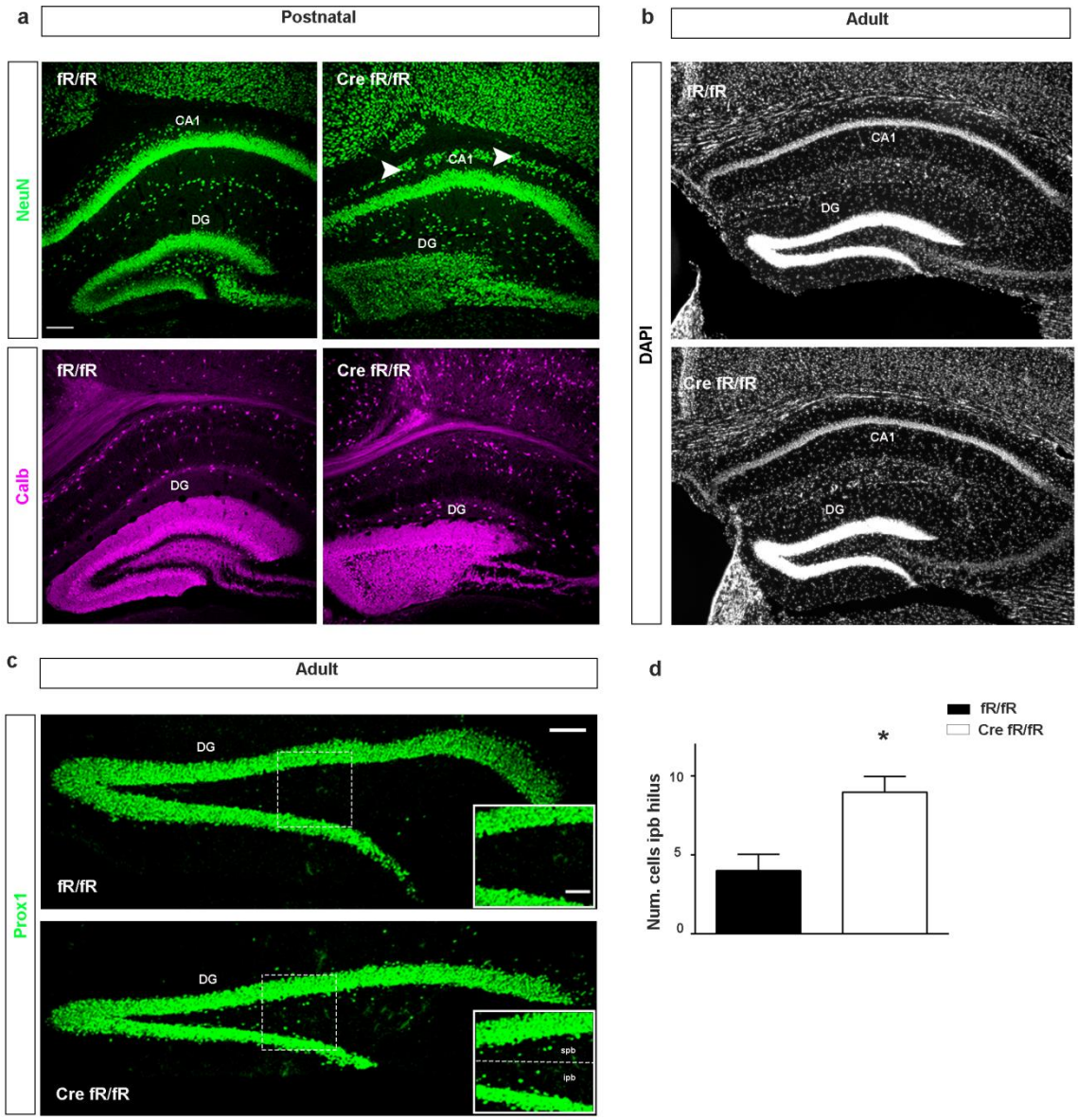

Figure R.3.5. | Conditional Reelin removal affects hippocampal cytoarchitecture. **a**, Representative hippocampal images immunostained with NeuN (top, green) and Calbindin (bottom, magenta) in the presence (fR/fR, right) or absence of Reelin (Cre fR/fR, left). Scale bar=100 µm. **b**, Representative confocal images of hippocampus (DAPI) in control (left) and Reelin deficient mice (right). **c**, Dentate gyrus Prox1+ cells in control (top) and Reelin deficient mice (bottom). Scale bar= 100 µm low magnification and 50 µm high magnification. **d**, Quantification of the number of Prox1+ cells misslocated in the lower blade hilus (data represents mean ± s.e.m; Unpaired t-test t= 3.452 df= 6 p= 0.0136, n= 4 fR/fR and 4 Cre fR/fR). CA1, Cornus Ammonis 1; DG, Dentate Gyrus; Calb, Calbindin; UB. upper blade; LB, lower blade.

3.5. Loss of Reelin during adulthood influences adult neurogenesis in the DG.

Previuos studies have suggested a posible role of Reelin in DG neurogenesis. In addition, despite *reeler* mice present reduced neurogenesis, these mutants display dramatic developmental alterations in the layering of the hippocampus (Forster et al., 2002) and consequently are not adequate to study the effects of the absence of the Reelin signaling pathway specifically on adult neurogenesis. To unravel the possible role of Reelin in adult neurogenesis in the SGZ of the DG we took advantage of conditional Cre fR/fR mice and analysed the different stages of the neurogenic process in adult mice.

First, we aimed to determine if proliferation in the SGZ of the DG was altered in the absence of Reelin in adult mice. Proliferation was analysed in mice injected with BrdU 24 hours before being sacrificed in order to label replicating cells. To ensure that Reelin was completely depleted, BrdU was administered two weeks after tamoxifen injection. The total number of BrdU+ cells in the SGZ of the DG was quantified and no significant differences were found in the total number of proliferating cells between fR/fR and Cre fR/fR mice **(Figure 3.6.a** and **Figure R.3.6.b**, top**)**. However, a number of BrdU+ cells were ectopically located in the hilus of Cre fR/fR mice **(Figure R.3.6.b,** bottom**)**. Thus, the loss of Reelin signaling during adulthood seems to not alter the number of progenitor cells in the DG, but impairs their location in the SGZ.

Once the proliferative stages conclude, the type 3 cells exit the cell-cycle and differenciate into immature GCs. At this time, postmitotic immature neurons start to migrate to their final position within the inner half of the GCL while they establish and receive synaptic contacts to become permanently integrated into the DG network for a long period of time. In order to visualize the effect of Reelin deficiency in the differentiation of DG progenitors an IHC was performed against doublecortin (DCX) to label immature neurons. In fR/fR mice immunoreactive DCX+ cells were found to be well organized, displaying a normal orientation, and located mainly in the inner part of the GCL **(Figure R.3.6.c,** top**)**. However, in Reelin deficient mice, many labeled cells appeared to display abnormal dendritic orientation within the GCL or were even ectopically oriented to the hilus **(Figure R.3.6.c,** bottom**)**. In addition, GC bodies in Cre fR/fR mice tended to be located deeper (toward the hilus aspect) in the GCL and sometimes displayed abnormal clusters or chains of presumptive migrating neuroblasts extending into the hilus from the SGZ. Despite the alterations observed in the morphology of these immature neurons, no differences in the total number and in the number of hilar ectopic DCX labelled cells were observed between genotypes **(Figure R.3.6.d)**.

Although the absence of Reelin in the adult brain did not seem to affect cellular proliferation in the DG, we wanted to explore if its deficiency could alter neuronal fate. By using the BrdU methodology, Reelin deficient mice injected with BrdU were sacrificed two months after injection, allowing the neurogenic process to finish. We performed double IHC against BrdU/NeuN in order to quantify the number of mature new-born neurons born at the same time. No significant differences were obtained in the total number of double BrdU+/NeuN+ cells between fR/fR and Cre fR/fR mice, in line with the proliferation results. To

further examine the involvement of Reelin in the migration of adult new-born neurons we analysed the position of the new-born neurons in the DG. In fR/fR mice, almost the total of cells were appropriately positioned in the GCL. By contrast, the absence of Reelin during adulthood resulted in a lower percentage of integrated newly generated neurons in the GCL and a higher percentage of ectopic newly generated neurons in the hilus of Cre fR/fR mice **(Figure 3.6.f)**. In addition to the position, the distance that neurons migrated from the SGZ through the GCL was measured, and although no statistical differences in the mean migrated distance were found between genotypes, a high percentage of BrdU/NeuN neurons migrated shorter distances compared to control mice **(Figure 3.6.g** and **Figure 3.6.h)**.

These findings indicate that many GCs after Reelin signaling supression, migrate and integrate aberrantly into the adult DG. This observation thus supports the notion that Reelin signaling influences the location, differentiation and migration of adult generated GCs.

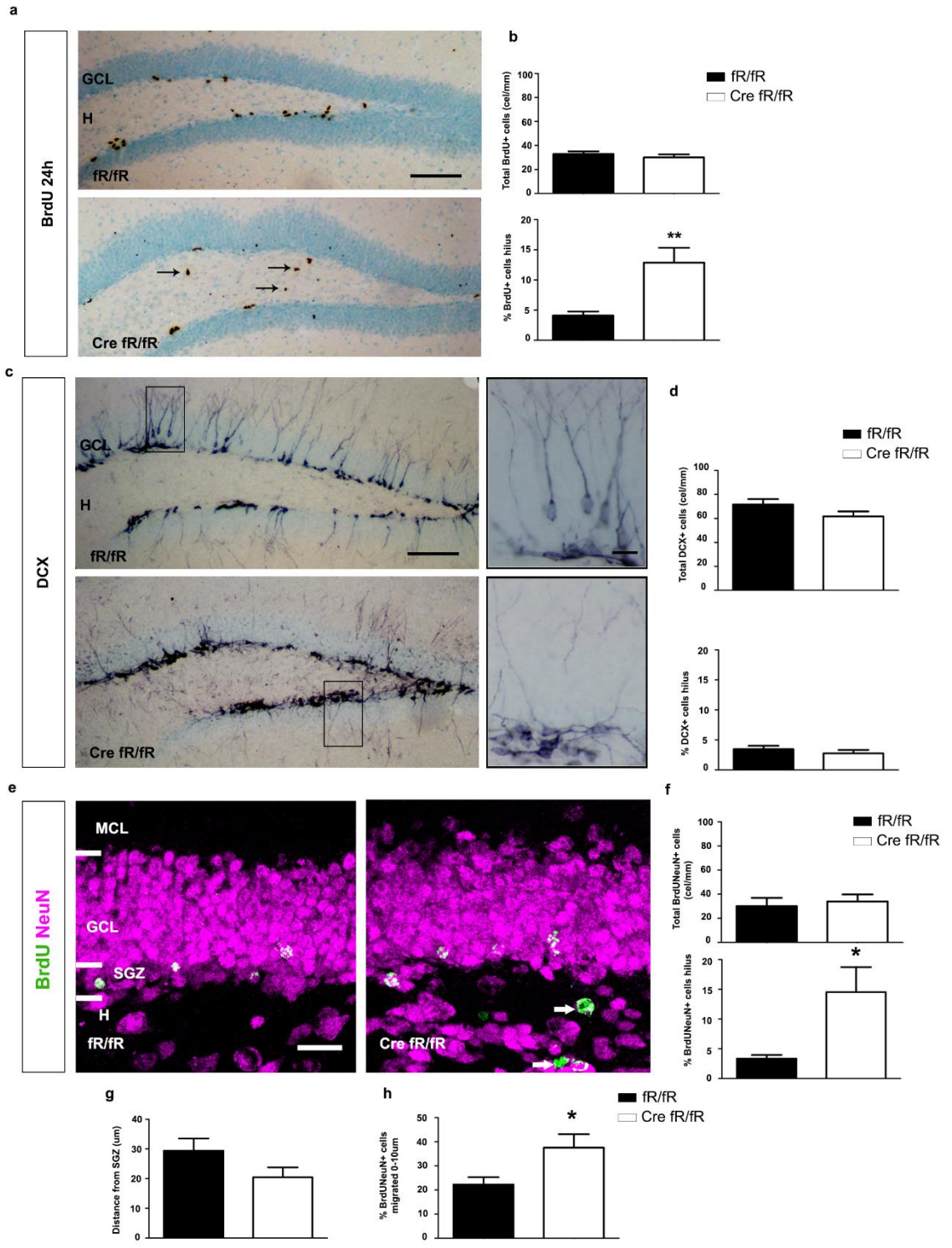

Figure R.3.6. | Effect of Reelin deficiency in adult neurogenesis. a, Immunohistochemical detection of BrdU positive cells in coronal sections of adult mice in the presence (fR/fR, left) and absence of Reelin from the whole brain (Cre fR/fR). All the slices were counterstained with Nissl. Arrows pointing ectopic BrdU+ cells in the hilus. Scale bar= 100 µm. **b**, Quantification of the total number of BrdU+ cells (top, data represents mean ± s.e.m, Unpaired two-tailed Student's t-test; t= 0.8696 df= 14 p= 0.3992, n.s. n=8 fR/fR and 8 Cre fR/fR), and the percentage of ectopic BrdU+ cells in the hilus normalized by the length of the spb of the DG (bottom, data represents mean ± s.e.m, Unpaired two-tailed Student's t-test; t= 3.443 df= 14 p= 0.0040, $^{**}P < 0.01$ n=8 fR/fR and 8 Cre fR/fR). **c**, Immunohistochemical detection of DCX positive neurons in coronal sections of adult

mice in the presence (fR/fR, left) and absence of Reelin (Cre fR/fR) All the slices were counterstained with Nissl. Arrows pointed ectopic BrdU+ cells in the hilus. Scale bar= 100 µm low magnification and 15 µm high magnification. **d**, Quantification of the total number of DCX+ cells (top, data represents mean ± s.e.m, Unpaired two-tailed Student's t-test; t= 1.608 df= 9 p= 0.1422, n.s. n=6 fR/fR and 5 Cre fR/fR), and the percentage of ectopic DCX+ cells in the hilus normalized by the length of the spb of the DG (bottom, data represents mean ± s.e.m, Unpaired two-tailed Student's t-test; t= 0.8452 df= 9 p= 0.4199, n.s. n=6 fR/fR and 5 Cre fR/fR). **e**, Representative images of BrdU+/NeuN+ cells in the DG in fR/fR and Cre fR/fR mice. Arrows pointing ectopically placed double BrdU/NeuN+ cells in the hilus. **f**, Quantification of the total number of double BrdU+/NeuN+ cells (top, data represents mean ± s.e.m, Unpaired two-tailed Student's t-test; t= 0.4123 df= 14 p= 0.6864, n.s. n=9 fR/fR and 7 Cre fR/fR) and the percentage of double BrdU/NeuN+ labeled cells in the hylus, normalized by the DG length (bottom, data represents mean ± s.e.m, Unpaired two-tailed Student's t-test; t= 2.619 df= 6 p=0.0396, $*P < 0.05$ n=9 fR/fR and 7 Cre fR/fR). **g**, Quantification of the mean distance migrated by double BrdU/NeuN labelled somas (Data represents mean ± s.e.m, Unpaired two-tailed Student's t-test; t= 0.4123 df= 14 p= 0.6864, n.s. n=9 fR/fR and 7 Cre fR/fR). **h**, Graph represents quantification of the percentage of new-neurons that migrate short distances (Data represents mean ± s.e.m, Unpaired two-tailed Student's t-test; t= 2.559 df= 14 p=0.0227, $*P < 0.05$ n=9 fR/fR and 7 Cre fR/fR)**.** MCL, Molecular cell layer; GCL, Granule cell layer; SGZ, Subgranular zone; H, Hilus.

3.6. Adult conditional loss of Reelin impairs dendritic orientation and migration of adult-generated GCs.

With the aim of exploring the impact of Reelin deficiency in adult plasticity, we analysed the development of adult-generated neurons at single-cell resolution after injections of GFP-expressing retrovirus (RV) in the DG of adult mice. This technique allows the study of a subset of newly generated neurons of a known age in order to quantify and compare parameters of neuronal maturation and dendritic arborisation. After virus infection, we injected tamoxifen to Cre fR/fR mice at different stages of neuronal maturation (2,4 and 8 weeeks) to assay the effect of Reelin supression in dendritic development. Four weeks after the injection of tamoxifen, mice were sacrificed in all the cases and brain tissue was collected to perform anti-GFP immunostaining. In the case of control fR/fR mice the labeled neurons displayed a normal morphology with predominantly one thick apical primary dendrite extended from the cell body through the GCL and the dendritic tree reaching deep into the molecular layer of hippocampus. In contrast, the Cre fR/fR labellled neurons surpringsily displayed aberrant basal dendrites projecting into the hilus. To substantie this observation, we quantified the number of apical and basal dendrites of GFP-labelled neurons. At all the experimental times analysed, adult-generated GCs in Cre fR/fR mice showed a statistically significant increase in the percentage of basal dendrites, when compared with fR/fR littermates. Moreover, we observed that Reelin depletion at early maturation stages (2 weeks) impaired labeled GC bodies location toward a deeper position in the GCL than in control counterparts as previously observed in the analysis of mature neurons. However, this difference was not detectable after depletion of Reelin at later maturation stages (4 and 8 weeks), once the dendritic tree is already formed and neurons present all the connections and are integrated in the existing circuitry.

These results suggested that the removal of Reelin signaling during adulthood might lead to aberrant positioning of the dendrites towards basal positions, both while adult-generated

neurons are still maturing, and once their maturation process is over. In addition, the loss of Reelin in the early stages of maturation affects the migration of adult generated neurons.

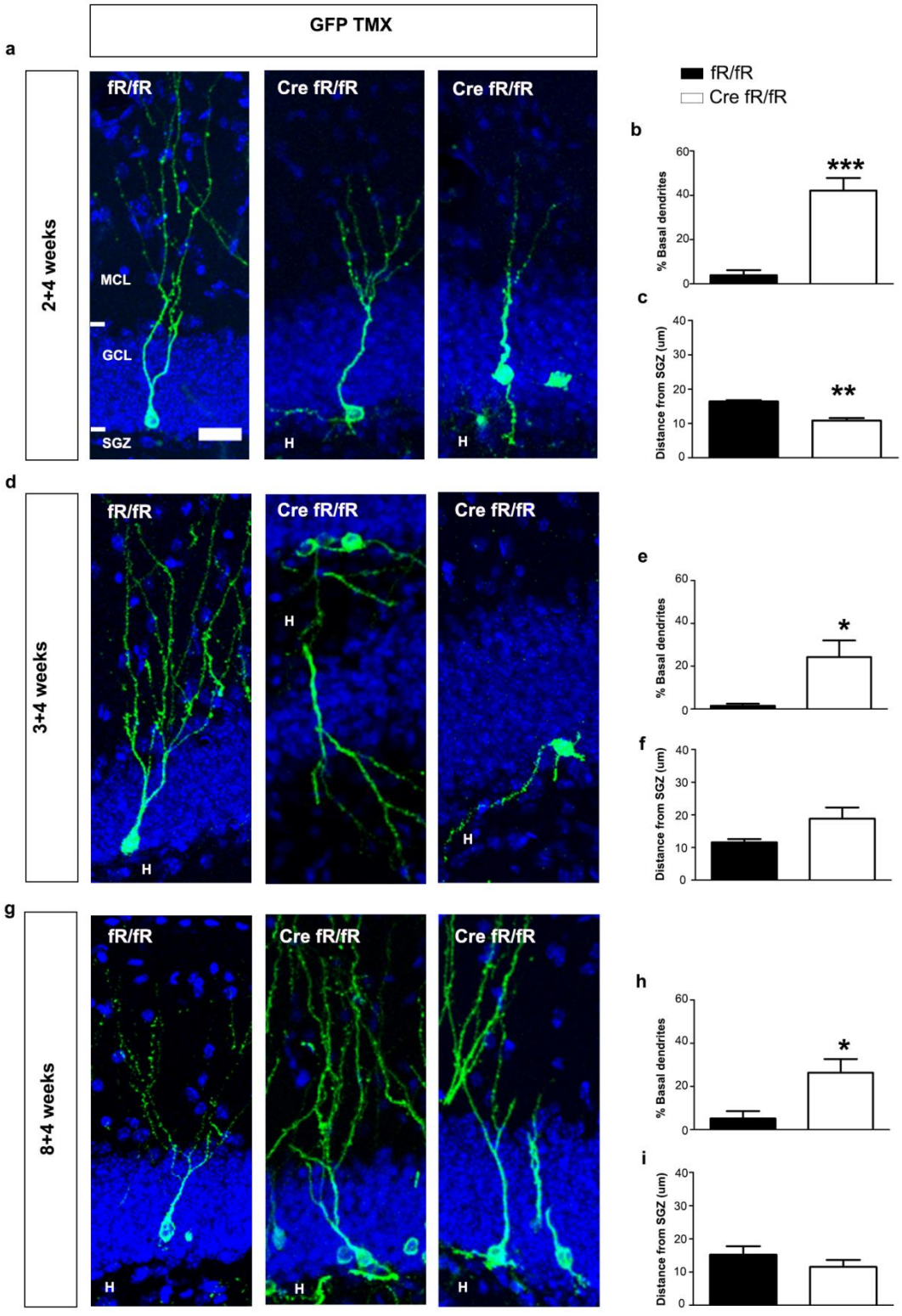

Figure R.3.7. | Effect of the adult conditional loss of Reelin in the dendritic morphology of new generated neurons and their migration at different maturation stages. a,d,g, Representative images of GFP+ labeled cells in the DG of fR/fR (left) and Cre fR/fR (center and right) mice counterstained with DAPI at 2 weeks (**a**), 3 weeks (**d**) and 8 weeks (**g**) after tamoxifen injection. **b,** Quantification of the percentage of apical dendrites of 6 weeks old neurons (Data represents mean ± s.e.m, Unpaired two-tailed Student's t-test; t= 7.163 df= 8 p<0.0001, ***$P < 0.0001$ n=5 fR/fR and 4 Cre fR/fR). **c,** Quantification of the mean distance migrated by GFP+ labelled soma of 6 weeks old (Data represents mean ± s.e.m, Unpaired two-tailed Student's t-test; t= 4.414 df= 8 p<0.0022, **$P < 0.01$ n=5 fR/fR and 4 Cre fR/fR). **e,** Quantification of the percentage of apical dendrites of 7 weeks old neurons (Data represents mean ± s.e.m, Unpaired two-tailed Student's t-test; t= 1.924 df= 8 p= 0.905, n.s. n=5 fR/fR and 5 Cre fR/fR). **f,** Quantification of the mean distance migrated by GFP+ labelled soma of 7 weeks old (Data represents mean ± s.e.m, Unpaired two-tailed Student's t-test; t= 2.210 df= 4 p= 0.0916, n.s. n=5 fR/fR and 5 Cre fR/fR). **h,** Quantification of the percentage of apical dendrites of 12 weeks old neurons (Data represents mean ± s.e.m, Unpaired two-tailed Student's t-test; t= 3.270 df= 6 p= 0.0170, *$p<0.05$ n=5 fR/fR and 3 Cre fR/fR). **i,** Quantification of the mean distance migrated by GFP+ labelled soma of 12 weeks old (Data represents mean ± s.e.m, Unpaired two-tailed Student's t-test; t= 0.9713 df= 6 p= 0.3689, n.s. n=5 fR/fR and 3 Cre fR/fR). MCL, Molecular cell layer; GCL, Granule cell layer; SGZ, Subgranular zone; H, Hilus.

3.7. Lack of Reelin impairs correct positioning of Purkinje cells in the cerebellum.

Ataxia in *reeler* mice results from a severe disorganization of the cerebellum, which present a severely diminished size without foliation derived from the reduction in the number of both granule and Purkinje cells (Rahimi-Balaei, Bergen, Kong, & Marzban, 2018) (Curran & D'Arcangelo, 1998) (Forster et al., 2006). In our mutant mouse model histological studies at P15 of the cerebellar foliation pattern revealed no major alterations at the level of foliation **(Figure R.3.8.a** and **Figure R.3.8.b)** between control fR/fR and Reelin deficient Cre fR/fR mice. However, in the cerebellum of Cre fR/fR mice many of the lobules displayed an irregular disposition of Purkinje cells (PC), whose severity varied according to the folia. Specially in VI-VII and IX-X folia, PCs location was severely disrupted with PC ectopically located underneath and in between the GCL, whereas in the medial III-V folia, PC appeared only partially misslocated. Anaysis of PC in the lateral folia, in which delamination is known to occur at later stages during postnatal development, showed all the lobules severely disrupted. Conversely, the granular cell disposition remained unaltered and well delimited in the whole of the cerebellum in the Cre fR/fR mice.

Analysis of the cerebellar laminar structure after Reelin depletion in adult mice demonstrated no major lamination defects **(Figure R.3.8.c)**. However, analysis of Purkinje cells disposition within the PC monolayer demonstrated that arround 30% of these PCs were misslocated in Cre fR/fR cerebellum when compared with fR/fR mice **(Figure R.3.8.d)**. Many of those cells were ectopically located in the GCL of Cre fR/fR mice, but accordingly with the previous results obtained after postnatal Reelin depletion, the PC distribution was not so milder in adult stages. Despite PC disorganization in Cre fR/fR mice, these mice did not show ataxia or apparent motor problems, which are features of *reeler* mice.

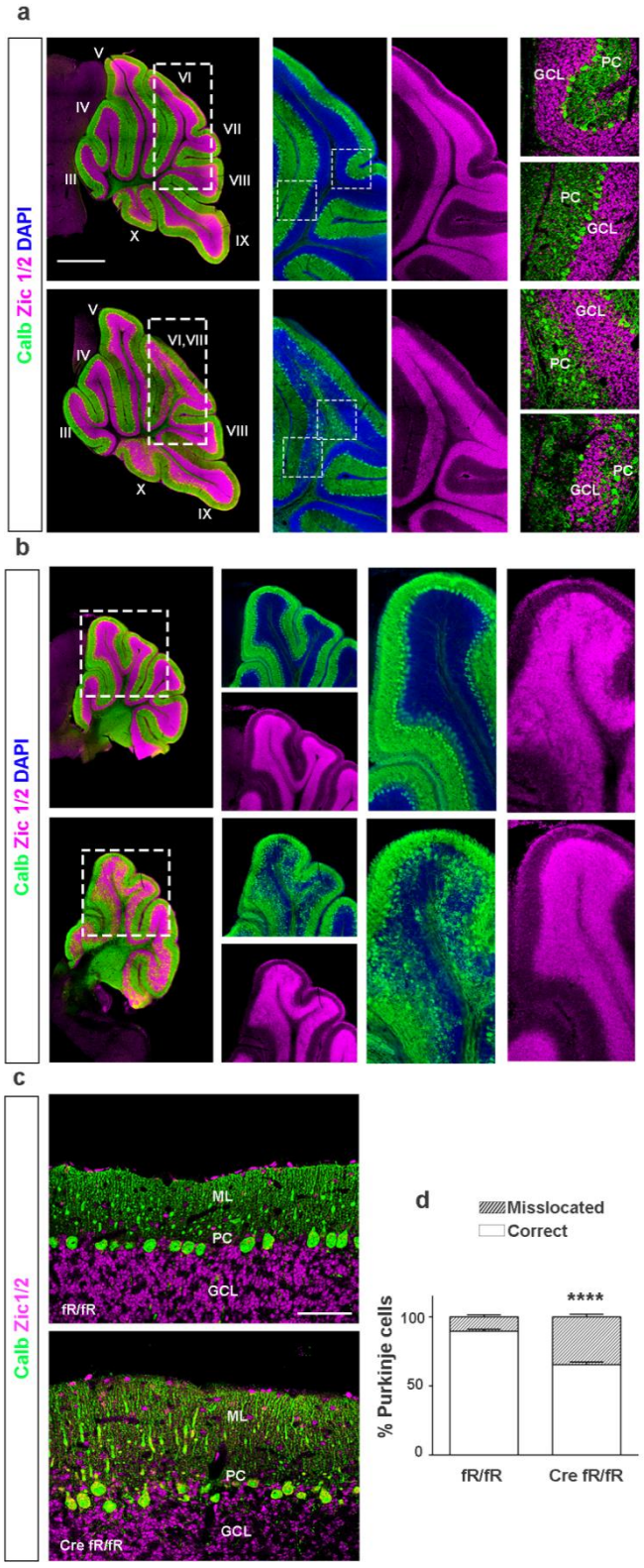

Figure R.3.8. | Cerebellum structure after Reelin depletion in postnatal and adult stages. **a-b**, Representative confocal images of the cerebellum distribution of Calbindin+ (Purkinje cells, green) and Zic 1/2+ cells (granule cells, magenta) at P15 in control (fR/fR, top) and Reelin deficient mice (Cre fR/fR, bottom) in vermis sections (**a**) and lateral cerebellum (**b**). Scale bar=700 µm. **c**, Representative confocal images of the cerebellum distribution of Calbindin+ (Purkinje cells, green) and Zic 2/3+ cells (granule cells, magenta) in adult control (fR/fR, top) and Reelin deficient mice (Cre fR/fR, bottom). **d**, Quantification of the percentage of Purkinje cells (Calbindin+, green) positioned properly in the Purkinje layer (correct) and misspositioned outside the Purkinje layer in adult mice (data represents mean ± s.e.m; Unpaired t-test t= 8.335 df= 17 ****p<0.0001, n= 10 fR/fR and 9 Cre fR/fR). GCL, Granular Cell Layer; PC, Purkinje Cells.

DISCUSSION

1. Role of Reelin in corticogenesis

Since its discovery (Falconer, 1951) the *reeler* brain phenotypes has been extensively studied. Several mouse models have been employed to analyse the contribution of Reelin signalling in the brain, including the Reelin deficient *reeler* mice (D'Arcangelo *et al.*, 1995), mice lacking one or two of the Reelin receptors VLDLR and ApoER2 (Hirota *et al.*, 2018) or mouse models with disrupted intracellular Dab1 protein (Teixeira *et al.*, 2012). However, nowadays several questions remain still unclear about how does Reelin influence neocortical neurons. The functions proposed for Reelin signalling include a permissive or attractive signal for migration and a guidance or positional signal (including stop signal). By using three new transgenic mouse models we have studied the specific role of Reelin selectively expressed by Calretinin positive cells or by Gad65 interneurons during corticogenesis as well as the role of Reelin in corticogenesis at different developmental stages and in the adult brain with the inducible mouse model.

1.1. PP splitting seems to occur normally after Reelin depletion from Calretinin positive cells.

During corticogenesis, the PP splitting is a crucial event that allows the organization of the mammalian cortex in birth-dependent inside-out manner. Once this process occurs, the superficial MZ and the SP remain separate after the incorporation of newly generated Layer VI neurons in the CP. CRC, the main population in the MZ, express Reelin protein, which has been suggested to direct both the PP splitting itself and the posterior migration and establishment of the cortical neuronal layers (Hirota & Nakajima, 2017)(Sekine *et al.*, 2014)(Chai & Frotscher, 2016).

To confirm that Reelin expressed by CRC plays a role in PP splitting, in neuronal migration and in neocortical lamination, we generated the CR fR/fR line. Once validated the model by the effective disappearance of Reelin from Calretinin positive cells, we explored the cortical layering at different stages during neocortical development. Our results from CR fR/fR mouse model suggest that PP splitting might be happening normally after Reelin suppression from CRC. First, immunofluorescence analysis of Calretinin positive cells in CR fR/fR mice, demonstrated that these cells, despite were Reelin negative, appeared in the MZ during all the developmental stages analysed. Second, observation of cortical neuronal distribution at E16 revealed that, unlike *reeler* mice, deeper layer neurons, recognizable by CTIP2 staining, were located underneath of upper layer neurons, labelled with Cux1 antibody. Moreover, the characteristic invasion of MZ by layer VI neurons in *reeler* cortices was not observed in CR fR/fR mice. However a transient number of Cux1 positive neurons overmigrated into MZ. Therefore, our results with the CR fR/fR mouse model pointed to a different interpretation of the role of Reelin-expressing CR cells during corticogenesis.

The expansion of the CRC layer during the growth phase of the cortex development is dependent on reciprocal interactions between CRC and ECM components and/or glia cells. Besides Reelin expressed by CR being the major component, the MZ contains other ECM

molecules that have been implicated in the organization of the MZ. In addition, previous studies have shown that meningeal cells also express ECM components that are essential for the assembly of the meningeal basement membrane. Notably, the defective anchorage of RGC processes to the meningeal surface is able to induce deficiencies in neuronal positioning including neuronal invasion to the MZ. Among the different ECM components, Lama-2 and Lama-4 participate in the attachment of the radial glia processes to the pial surface. Specifically, expression of Lama-4 has been reported to be regulated by vascular Reelin signalling. Moreover, β1 integrin, which is expressed by cortical neurons and glial cells has been shown to regulate glial end feet anchorage, the assembly of the meningeal basement membrane and the formation of CRC layer. Thus, either the presence of Reelin in the vessels from a different source to CRC or the contribution of different ECM components, could explain how in the CR fR/fR mice PP splitting occurs (Segarra *et al.*, 2018)(Graus-Porta *et al.*, 2001)(Franco & Muller, 2011)(Chai & Frotscher, 2016).

Another noticeable feature observed in CR fR/fR was the absence of the characteristic outside-in lamination of *reeler* cortices. In Reelin deficient mice, pyramidal layer VI neurons appear located in the outermost part of the cerebral cortex, in close proximity to the pial surface, even invading the MZ, demonstrating a failed formation of the CP during PP splitting. Exists some controversial about how the CP formation occurs, and two different models have been proposed to account for the appearance of layer VI cortical neurons within the PP. Some data suggests that PP splitting takes place after reorganization of Layer VI cortical neurons that are distributed in the PP intermixed with Calretinin expressing PP neurons. An alternative theory suggests that layer VI cortical neurons rapidly move from VZ into the PP by somal translocation. In any case, PP splitting seems to be initiated by the polarized dendritic growth of layer VI neurons (Olson, 2014). Compelling evidences support that functional ApoER2 is present in these premigratory neurons, suggesting a role of Reelin in neuronal polarization of early generated neurons through the activation of Dab1-Crk/CrkL-C3G-Rap1/Cdc42 pathway, which in turn controls cytoskeleton dynamics. In addition, the presence of the so called ‘’deep’’ Reelin in the lower IZ/VZ by an unknown source different from CRC has been also reported (Uchida *et al.*, 2009)(Yoshida *et al.*, 2006) (Sekine *et al.*, 2014). Thus, in line with our results, the deep Reelin present in the IZ/VZ could be responsible of PP splitting, more than Reelin expressed by CRC.

1.2. Loss of Reelin from Calretinin positive cells triggers defective migration of CP neurons without *reeler*-like layer inversion.

A general disposition of Cux1 and CTIP2 positive neurons in the upper and the lower part of the CP respectively, was recognizable in CR fR/fR mice at E16, and P1, suggesting that some later-born neurons were able to migrate long distances going through early-born neurons. However, some defects in cortical distribution were observed. Particularly, analysis of CR fR/fR embryos showed an upward shift of later-born neurons. Furthermore, a number of Cux1 and CTIP2 positive neurons failed to migrate and remained in the IZ. These observations suggest specific functions of Reelin expressed by CRC in somal and terminal translocation rather than in locomotion.

Deeper layer neurons, including layer V-VI neurons, migrate using somal translocation instead of locomotion mode to occupy their final position in the CP. During somal translocation, deeper layer neurons extend a leading process to the MZ, where they contact with CRC, triggering the shortening of the leading process. In this process, Reelin controls the actin cytoskeleton via cofilin and the N-cadherin-mediated stabilization of the leading process, but also regulates the cellular interactions between migrating neurons and CRC through nectin-mediated cellular interactions (Hirota & Nakajima, 2017)(Santana & Marzolo, 2017). We hypothesize that early-born neurons in CR fR/fR mice were able to extend a leading process. However, the absence of Reelin from CRC, could prevent the expression of the nectin system and consequently their contact with the leading process, triggering the overmigration of CTIP2 neurons that occupied a higher position in the CP. As we mentioned before regarding layer VI neurons, a possible explanation is that deep Reelin was enough to induce the formation of the leading process and the expression of N-cadherin in the membrane of migrating neurons.

At stages, upper layer neurons change their migration modes. First, multipolar postmitotic neurons become bipolar in the IZ with a defined leading process and a trailing axon and start radial migration. During polarization, Reelin signalling influences the expression of N-cadherin and the control of the actin cytoskeleton necessary for neuronal migration in the IZ. As we proposed above, the presence of Reelin in the IZ/VZ could be sufficient to allow migration of newly-generated neurons in the absence of Reelin from CRC. However, the abnormal migration defects observed at E16 differ between early and late-born neurons. Whereas CTIP2 neurons occupied a more confined layer, Cux1 neurons were widely distributed through all the cortical layers. Since downregulation of N-cadherin results in a delay of polarization and migration, it is conceivable that a delay in migration may occur in CR fR/fR mice, and thus, Cux1 positive cells present in the lower part of the CP at E16 correspond to cells that are still migrating. Another possible hypothesis is the consumption of Reelin protein in the IZ/VZ. Despite the presence of the Reelin-expressing cells in the IZ/VZ, the protein levels detected are very faint and Reelin seems to be only transiently expressed (Yoshida *et al.*, 2006). Supporting this hypothesis, we found defects in the polarization of neurons born at E14 in the lower part of the neocortex after electroporation in CR fR/fR mice. GFP-labelled neurons that reached the upper part of the CP showed a defined leading process, although in some cases they were missaligned and failed to reach the MZ. However, neurons retained in the lower part of the CP showed a multipolar morphology in which the leading process was not clearly distinguishable.

Then, bipolar neurons, with one extending leading process, start to move through CP using the locomotion mode which is RG-dependent migration (Chai & Frotscher, 2016). A number of studies have shown that Reelin signalling is not required for glia-guided locomotion (Sekine *et al.*, 2011). In addition, locomotion alone is not sufficient to establish the proper inside-out structure of the cortex. Finally, when migrating neurons arrive beneath the outermost region of the CP, the MZ, they transiently pause their migration within the primitive cortical zone and switch to terminal translocation mode. Our studies suggest that Reelin expressed by CRC is not necessary for glial-guided motility, since Cux1 positive neurons were able to migrate long distances and appeared distributed along the entire cortex. However, the presence of Reelin in the MZ seems to be essential as stop signal during terminal translocation in the final stages of cortical migration, avoiding overmigration. Thus we can conclude that layer order does not depend exclusively of Reelin expressed by CRC in the MZ of the neocortex. However it influences layer refinement.

1.3. Reelin in the ourtermost part of the cortex acts as stop signal during development and in adult stages.

To investigate the effects of Reelin deficiency in the early postnatal development we generated the inducible conditional transgenic model (Cre fR/fR). It represents a suitable animal model to bypass the deleterious consequences of the embryonic absence of Reelin in the developing brain. To unravel the function of Reelin at this period, depletion of Reelin was induced by tamoxifen administration to newborn (P1 to P3) pups that were then sacrificed at P15. Once confirmed the completely disappearance of Reelin protein at P6 by WB and further validated by Reelin IHC at P15, we analysed the neuronal cortical distribution. Observations of the laminar structure of the cortex, centred upon the primary somatosensory cortex, revealed a displacement of upper-layer neurons (Cux1), but not lower-layer neurons (Trb1, CTIP2). Remarkably, Cux1 positive neurons were shifted upwards and ectopically over migrated in the cortical layer I. This results suggest that Reelin deficiency during early postanatal stages specifically alters the migration and positioning of late born neurons.

Interestingly, at this particular stage, the expression pattern of Reelin changes. Whereas the main population of Reelin-expressing cells in the neocortex, the CRC, disappear during the first postanatal weeks, a number of GABAergic interneurons distributed along the cortex start to express Reelin, becoming the main source of this protein in late postnatal and adult stages (Knuesel, 2010) (Wasser & Herz, 2017)(Jossin & Goffinet, 2007)(Alcantara *et al.*, 1998).

To decipher the function of Reelin selectively expressed by GABAergic interneurons we generated the Gad fR/fR mouse model. Once validated the model, we analysed the cortical distribution of upper and lower layer neurons. Whereas no differences were observed at E16 between controls and Gad fR/fR mice, at P1, Cux1 staining displayed a dense packed band in the upper boundary of the layers that they are normally destined to. Furthermore, analysis of the cortical distribution at later stages in Gad fR/fR mice, from P15 onward, showed a remarkable overmigration of Cux1 labeled neurons in cortical layer I, which is usually a cell sparse layer.

The observed results of over-migration of upper-layer neurons is consistent with the hypothesized role of Reelin as a stopping signal in migration during terminal translocation. Once the leading process of migrating postmitotic neurons reaches the MZ, neurons detach from their glial scaffold and the soma moves rapidly toward the top of the CP within the PCZ. In the PCZ, locomoting neurons stop transiently before change their migratory mode to terminal translocation. The thickness of the PCZ structure is similar to the distance of terminal translocation, that in turn counterparts the length of the leading process (Forster *et al.*, 2010) (Sekine 2014). Interestingly, the PCZ is a transitory cell dense region where immature migrating neurons differentiate into mature neurons, and then a new PCZ is formed with a new batch of migrating neurons, from inside-to-outside.

Thus, two requirements are necessary for migration arrest in the cortex. First, migrating neurons have to detach from the radial glial scaffold. Second, the cytoskeleton of migrating neurons should be stabilized to allow polarized dendritogenesis. The detachment function of Reelin is likely to be mediated by α3β1 integrin interactions. Reelin-mediated reorganization of actin and microtubules cytoskeleton has been demonstrated to be essential during cortical dendritogenesis and migration arrest. On the one hand, Reelin signalling stabilizes the leading process of migrating neurons, likely by stabilizing the actin cytoskeleton, allowing the proper anchorage of the leading process to the MZ. This function seems to be mediated by cofilin (via LIM-K). Thus, the phosphorylated form of cofilin, which is inactive, stabilizes the leading process. In the MZ high levels of p-cofilin are found, whereas in *reeler* cortices, this level is down-regulated. It has been proposed that cofilin phosphorylation is induced after binding of Reelin to ApoER2. On the other hand, stability of microtubule cytoskeleton is controlled by Reelin-mediated dephosphorylation of tau. In *reeler* mice, increased activity of GSK3β (the main kinase of tau) as well as hiperphosphorylated tau, result in destabilization of the tubulin cytoskeleton. Furthermore, abnormal arrangement of MAP2 in dendritic processes has been shown in models of defective Reelin signalling (Jakob *et al.*, 2017)(Zhao & Frotscher, 2010).

However, additional mechanism seem to be required to act as a stop signal. Previous reports have suggested that Reelin also controls nuclear translocation in the final phase of migration by regulating Lis1 function. Lis1 acts by stabilizing the microtubules through its binding to the Pafah1b complex. After Dab1 phosphorylation induced by the binding of Reelin to VLDLR, the Reelin-VLDLR complex is endocyted. At the same time, Pafah1b complex which is able to bind the citoplasmatic domain of VLDLR but not ApoER2, may displace phosphorylated Dab1 from its binding site on VLDLR, and promote its interaction with Lis1. Thus Reelin seems to stabilize actin cytoskeleton by its binding to ApoER2 (mainly localized in the soma) and the microtubule cytoskeleton through the binding of VLDLR (which is preferentially placed in the distal portion of the leading process), promoting nuclear translocation. In addition, the Reelin ApoER2-induced activation is not accompanied by a reduction of Reelin, whereas binding of Reelin to VLDLR rapidly induce the internalization of the Reelin/VLDLR complex. Then, endocytosis of the Reelin/VLDLR complex results in a rapid local decrease of extracellular Reelin and the proteasome degradation of Dab1 signalling via SOCS7-Cul5-Rbx2, which have been suggested to prevent neuronal overmigration (Hirota & Nakajima, 2017)(Sekine *et al.*, 2011)(Chai & Frotscher, 2016).

1.4. Reelin is required for the maintenance of cortical layering in the adult.

One of the most interesting results derived from this thesis, was the observation of Reelin influence in a novel form of cortical plasticity. Taking advantage of the newly generated Cre fR/fR mice, we depleted Reelin signalling during adulthood. Surprisingly, we observed the presence of adult postmitotic neurons invading the layer I. Despite this novel phenotype was not as strong as the overmigrated phenotype observed at postnatal stages, this findings highlight that Reelin signalling is indeed required for the maintenance of the cortical cytoarchitecture in the adult brain.

As we mentioned above, Reelin signalling has been shown to regulate the stabilization of the actin and microtubule cytoskeleton. Thus, we suggest that Reelin deficiency during adulthood could induce cytoskeleton disorganization. However, two different hypothesis could explain the presence of layer II-III neurons in the outermost part of the cortex. The first one is that as a result of the cytoskeleton destabilization, the dendritic trees become disordered and dendrites retract, losing their arborisation. Consequently, the cortical layer I, that consists mostly of neuropil, a tangle of neurites and glia, would remain free of dendrites and disappear. However, when we measured the cortical width, no differences were observed after Reelin depletion. The second one, it refers to the invasion of layer I as a result of somal translocation. As we mentioned before, Reelin signalling controls somal translocation as a results of Reelin-dependant degradation of Dab1 by means of the ubiquitin-proteasome system (Simo & Cooper, 2013). In accordance with this assumption, increased Dab1 protein levels were observed by WB in parallel with Reelin deletion.

2. Role of Reelin in the formation of the hippocampus.

2.1. Reelin expressed by Calretinin positive neurons is essential for the proper lamination of the hippocampus.

The hippocampal formation is essential for the consolidation of cognitive abilities including short- to long-term memory, as well as spatial memory (Deng *et al.*, 2010). In addition, it is also associated with the emergence of several neuropsychiatric disorders, including epilepsy, mental retardation and Alzheimers disease (AD). During development of the mammalian hippocampus, defects in neuronal migration results in aberrant hippocampal lamination, neuronal differentiation disorders and neural circuit defects, leading to the appearance of multiple disorders.

The mammalian hippocampal region consists in the hippocampal formation together with the "periallocortical region" which is made up of the area retrosplenialis, the presubiculum, the parasubiculum and the entorhinal cortex. The hippocampal formation is formed by the fascia dentata or dentate gyrus, the hippocampus proper o cornus Ammonis, and the subiculum (Khalaf-Nazzal & Francis, 2013).

The development and formation of the Cornus Ammonis (CA) occurs similarly to neocortical development with some slight differences. Pyramidal cells that will form the CA layer are generated in the VZ from E12 to E18 and then migrate radially toward the pial surface, settling into the hippocampal plate, the future pyramidal cell layer. Development of this layer takes place following an inside-out pattern of migration as occurs in the neocortex. Thus, early born pyramidal cells are placed in the deeper part of the pyramidal cell layer, whereas late born pyramidal cells pass the older neurons to reach the upper part. However, whereas neocortical migrating neurons use a single radial fiber as scaffold, in the case of hippocampal pyramidal neurons migration occurs through the use of multiple radial glial fibers leading to a zigzag movement. In addition, migration of hippocampal pyramidal neurons occurs obliquely so that neurons are distributed in a more horizontal manner, not in a well-defined vertical column as in the case of neocortical pyramidal cells. It has been proposed that early Reelin expression presumably plays a role for pyramidal cell migration in the CA1 region. This assumption is supported by the fact that pyramidal cells of CA1 migrate towards the Reelin-rich region of CRC in the dentate gyrus pial surface and that in *reeler* hippocampus pyramidal cells appeared malpositioned as early as E15.5 (Hatami *et al.*, 2018)(Hayashi *et al.*, 2015).

The analysis of CA1 region evidenced that in contrast to *reeler* mice, no major lamination defects were observed in the CR fR/fR hippocampus. However a subset of pyramidal neurons appeared dispersed in the so and sr, which correlates with a thicker CA1 compared to control mice. In addition, analysis of BrdU labelled cells distribution showed that later born neurons (BrdU injected at E15.5) remained in the deeper part on the CA1 in CR fR/fR mice, suggesting a role of Reelin expressed by Calretinin positive cells in the proper migration on these cells. In line with the observed defects in neocortical migration, early born neurons (defined by BrdU injection at E12), were mainly positioned in the lower part of the pyramidal

layer in both genotypes, suggesting that Reelin-expressed by CRC during embryonic development is not essential for the proper migration of these cells. As we mentioned above, the expression of Reelin by a different source from CRC, such as the "deep" Reelin, could control the migration of early-generated hippocampal pyramidal neurons. However, this signal would not be sufficient to promote migration of late-generated pyramidal neurons properly.

Generation of GCs that forms the supra and infra-pyramidal blades of the DG is known to occur in two phases. In the first migratory route, early dentate granule cells as well as precursor cells originated in the SDM (which is formed at E15.5) migrate towards the hippocampal fissure along the primary RG fibers and become arranged in a rudimentary supra-pyramidal blade (SPB) of the DG by E18. The primary radial glial scaffold is originated in the fimbria region and leads to the pial side of the cortex and the hippocampal fissure. Additionally, CRC, originated in the cortical hem migrate tangentially towards the hippocampal fissure. Like RG cells in the neocortex, primary RG cells of the DG show no major defects in *reeler* hippocampus and presumably, the chemokine Stromal cell-derived factor 1 (SDF1, CXCL12) rather than Reelin, controls this early phase of development in the DG. At this time however, a second wave of dentate GCs migrate from the SDM and remain in the hilus, where they maintain their proliferative capacity in the TDM. About 85% of dentate GCs are generated postnatally in the TDM, with a peak of proliferation by P1. Between P10 and P14 the secondary RGCs of the TDM differentiate into astrocytes, following the formation of the second radial glial fiber scaffold. In *reeler* mice secondary RGCs present a severely altered morphology (failed to establish radial processes) and positioning (distributed throughout the DG). The compaction of the GCL occurs simultaneously to the developing of the secondary glial scaffold so that the final width of the GCL corresponds with the exact length of the radial processes of secondary RG cells. Finally, by P14 the TDM turns into SGZ (Wang *et al.*, 2018)(Fan *et al.*, 2018)(Hatami *et al.*, 2018) (Brunne *et al.*, 2013) (Forster *et al.*, 2002).

Our data revealed for the first time the specific contribution of Reelin expressed by CRC and by Calretinin positive interneurons to the formation of the DG. In line with previous studies, we believe that in CR fR/fR mice the formation of the spb which is known to occur early during development, occurs regardless of Reelin from CRC. In addition, we hypothesize that the signal of SDF1 could be responsible of the formation of the primary radial glia and the migration of the first wave of GCs from the SDM. However, analysis of P1 hippocampus showed masses of presumably CRC (defined by Calretinin positive immunostaining) that were ectopically located in the GCL. These observations could suggest that the lack of Reelin in Calretinin positive cells alters the lamination pattern of CRC in the hippocampus and thus, the proper migration and location of GCs. Nevertheless, this observation is contrary to what was previously published. Previous data pointed that CRC-themselves are able to migrate and positioned correctly by the expression of C-X-C motif G-protein coupled chemokine receptors (CXCR) 4 and CXCR7 and the binding of the ligand SDF1 that is mainly expressed by meninges and astrocytes. Nonetheless, a relative increase of SDF-1 levels has been observed in *reeler* hippocampus, together with a reduced number of CRC residing closer to the hippocampal fissure and in the ipb of the DG (Anstotz *et al.*, 2019). Thus, the up-regulation of SDF-1 in the absence of Reelin may account for the aberrant CRC location. Another possible explanation is that Reelin from a different source, likely GABAergic interneurons, could be enough for spb formation. However, several studies have demonstrated that Reelin has to be present in a

specific topical location, presumably in a compact band CRC, to induce the proper GCs migration and compactation into the GCL (Zhao *et al.*, 2006)(Forster, Zhao, *et al.*, 2006)(Zhao & Frotscher, 2010).

In addition, Reelin-expressed by CRC of the hippocampal fissure seems to act as chemoattractive signalling for migrating GC neurons and control their proper location. As we observed with Prox1 labelling and BrdU experiments, in CR fR/fR mice a number of early GCs failed to migrate properly trough the emerging GCL and remained in the inner part of the spb. As we mentioned above the majority of GCs are generated in the TDM during the first postnatal week. At this time, CRC population decline by apoptosis coinciding with the shift of Reelin expression to GABAergic interneurons. Strikingly, the more surprising abnormalities observed in CR fR/fR hippocampus became evident at later stages. The analysis of hippocampal lamination at P30 showed that the ipb (including both the GCL and the ML) was either not well developed or absent in some cases. The formation of ipb is known to occur postnatally, being clearly distinguishable by P14 when the main source of Reelin protein comes from GABAergic interneurons. However, our data showed that Reelin postnatally expressed by these population of neurons is not necessary for the correct lamination of hippocampal structures. Therefore, our results suggest that Reelin expressed by CRC could be essential for the proper location of these cells in the fissure, that in turn, control the correct development of the second radial glial fiber scaffold. This process that takes places between P10-P14, develops at the same time that the formation of the ipb. In addition, defects in migration of later born GCs were also oberved in CR fR/fR, as demonstrated a wider distribution of BrdU labeled neurons at postanatal stages in the spb, displaying irregular boundaries between the outermost part of the GCL and the ML that correlate with increased width of the GCL. A similar phenotype, was previously observed after deletion of CTR region of Reelin protein, which has been proposed to preferably bind to VLDLR (Ha *et al.*, 2017).

To sum, all these evidences suggest that the formation of the spb occurs influenced by the formation of the primary radial glial scaffold, which is not strictly dependent of the effect of Reelin signaling expressed by Calretinin positive cells. This primary scaffold could serve as a guide for the migration of early born GCs neurons. In addition, Reelin expressed by other source, such as GABAergic interneurons, that is detectable from P1, could serve as signal for GCs migration. However, the absence of a well developed ipb and the aberrant location of GCs within the GCL pointed an essential role of Reelin expressed by Calretinin positive cells.

2.2. Postanatal loss of Reelin causes structural alteration in the hippocampus resembling those of *reeler* mice.

In recent years several mouse models have been developed to try to elucidate the roles of Reelin in migration and lamination of the developing hippocampus. However, the precise function of Reelin in the different process of hippocampal formation has been difficult to ascertain because of the complexity of the *reeler* phenotype. To bypass the deleterious consequences of Reelin deficiency during embryonic stages and analyse the specific role of Reelin in the development of the hippocampus at postnatal stages we use the inducible Cre fR/fR mice.

The histological study of laminar structures of the hippocampus revealed expected alterations in the hippocampal morphology of Cre fR/fR mice resembling those observed in the *reeler* mice and is consistent with the late development of this particular structure (Forster, Zhao, *et al.*, 2006). Specifically, hippocampal pyramidal cells were misspositioned in the Ammon's horn, with some neurons aberrantly positioned in the so and sr and even forming ectopic islands of cells in the white matter. In addition, the dentate gyrus failed to form correctly and granule cells were scattered along the entire DG.

However, the observed phenotype in the hippocampus of Cre fR/fR mice contrasted with the results observed in CR fR/fR mice and Gad fR/fR. Hippocampus of Gad fR/fR mice did not showed any alteration in the layering of the hippocampal structures, suggesting that Reelin expressed by Gad65 interneurons is not necessary for the formation of the hippocampus. Thus, we could hypothesize that the Reelin from the remaining CRC is enough to maintain the conformation of these structures intact. Nevertheless, the observed phenotype in CR fR/fR hippocampus was not altered as in the Cre fR/fR mice, since the formation of an altered but visible spb was distinguishable in the DG of CR fR/fR. Therefore, we need to consider an additional source of Reelin implicated in the proper layering of the DG.

As we previously mentioned the hippocampus is functionally connected in a unidirectional "tri-synaptic" circuit, the perforant pathway. In the perforant pathway, the ingrowing axons from the entorhinal fibers enter specifically into the stratum lacunosum moleculare of the hippocampus to further innervate the outermost part of the molecular layer of the DG, following a lamina-specific distribution without invading the adjacent ventrolateral isocortex. This axonal wiring and the pattern of connections are well established from the very beginning during development. In mice, the extreme of entorhinal fibers reaches the axons of CRC located in the molecular layer of the developing DG by E17. Thus, CRC serve as scaffolds for neuronal projection from the EC, which is the starting signal of the trisynaptic circuit. From this moment on the perforant network maturates following a stereotyped sequence in which the correct laminar specificity of hippocampal afferent fibre projections is controlled by specific molecular interactions between the fibres and their targets (Super *et al.*, 1998)(Forster, Zhao, *et al.*, 2006)(Khalaf-Nazzal & Francis, 2013)(Song *et al.*, 2016)(Gil & Del Rio, 2019)(Donato *et al.*, 2017). However, some of the axonal guidance molecules and the receptors involved in the definition of this particular connection as well as those that define cell-axon recognition and connectivity at a cellular level remain to be elucidated.

Furthermore, Reelin expression in the entorhinal cortex is detectable from early embryonic stages to postnatal and adult stages. During neocortical development Reelin is expressed by CRC of the MZ, but from E18 onwards, Reelin is mainly expressed by a population of layer II cortical neurons of the entorhinal cortices, the stellate neurons (Ray & Brecht, 2016). Thus, since these neurons are known to project to the DG, we hypothesize that entorhinal-expressed Reelin could play a role in the formation of the hippocampus. Supporting this assumption, the appearance of the spb in CR fR/fR mice could demonstrate that Reelin-expressed by stellate neurons acts as signal for migration of GC neurons in the spb of the DG in these mice. In addition, the *reeler* mutant mice also exhibit alterations in the entorhinohippocampal afferents, including abnormal termination of the circuit as well as reduced axonal branching and aberrant synaptogenesis, suggesting a role of Reelin in the development of the perforant pathway (Borrell *et al.*, 1999). However, in Cre fR/fR mice the depletion of Reelin from hippocampal CRC and from layer II stellate neurons drives the formation of a hypomorphic DG as occurs in *reeler* mice.

3. Role of Reelin in adult neurogenesis in the SGZ of the DG.

Adult hippocampal neurogenesis describes the active process in which adult-born neurons are continuously generated from NSCs throughout life in the DG. Normal proliferation and maturation of local NSCs in the DG contributes to affective behaviours and cognitive function, and impairments in these processes are thought to underlie anxiety, mood disorders and/or learning and memory in several neuropsychiatric disorders (Eisch *et al.*, 2009) (Zhao *et al.*, 2008) (Terrillion *et al.*, 2017). Thus, several studies during the last few years have focused in the study of adult hippocampal neurogenesis. Loss of Reelin was first related to a decreased adult neurogenesis in the *reeler* mouse model (Won *et al.*, 2006) and since then, several studies have been performed in order to unravel the possible role that Reelin could have in adult neurogenesis.

3.1. Conditional loss of Reelin during adulthood does not alter proliferation in the DG.

Cell differentiation and proliferation were found to be severely altered in the DG of the *reeler* mice (Won *et al.*, 2006)(Zhao *et al.*, 2007) (Sibbe *et al.*, 2015). However, altered adult neurogenesis in these mice seems to be influenced by the accumulated defects during development that these mice present in the strictly ordered structure of the DG (Brunne *et al.*, 2013). As both, Reelin signalling and granule cell arrangement are altered in *reeler* mice, new studies have focused in the analysis of the conditional loss of Reelin in adult neurogenesis. After supression of this pathway in adult progenitor cells, they change their fate toward glial cells (Teixeira *et al.*, 2012). A similar imbalance between glial and neuronal fates of SGZ progenitors has also been described in adult *reeler* mutants (Zhao et al., 2007). In addition, induced Reelin overexpression has been shown to increase the rate of adult neurogenesis and causes abnormal cell migration and integration of the new-born granule cells (Pujadas *et al.*, 2010a).

In this context, we investigated the impact of the conditional loss of Reelin on adult neurogenesis in the DG by using the Cre fR/fR mice. Our data indicates that Reelin signalling influences multiple stages of adult hippocampal neurogenesis. The number and distribution of dividing cells, presumably mitotic progenitors, was determined after BrdU incorporation in an adult Reelin deficient mice and no differences were found in cell division rate. In addition, the number of immature neurons defined by DCX immunostaining, did not differ between controls and Reelin deficient mice. Although type 3 progenitors could not be distinguished from immature neurons by DCX labelling, DCX has been described as a good marker of immature neurons, and good for dendritogenesis studies (Rao & Shetty, 2004). Furthermore, we explored if Reelin deficiency in adult stages could imbalance neuronal/glial fate as was previously reported (Won *et al.*, 2006)(Zhao et al., 2007) (Teixeira *et al.*, 2012) (Korn *et al.*, 2016). We analyzed the number of double BrdU/NeuN neurons in order to quantify the number of mature new-born neurons born at the same time and no significant differences were obtained. Thus, our results suggest that the conditional loss of Reelin in adulthood might not be critical for adult proliferation when the development has occurred normally.

Nevertheless, our data present some discrepancies with previously published data because we found no differences in the neuronal/glial fate. In agreement with the data presented in this project, it was previously published that Reelin signalling is crucial for the recruitment of the quiescent stem cells in the SGZ in the adult DG, but once quiescent stem cells start the proliferation process, the balance between glial and neuronal fates of SGZ progenitors does not depend on Reelin (Sibbe *et al.*, 2015) (Brunne *et al.*, 2013).

3.2. Conditional loss of Reelin during adulthood impairs GCs location.

In the adult DG, neurogenesis is mainly restricted to the SGZ of the DG. In this zone, proliferative niches are important to protect precursor cells against an environment that overall is non-permissive to proliferation. They depend on cell arrangement and cell morphology, which are both disturbed in the *reeler* DG. In addition Reelin signalling has been shown to influence secondary radial glial cells morphology that in turn is necessary for the correct positioning and compaction of granule neurons. Conversely, in a bidirectional interaction, GCL arrangement depends on radial glial cell morphology (Brunne *et al.*, 2013). In *reeler* mutants and in mutant of the Reelin signalling cascade, granule cells display scattered distribution, often invading the ML and the hilus (Frotscher et al., 2003)(Korn *et al.*, 2016) (Teixeira *et al.*, 2012). However, it remains unclear whether Reelin signalling influences glial scaffold guiding migration or if acts on the migratory process itself, controlling migration directionally and/or migratory speed.

Migrating granule cells could pass through three different modes of migration. During radial migration granule cells extend their leading process radially to the GCL and migrate through this layer. Tangential migration is defined by the extension of a leading process oriented in parallel to the granule cell layer followed by nuclear translocation. Finally, the third migratory mode, the converted tangential migration, is referred to a process of tangential migration that is converted to radial migration. In this case, neurons initially extend a leading process parallel to the GCL and then, a second leading process is formed with a radial orientation allowing the cell to migrate within the GCL. This process requires cytoskeletal reorganization, to allow leading process retraction and extension. In *reeler* cortices, granule cells are able to migrate by extending a leading and trailing process, however, since the leading process points to multiple directions, a preferential migration is not observed (Wang *et al.*, 2018).

Despite no major lamination defects were observed in the DG after depletion of Reelin in adult stages, suggesting that radial glial scaffold formed normally, a number of cells ectopically located on the hilus was found in Cre fR/fR mice. Noteworthy, some proliferative cells were observed in the hilar region, suggesting that Reelin signalling is essential to maintain precursor cells in the proper location within the SGZ. Furthermore, the absence of Reelin during adulthood resulted in a lower percentage of integrated newly generated neurons in the GCL and a higher percentage of ectopic newly generated neurons in the hilus. In addition, Prox1 immunostaining demonstrated granule cell dispersion in the hilus. Altogether, our data suggest that Reelin is essential for the correct positioning of cells in the DG during adulthood and that its deficiency prevents the correct integration of new generated cells.

In addition to the position, we also analysed the distance that neurons migrated from the SGZ through the GCL and we found that integrated neurons were preferentially located in the lower half of the GCL, defined by a migration below 10 microns, in the absence of Reelin, suggesting that Reelin signalling might be impairing also their migration. However, it is not possible to discriminate if the effects observed in positioning are due to misslocation of progenitor cells in the hilus or impaired migration.

An increased number of adult-born neurons that migrate and integrate aberrantly into existing DG circuitry has been observed in murine models of mesial temporal lobe epilepsy (mTLE) and acute seizures, and this phenotype has been related to Reelin decrease (Gong et al., 2007)(Teixeira *et al.*, 2012). Particulary, adult granule neurons that exhibit hilar disposition and hilar basal dendrites (HBDs) are suggested to be pro-epileptogenic. In additon, dispersion of GCL is one of the main features observed in human with mTLE and can be reproduced in animal models of induced status epilepticus (SE) with kainic acid or pilocarpine (Korn *et al.*, 2016). Besides these results in Reelin deficient mouse models, overexpression of Reelin also alters the distribution of new-born neurons along the GCL, indicating an abnormal cell positioning when Reelin levels are altered (Pujadas et al., 2010).

3.3. Adult Reelin signalling is essential to establish and maintain the dendritic orientation of GCs in the DG.

Analysis of immature granule neurons based on DCX immunostaining confirmed the previously described phenotype of altered dendritic development caused by lack of Reelin signaling (Teixeira *et al.*, 2012). In Cre fR/fR mice, many labeled cells appeared to display abnormal dendritic orientation within the GCL or were even ectopically located in the hilus. To further characterize the influence of Reelin signalling in dendritogenesis, we analysed the dendritic orientation of new generated neurons after Reelin depletion at different maturation stages (2, 4 and 8 weeks). In all the cases Reelin depletion resulted in an aberrant dendritic tree morphology, with abundance of basal dendrites that ectopically project into the hilus. These results suggest that Reelin signalling pathway is required for a proper dendritic orientation of granule neurons at both stages, during dendritogenesis and also when mature granule neurons are already integrated in the existing circuitry.

The maturation and integration of a new-generated neuron begins with the extension of neuritic filopodia which develop into axon and dendrites. The fine-tuning of dendritic development and outgrowth seems to be controlled by several Reelin-induced pathways. First, activation of ApoER2/Dab1/PI3K pathway induces the extension of the growth cone, promoting the extension of filopodia trough activation of the RhoGTPases Cdc42 and Rac1 that influence actin cytoskeleton. As neuronal polarization occurs in a nascent neuron, an axon emerges and stabilizes in the future basal site of the mature neuron. Then, opposite to the axon, the major apical dendritic tree is developed. The establishment of this symmetry is controlled by positioning of the Golgi apparatus. Thus, dispersion of the Golgi apparatus results in a loss of dendritic asymmetry, with an equal distribution of apical and basal dendrites (Matsuki *et al.*, 2010). It has been shown that the GTPases Rac1 and Cdc42 are involved in Golgi complex translocation to the primary apical dendrite, which is selected by its

proximity to a Reelin source (Meseke *et al.*, 2013). Furthermore, dendritic complexity is increased in dendrites containing Golgi outpost (GOPs). The GOPs are defined as discrete mini-organelles originated from Golgi complex deployment that participate in trafficking of multiple proteins associates with dendritic development and synaptic function. Reelin signalling has been shown to play important roles in Golgi dynamics and fragmentation as well as in GOPs formation (Caracci *et al.*, 2019). Specifically, stabilization of the cytoskeleton is controlled by Reelin signalling trough the activation of Lis1 and by the phosphorylation and inactivation of cofilin through LIMK1, which also participate in Golgi complex fragmentation and GOPs fission (Quassollo *et al.*, 2015) (Wasser & Herz, 2017). In addition, the dynamics of Golgi apparatus is closely related with microtubules nucleation. Thus, the microtubule nucleating protein CLASP2 is found associated to the Golgi complex, where acts as a centrosomal nucleation site enhancing dendritic branching.

All these evidences support our observed results. We suggest that Reelin could control the location of the Golgi apparatus during neuronal polarization that in turn allows the definition of the apical processes. However, depletion of Reelin at early stages of neuronal maturation retains Golgi apparatus into the soma preventing its fragmentation and/or limiting the trafficking of discrete Golgi units through apical positions. Furthermore, we propose that at later maturation stages, Reelin is a signal for the correct position of GOPs into apical dendrites, through which proteins associated with synaptic function traffic. Therefore, in a context without Reelin, Golgi structures that are known to be highly dynamic, could vary their position towards basal positions. In addition, a recent study suggest that Reelin signalling interference could reactivate a dendritic outgrowth of mature neurons (Ampuero *et al.*, 2017). So far, the obtained results are supported by previous studies focused dendritogenesis. *Reeler* mice showed a reduced complexity of the dendritic tree in hippocampal new-born neurons, suggesting a role of Reelin in dendritogenesis during development (Niu *et al.*, 2004). More recently, another study described that Reelin overexpressing mice showed an accelerated dendritic development. In contrast, using conditional Dab1 deficient mice, it was shown that the dendritic tree complexity was altered by cell-autonomus inactivation of the Reelin signalling pathway in adulthood, suggesting that Reelin signalling pathway is required for a proper dendritic orientation of adult newly generated neurons (Teixeira *et al.*, 2012).

4. Role of Reelin in the formation of the cerebellum

In the *reeler* mouse model cerebellar granular cells and Purkinje cells are reduced in number and in addition Purkinje cells are abnormally positioned with less branched dendrites (Curran & D'Arcangelo, 1998) (Forster, Jossin, *et al.*, 2006). Due to the reduction in the number of PC and granule cells, the size of the *reeler* cerebellum is severely diminished and abnormally foliated (Rahimi-Balaei *et al.*, 2018) (Cocito *et al.*, 2016).

We have shown that, unlike *reeler* mutants, CR fR/fR and Gad fR/fR mice have normal cerebellar foliation, lobule IV was larger and lobules VI and VII were simpler, and they were not ataxic, suggesting that as expected Reelin deficiency from both Calretinin positive cells and Gad65 interneurons does not alter neuronal distribution in the cerebellum. However, we have been able to confirm that postnatal and adult loss of Reelin alters normal cerebela foliation and induces misspositioning of Purkinje cells, leaving granular cells unaffected even in the later-formed folia. Thus, Reelin seems to regulate the proper refinement of the Punkinje cell alignment and therefore we could hypothesize that the alterations seen in *reeler* mice are most likely due to the misspositioning of Purkinje cells.

CONCLUSIONS

The results obtained in this study allow us to raise the following conclusions:

1. Reelin expressed by Calretinin positive cells is not necessary for preplate splitting.
2. The selective depletion of Reelin from Calretinin positive cells leads to defective migration of cortical neurons without *reeler*-like layering inversion.
3. Perinatal expression of Reelin from GAD65 interneurons partially rescues the aberrant distribution of cortical neurons in Calretinin positive Reelin deficient mice. Specifically, by restoring layer I structure and reducing the number of layer II-II neurons ectopically located in deeper layers.
4. Reelin in the postnatal and adult brain is essential for the maintenance of the cortical neurons distribution. Particularly, Reelin expressed by Gad65 interneurons seems to be essential to preserve layer I cytoarchitecture.
5. Postnatal Reelin expression controls the correct formation of the hippocampal laminar structures.
6. Reelin from hippocampal Calretinin positive cells, and not one from Gad65 interneurons, is essential for the correct lamination of hippocampal structures, especially for the infrapyramidal blade of the dentate gyrus.
7. The density of mitotic neuronal progenitors, immature neurons and mature neurons remains unaltered after conditional depletion of Reelin expression in the adult brain. However, Reelin deficiency significantly increases the number of progenitor and granule cells ectopically located in the hilus of the dentate gyrus.
8. Reelin expression is required for the proper migration of the newly generated neurons during adulthood.
9. Adult Reelin expression is essential to establish and maintain the dendritic orientation of granule cells in the dentate gyrus.
10. Reelin expression in the cerebellum at postnatal and adult stages is necessary for the correct positioning of Purkinje cells.

REFERENCES

Abraham, H. & Meyer, G. (2003) Reelin-expressing neurons in the postnatal and adult human hippocampal formation. *Hippocampus*, **13**, 715–727.

Alcantara, S., Ruiz, M., D'Arcangelo, G., Ezan, F., de Lecea, L., Curran, T., Sotelo, C., & Soriano, E. (1998) Regional and cellular patterns of reelin mRNA expression in the forebrain of the developing and adult mouse. *J. Neurosci.*, **18**, 7779–7799.

Ampuero, E., Jury, N., Hartel, S., Marzolo, M.-P., & van Zundert, B. (2017) Interfering of the Reelin/ApoER2/PSD95 Signaling Axis Reactivates Dendritogenesis of Mature Hippocampal Neurons. *J. Cell. Physiol.*, **232**, 1187–1199.

Andrade, N., Komnenovic, V., Blake, S.M., Jossin, Y., Howell, B., Goffinet, A., Schneider, W.J., & Nimpf, J. (2007) ApoER2/VLDL receptor and Dab1 in the rostral migratory stream function in postnatal neuronal migration independently of Reelin. *Proc. Natl. Acad. Sci. U. S. A.*, **104**, 8508–8513.

Anstotz, M., Karsak, M., & Rune, G.M. (2019) Integrity of Cajal-Retzius cells in the reeler-mouse hippocampus. *Hippocampus*, **29**, 550–565.

Anstotz, M., Quattrocolo, G., & Maccaferri, G. (2018) Cajal-Retzius cells and GABAergic interneurons of the developing hippocampus: Close electrophysiological encounters of the third kind. *Brain Res.*, **1697**, 124–133.

Bartolini, G., Sanchez-Alcaniz, J.A., Osorio, C., Valiente, M., Garcia-Frigola, C., & Marin, O. (2017) Neuregulin 3 Mediates Cortical Plate Invasion and Laminar Allocation of GABAergic Interneurons. *Cell Rep.*, **18**, 1157–1170.

Berg, D.A., Bond, A.M., Ming, G.-L., & Song, H. (2018) Radial glial cells in the adult dentate gyrus: what are they and where do they come from? *F1000Research*, **7**, 277.

Borrell, V. & Marin, O. (2006) Meninges control tangential migration of hem-derived Cajal-Retzius cells via CXCL12/CXCR4 signaling. *Nat. Neurosci.*, **9**, 1284–1293.

Borrell, V., Ruiz, M., Del Rio, J.A., & Soriano, E. (1999) Development of commissural connections in the hippocampus of reeler mice: evidence of an inhibitory influence of Cajal-Retzius cells. *Exp. Neurol.*, **156**, 268–282.

Bosch, C., Masachs, N., Exposito-Alonso, D., Martinez, A., Teixeira, C.M., Fernaud, I., Pujadas, L., Ulloa, F., Comella, J.X., DeFelipe, J., Merchan-Perez, A., & Soriano, E. (2016) Reelin Regulates the Maturation of Dendritic Spines, Synaptogenesis and Glial Ensheathment of Newborn Granule Cells. *Cereb. Cortex*, **26**, 4282–4298.

Boyle, M.P., Bernard, A., Thompson, C.L., Ng, L., Boe, A., Mortrud, M., Hawrylycz, M.J., Jones, A.R., Hevner, R.F., & Lein, E.S. (2011) Cell-type-specific consequences of Reelin deficiency in the mouse neocortex, hippocampus, and amygdala. *J. Comp. Neurol.*, **519**, 2061–2089.

Brunne, B., Franco, S., Bouche, E., Herz, J., Howell, B.W., Pahle, J., Muller, U., May, P., Frotscher, M., & Bock, H.H. (2013) Role of the postnatal radial glial scaffold for the development of the dentate gyrus as revealed by Reelin signaling mutant mice. *Glia*, **61**, 1347–1363.

Caracci, M.O., Fuentealba, L.M., & Marzolo, M.-P. (2019) Golgi Complex Dynamics and Its Implication in Prevalent Neurological Disorders. *Front. cell Dev. Biol.*, **7**, 75.

Carleton, A., Petreanu, L.T., Lansford, R., Alvarez-Buylla, A., & Lledo, P.-M. (2003) Becoming a new neuron in the adult olfactory bulb. *Nat. Neurosci.*, **6**, 507–518.

Castillo, P.E. (2012) Presynaptic LTP and LTD of excitatory and inhibitory synapses. *Cold Spring*

Harb. Perspect. Biol., **4**.

Castillo, P.E., Chiu, C.Q., & Carroll, R.C. (2011) Long-term plasticity at inhibitory synapses. *Curr. Opin. Neurobiol.*, **21**, 328–338.

Chai, X., Forster, E., Zhao, S., Bock, H.H., & Frotscher, M. (2009) Reelin stabilizes the actin cytoskeleton of neuronal processes by inducing n-cofilin phosphorylation at serine3. *J. Neurosci.*, **29**, 288–299.

Chai, X. & Frotscher, M. (2016) How does Reelin signaling regulate the neuronal cytoskeleton during migration? *Neurogenes. (Austin, Tex.)*, **3**, e1242455.

Christian, K.M., Song, H., & Ming, G. (2014) Functions and dysfunctions of adult hippocampal neurogenesis. *Annu. Rev. Neurosci.*, **37**, 243–262.

Cocito, C., Merighi, A., Giacobini, M., & Lossi, L. (2016) Alterations of Cell Proliferation and Apoptosis in the Hypoplastic Reeler Cerebellum. *Front. Cell. Neurosci.*, **10**, 141.

Colangelo, A.M., Cirillo, G., Alberghina, L., Papa, M., & Westerhoff, H. V (2019) Neural plasticity and adult neurogenesis: the deep biology perspective. *Neural Regen. Res.*, **14**, 201–205.

Colgan, L.A. & Yasuda, R. (2014) Plasticity of dendritic spines: subcompartmentalization of signaling. *Annu. Rev. Physiol.*, **76**, 365–385.

Cooper, J.A. (2008) A mechanism for inside-out lamination in the neocortex. *Trends Neurosci.*, **31**, 113–119.

Cope, E.C. & Gould, E. (2019) Adult Neurogenesis, Glia, and the Extracellular Matrix. *Cell Stem Cell*, **24**, 690–705.

Curran, T. & D'Arcangelo, G. (1998) Role of reelin in the control of brain development. *Brain Res. Brain Res. Rev.*, **26**, 285–294.

D'Arcangelo, G. & Curran, T. (1998) Reeler: new tales on an old mutant mouse. *Bioessays*, **20**, 235–244.

D'Arcangelo, G., Miao, G.G., Chen, S.C., Soares, H.D., Morgan, J.I., & Curran, T. (1995) A protein related to extracellular matrix proteins deleted in the mouse mutant reeler. *Nature*, **374**, 719–723.

De Vincenti, A.P., Rios, A.S., Paratcha, G., & Ledda, F. (2019) Mechanisms That Modulate and Diversify BDNF Functions: Implications for Hippocampal Synaptic Plasticity. *Front. Cell. Neurosci.*, **13**, 135.

Del Rio, J.A., Heimrich, B., Borrell, V., Forster, E., Drakew, A., Alcantara, S., Nakajima, K., Miyata, T., Ogawa, M., Mikoshiba, K., Derer, P., Frotscher, M., & Soriano, E. (1997) A role for Cajal-Retzius cells and reelin in the development of hippocampal connections. *Nature*, **385**, 70–74.

del Rio, J.A., Sole, M., Borrell, V., Martinez, A., & Soriano, E. (2002) Involvement of Cajal-Retzius cells in robust and layer-specific regeneration of the entorhino-hippocampal pathways. *Eur. J. Neurosci.*, **15**, 1881–1890.

Del Turco, D., Gebhardt, C., Burbach, G.J., Pleasure, S.J., Lowenstein, D.H., & Deller, T. (2004) Laminar organization of the mouse dentate gyrus: insights from BETA2/Neuro D mutant mice. *J. Comp. Neurol.*, **477**, 81–95.

Deng, W., Aimone, J.B., & Gage, F.H. (2010) New neurons and new memories: how does adult hippocampal neurogenesis affect learning and memory? *Nat. Rev. Neurosci.*, **11**, 339–

350.

Dlugosz, P. & Nimpf, J. (2018) The Reelin Receptors Apolipoprotein E receptor 2 (ApoER2) and VLDL Receptor. *Int. J. Mol. Sci.*, **19**.

Doehner, J. & Knuesel, I. (2010) Reelin-mediated Signaling during Normal and Pathological Forms of Aging. *Aging Dis.*, **1**, 12–29.

Donato, F., Jacobsen, R.I., Moser, M.-B., & Moser, E.I. (2017) Stellate cells drive maturation of the entorhinal-hippocampal circuit. *Science*, **355**.

Eisch, A.J., Cameron, H.A., Encinas, J.M., Meltzer, L.A., & Overstreet-wadiche, L.S. (2009) Adult Neurogenesis, Mental Health, and Mental Illness: Hope or Hype? *J Neurosci*, **28**, 11785–11791.

Fan, S.-J., Sun, A.-B., & Liu, L. (2018) Epigenetic modulation during hippocampal development. *Biomed. reports*, **9**, 463–473.

Feng, L., Allen, N.S., Simo, S., & Cooper, J.A. (2007) Cullin 5 regulates Dab1 protein levels and neuron positioning during cortical development. *Genes Dev.*, **21**, 2717–2730.

Ferrer-Ferrer, M. & Dityatev, A. (2018) Shaping Synapses by the Neural Extracellular Matrix. *Front. Neuroanat.*, **12**, 40.

Flames, N. & Marin, O. (2005) Developmental mechanisms underlying the generation of cortical interneuron diversity. *Neuron*, **46**, 377–381.

Forster, E., Bock, H.H., Herz, J., Chai, X., Frotscher, M., & Zhao, S. (2010) Emerging topics in Reelin function. *Eur. J. Neurosci.*, **31**, 1511–1518.

Forster, E., Jossin, Y., Zhao, S., Chai, X., Frotscher, M., & Goffinet, A.M. (2006) Recent progress in understanding the role of Reelin in radial neuronal migration, with specific emphasis on the dentate gyrus. *Eur. J. Neurosci.*, **23**, 901–909.

Forster, E., Tielsch, A., Saum, B., Weiss, K.H., Johanssen, C., Graus-Porta, D., Muller, U., & Frotscher, M. (2002) Reelin, Disabled 1, and beta 1 integrins are required for the formation of the radial glial scaffold in the hippocampus. *Proc. Natl. Acad. Sci. U. S. A.*, **99**, 13178–13183.

Forster, E., Zhao, S., & Frotscher, M. (2006) Laminating the hippocampus. *Nat. Rev. Neurosci.*, **7**, 259–267.

Franco, S.J., Martinez-Garay, I., Gil-Sanz, C., Harkins-Perry, S.R., & Muller, U. (2011) Reelin regulates cadherin function via Dab1/Rap1 to control neuronal migration and lamination in the neocortex. *Neuron*, **69**, 482–497.

Franco, S.J. & Muller, U. (2011) Extracellular matrix functions during neuronal migration and lamination in the mammalian central nervous system. *Dev. Neurobiol.*, **71**, 889–900.

Frotscher, M. (1998) Cajal-Retzius cells, Reelin, and the formation of layers. *Curr. Opin. Neurobiol.*, **8**, 570–575.

Frotscher, M., Chai, X., Bock, H.H., Haas, C.A., Forster, E., & Zhao, S. (2009) Role of Reelin in the development and maintenance of cortical lamination. *J. Neural Transm.*, **116**, 1451–1455.

Frotscher, M., Haas, C.A., Förster, E., Institut, A., & Freiburg, U. (2003) Reelin Controls Granule Cell Migration in the Dentate Gyrus by Acting on the Radial Glial Scaffold 634–640.

Frotscher, M., Studer, D., Graber, W., Chai, X., Nestel, S., & Zhao, S. (2014) Fine structure of

synapses on dendritic spines. *Front. Neuroanat.*, **8**, 94.

Gelman, D.M. & Marin, O. (2010) Generation of interneuron diversity in the mouse cerebral cortex. *Eur. J. Neurosci.*, **31**, 2136–2141.

Gil-Sanz, C., Franco, S.J., Martinez-Garay, I., Espinosa, A., Harkins-Perry, S., & Muller, U. (2013) Cajal-Retzius cells instruct neuronal migration by coincidence signaling between secreted and contact-dependent guidance cues. *Neuron*, **79**, 461–477.

Gil, V. & Del Rio, J.A. (2019) Functions of Plexins/Neuropilins and Their Ligands during Hippocampal Development and Neurodegeneration. *Cells*, **8**.

Gong, C., Wang, T., Huang, H.S., & Parent, J.M. (2007) Reelin Regulates Neuronal Progenitor Migration in Intact and Epileptic Hippocampus **27**, 1803–1811.

Graus-Porta, D., Blaess, S., Senften, M., Littlewood-Evans, A., Damsky, C., Huang, Z., Orban, P., Klein, R., Schittny, J.C., & Muller, U. (2001) Beta1-class integrins regulate the development of laminae and folia in the cerebral and cerebellar cortex. *Neuron*, **31**, 367–379.

Greene, N.D.E. & Copp, A.J. (2014) Neural tube defects. *Annu. Rev. Neurosci.*, **37**, 221–242.

Ha, S., Tripathi, P.P., Mihalas, A.B., Hevner, R.F., & Beier, D.R. (2017) C-Terminal Region Truncation of RELN Disrupts an Interaction with VLDLR, Causing Abnormal Development of the Cerebral Cortex and Hippocampus. *J. Neurosci.*, **37**, 960–971.

Haas, C.A. & Frotscher, M. (2010) Reelin deficiency causes granule cell dispersion in epilepsy. *Exp. brain Res.*, **200**, 141–149.

Hack, I., Bancila, M., Loulier, K., Carroll, P., & Cremer, H. (2002) Reelin is a detachment signal in tangential chain-migration during postnatal neurogenesis. *Nat. Neurosci.*, **5**, 939–945.

Hatami, M., Conrad, S., Naghsh, P., Alvarez-Bolado, G., & Skutella, T. (2018) Cell-Biological Requirements for the Generation of Dentate Gyrus Granule Neurons. *Front. Cell. Neurosci.*, **12**, 402.

Hayashi, K., Kubo, K.-I., Kitazawa, A., & Nakajima, K. (2015) Cellular dynamics of neuronal migration in the hippocampus. *Front. Neurosci.*, **9**, 135.

He, C.-W., Liao, C.-P., & Pan, C.-L. (2018) Wnt signalling in the development of axon, dendrites and synapses. *Open Biol.*, **8**.

Hiesberger, T., Trommsdorff, M., Howell, B.W., Goffinet, A., Mumby, M.C., Cooper, J.A., & Herz, J. (1999) Direct binding of Reelin to VLDL receptor and ApoE receptor 2 induces tyrosine phosphorylation of disabled-1 and modulates tau phosphorylation. *Neuron*, **24**, 481–489.

Hirota, Y., Kubo, K.-I., Fujino, T., Yamamoto, T.T., & Nakajima, K. (2018) ApoER2 Controls Not Only Neuronal Migration in the Intermediate Zone But Also Termination of Migration in the Developing Cerebral Cortex. *Cereb. Cortex*, **28**, 223–235.

Hirota, Y. & Nakajima, K. (2017) Control of Neuronal Migration and Aggregation by Reelin Signaling in the Developing Cerebral Cortex. *Front. cell Dev. Biol.*, **5**, 40.

Hunt, D.L. & Castillo, P.E. (2012) Synaptic plasticity of NMDA receptors: mechanisms and functional implications. *Curr. Opin. Neurobiol.*, **22**, 496–508.

Ikeda, Y. & Terashima, T. (1997) Expression of reelin, the gene responsible for the reeler mutation, in embryonic development and adulthood in the mouse. *Dev. Dyn.*, **210**, 157–

172.

Ishii, K., Kubo, K.-I., & Nakajima, K. (2016) Reelin and Neuropsychiatric Disorders. *Front. Cell. Neurosci.*, **10**, 229.

Jakob, B., Kochlamazashvili, G., Japel, M., Gauhar, A., Bock, H.H., Maritzen, T., & Haucke, V. (2017) Intersectin 1 is a component of the Reelin pathway to regulate neuronal migration and synaptic plasticity in the hippocampus. *Proc. Natl. Acad. Sci. U. S. A.*, **114**, 5533–5538.

Jossin, Y., Bar, I., Ignatova, N., Tissir, F., De Rouvroit, C.L., & Goffinet, A.M. (2003) The reelin signaling pathway: some recent developments. *Cereb. Cortex*, **13**, 627–633.

Jossin, Y. & Goffinet, A.M. (2007) Reelin signals through phosphatidylinositol 3-kinase and Akt to control cortical development and through mTor to regulate dendritic growth. *Mol. Cell. Biol.*, **27**, 7113–7124.

Kang, E., Wen, Z., Song, H., Christian, K.M., & Ming, G.-L. (2016) Adult Neurogenesis and Psychiatric Disorders. *Cold Spring Harb. Perspect. Biol.*, **8**.

Kawauchi, T., Sekine, K., Shikanai, M., Chihama, K., Tomita, K., Kubo, K., Nakajima, K., Nabeshima, Y.-I., & Hoshino, M. (2010) Rab GTPases-dependent endocytic pathways regulate neuronal migration and maturation through N-cadherin trafficking. *Neuron*, **67**, 588–602.

Kempermann, G. & Gage, F.H. (2015) Neurogenesis in the adult hippocampus. *Cold Spring Harb. Perspect. Biol.*, **231**, 220–235.

Khalaf-Nazzal, R. & Francis, F. (2013) Hippocampal development - old and new findings. *Neuroscience*, **248**, 225–242.

Kim, W.R. & Sun, W. (2011) Programmed cell death during postnatal development of the rodent nervous system. *Dev. Growth Differ.*, **53**, 225–235.

Knuesel, I. (2010) Reelin-mediated signaling in neuropsychiatric and neurodegenerative diseases. *Prog. Neurobiol.*, **91**, 257–274.

Kohno, T., Honda, T., Kubo, K.-I., Nakano, Y., Tsuchiya, A., Murakami, T., Banno, H., Nakajima, K., & Hattori, M. (2015) Importance of Reelin C-terminal region in the development and maintenance of the postnatal cerebral cortex and its regulation by specific proteolysis. *J. Neurosci.*, **35**, 4776–4787.

Korn, M.J., Mandle, Q.J., & Parent, J.M. (2016) Conditional Disabled-1 Deletion in Mice Alters Hippocampal Neurogenesis and Reduces Seizure Threshold. *Front. Neurosci.*, **10**, 63.

Kristianto, J., Johnson, M.G., Zastrow, R.K., Radcliff, A.B., & Blank, R.D. (2017) Spontaneous recombinase activity of Cre-ERT2 in vivo. *Transgenic Res.*, **26**, 411–417.

Lakoma, J., Garcia-Alonso, L., & Luque, J.M. (2011) Reelin sets the pace of neocortical neurogenesis. *Development*, **138**, 5223–5234.

Lane-donovan, C., Philips, G.T., Wasser, C.R., Durakoglugil, M.S., Masiulis, I., Upadhaya, A., Pohlkamp, T., Coskun, C., Kotti, T., Steller, L., Hammer, R.E., Frotscher, M., Bock, H.H., & Herz, J. (2015) Reelin protects against amyloid b toxicity in vivo **8**, 1–13.

Lanoue, V. & Cooper, H.M. (2019) Branching mechanisms shaping dendrite architecture. *Dev. Biol.*, **451**, 16–24.

Laumonnerie, C. & Solecki, D.J. (2018) Regulation of Polarity Protein Levels in the Developing Central Nervous System. *J. Mol. Biol.*, **430**, 3472–3480.

Ledda, F. & Paratcha, G. (2017) Mechanisms regulating dendritic arbor patterning. *Cell. Mol. Life Sci.*, **74**, 4511–4537.

Lee, G.H. & D'Arcangelo, G. (2016) New Insights into Reelin-Mediated Signaling Pathways. *Front. Cell. Neurosci.*, **10**, 122.

Leung, B. & Shimeld, S.M. (2019) Evolution of vertebrate spinal cord patterning. *Dev. Dyn.*,.

Lewis, T.L.J., Courchet, J., & Polleux, F. (2013) Cell biology in neuroscience: Cellular and molecular mechanisms underlying axon formation, growth, and branching. *J. Cell Biol.*, **202**, 837–848.

Li, G. & Pleasure, S.J. (2005) Morphogenesis of the dentate gyrus: what we are learning from mouse mutants. *Dev. Neurosci.*, **27**, 93–99.

Lim, D.A. & Alvarez-Buylla, A. (2016) The Adult Ventricular-Subventricular Zone (V-SVZ) and Olfactory Bulb (OB) Neurogenesis. *Cold Spring Harb. Perspect. Biol.*, **8**.

Lussier, A.L., Weeber, E.J., & Rebeck, G.W. (2016) Reelin Proteolysis Affects Signaling Related to Normal Synapse Function and Neurodegeneration. *Front. Cell. Neurosci.*, **10**, 75.

Marzban, H., Del Bigio, M.R., Alizadeh, J., Ghavami, S., Zachariah, R.M., & Rastegar, M. (2015) Cellular commitment in the developing cerebellum . *Front. Cell. Neurosci.* ,.

Matsuki, T., Matthews, R.T., Cooper, J.A., van der Brug, M.P., Cookson, M.R., Hardy, J.A., Olson, E.C., & Howell, B.W. (2010) Reelin and stk25 have opposing roles in neuronal polarization and dendritic Golgi deployment. *Cell*, **143**, 826–836.

Meseke, M., Rosenberger, G., & Forster, E. (2013) Reelin and the Cdc42/Rac1 guanine nucleotide exchange factor alphaPIX/Arhgef6 promote dendritic Golgi translocation in hippocampal neurons. *Eur. J. Neurosci.*, **37**, 1404–1412.

Ming, G. li & Song, H. (2011) Adult Neurogenesis in the Mammalian Brain: Significant Answers and Significant Questions. *Neuron*, **70**, 687–702.

Miyata, T., Nakajima, K., Aruga, J., Takahashi, S., Ikenaka, K., Mikoshiba, K., & Ogawa, M. (1996) Distribution of a reeler gene-related antigen in the developing cerebellum: an immunohistochemical study with an allogeneic antibody CR-50 on normal and reeler mice. *J. Comp. Neurol.*, **372**, 215–228.

Miyata, T., Ono, Y., Okamoto, M., Masaoka, M., Sakakibara, A., Kawaguchi, A., Hashimoto, M., & Ogawa, M. (2010) Migration, early axonogenesis, and Reelin-dependent layer-forming behavior of early/posterior-born Purkinje cells in the developing mouse lateral cerebellum. *Neural Dev.*, **5**, 23.

Mosley, M., Shah, C., Morse, K.A., Miloro, S.A., Holmes, M.M., Ahern, T.H., & Forger, N.G. (2017) Patterns of cell death in the perinatal mouse forebrain. *J. Comp. Neurol.*, **525**, 47–64.

Nadarajah, B. & Parnavelas, J.G. (2002) Modes of neuronal migration in the developing cerebral cortex. *Nat. Rev. Neurosci.*, **3**, 423–432.

Nakamura, K., Beppu, M., Sakai, K., Yagyu, H., Matsumaru, S., Kohno, T., & Hattori, M. (2016) The C-terminal region of Reelin is necessary for proper positioning of a subset of Purkinje cells in the postnatal cerebellum. *Neuroscience*, **336**, 20–29.

Namba, T., Funahashi, Y., Nakamuta, S., Xu, C., Takano, T., & Kaibuchi, K. (2015) Extracellular and Intracellular Signaling for Neuronal Polarity. *Physiol. Rev.*, **95**, 995–1024.

Nikolopoulou, E., Galea, G.L., Rolo, A., Greene, N.D.E., & Copp, A.J. (2017) Neural tube closure: cellular, molecular and biomechanical mechanisms. *Development*, **144**, 552–566.

Nishijima, T., Kawakami, M., & Kita, I. (2013) Long-Term Exercise Is a Potent Trigger for ΔFosB Induction in the Hippocampus along the dorso – ventral Axis **8**, 1–17.

Niu, S., Renfro, A., Quattrocchi, C.C., Sheldon, M., & Arcangelo, G.D. (2004) Reelin Promotes Hippocampal Dendrite Development through the VLDLR / ApoER2-Dab1 Pathway Program in Neuroscience **41**, 71–84.

Obernier, K. & Alvarez-Buylla, A. (2019) Neural stem cells: origin, heterogeneity and regulation in the adult mammalian brain. *Development*, **146**.

Olson, E.C. (2014) Analysis of preplate splitting and early cortical development illuminates the biology of neurological disease. *Front. Pediatr.*, **2**, 121.

Praag, H. Van, Schinder, A.F., Christie, B.R., Toni, N., Palmer, T.D., & Gage, F.H. (2002) Functional neurogenesis in the adult hippocampus **415**, 1030–1034.

Prigge, C.L. & Kay, J.N. (2018) Dendrite morphogenesis from birth to adulthood. *Curr. Opin. Neurobiol.*, **53**, 139–145.

Pujadas, L., Gruart, A., Bosch, C., Delgado, L., Teixeira, C.M., Rossi, D., de Lecea, L., Martinez, A., Delgado-Garcia, J.M., & Soriano, E. (2010a) Reelin regulates postnatal neurogenesis and enhances spine hypertrophy and long-term potentiation. *J. Neurosci.*, **30**, 4636–4649.

Pujadas, L., Gruart, A., Bosch, C., Delgado, L., Teixeira, C.M., Rossi, D., de Lecea, L., Martinez, A., Delgado-Garcia, J.M., & Soriano, E. (2010b) Reelin Regulates Postnatal Neurogenesis and Enhances Spine Hypertrophy and Long-Term Potentiation. *J. Neurosci.*, **30**, 4636–4649.

Quassollo, G., Wojnacki, J., Salas, D.A., Gastaldi, L., Marzolo, M.P., Conde, C., Bisbal, M., Couve, A., & Caceres, A. (2015) A RhoA Signaling Pathway Regulates Dendritic Golgi Outpost Formation. *Curr. Biol.*, **25**, 971–982.

Rahimi-Balaei, M., Bergen, H., Kong, J., & Marzban, H. (2018) Neuronal Migration During Development of the Cerebellum. *Front. Cell. Neurosci.*, **12**, 484.

Ranaivoson, F.M., von Daake, S., & Comoletti, D. (2016) Structural Insights into Reelin Function: Present and Future. *Front. Cell. Neurosci.*, **10**, 137.

Rao, M.S. & Shetty, A.K. (2004) Eficacy of doublecortin as a marker to analyse the absolute number and dendritic growth of newly generated neurons in the adult dentate gyrus **19**.

Ray, S. & Brecht, M. (2016) Structural development and dorsoventral maturation of the medial entorhinal cortex. *Elife*, **5**, e13343.

Rio, C., Rieff, H.I., Qi, P., Khurana, T.S., & Corfas, G. (1997) Neuregulin and erbB receptors play a critical role in neuronal migration. *Neuron*, **19**, 39–50.

Rodriguez-Iglesias, N., Sierra, A., & Valero, J. (2019) Rewiring of Memory Circuits: Connecting Adult Newborn Neurons With the Help of Microglia. *Front. cell Dev. Biol.*, **7**, 24.

Rossi, D.J., Jamieson, C.H.M., & Weissman, I.L. (2008) Stems Cells and the Pathways to Aging and Cancer 681–696.

Royaux, I., Lambert de Rouvroit, C., D'Arcangelo, G., Demirov, D., & Goffinet, A.M. (1997) Genomic organization of the mouse reelin gene. *Genomics*, **46**, 240–250.

Ruzankina, Y., Pinzon-Guzman, C., Asare, A., Ong, T., Pontano, L., Cotsarelis, G., Zediak, V.P., Velez, M., Bhandoola, A., & Brown, E.J. (2007) Deletion of the developmentally essential gene ATR in adult mice leads to age-related phenotypes and stem cell loss. *Cell Stem Cell*, **1**, 113–126.

Sakai, K., Shoji, H., Kohno, T., Miyakawa, T., & Hattori, M. (2016) Mice that lack the C-terminal region of Reelin exhibit behavioral abnormalities related to neuropsychiatric disorders. *Sci. Rep.*, **6**, 28636.

Santana, J. & Marzolo, M.-P. (2017) The functions of Reelin in membrane trafficking and cytoskeletal dynamics: implications for neuronal migration, polarization and differentiation. *Biochem. J.*, **474**, 3137–3165.

Sathyanesan, A., Zhou, J., Scafidi, J., Heck, D.H., Sillitoe, R. V, & Gallo, V. (2019) Emerging connections between cerebellar development, behaviour and complex brain disorders. *Nat. Rev. Neurosci.*,.

Schelski, M. & Bradke, F. (2017) Neuronal polarization: From spatiotemporal signaling to cytoskeletal dynamics. *Mol. Cell. Neurosci.*, **84**, 11–28.

Segarra, M., Aburto, M.R., Cop, F., Llao-Cid, C., Hartl, R., Damm, M., Bethani, I., Parrilla, M., Husainie, D., Schanzer, A., Schlierbach, H., Acker, T., Mohr, L., Torres-Masjoan, L., Ritter, M., & Acker-Palmer, A. (2018) Endothelial Dab1 signaling orchestrates neuro-glia-vessel communication in the central nervous system. *Science*, **361**.

Seki, T., Sato, T., Toda, K., Osumi, N., Imura, T., & Shioda, S. (2014) Distinctive population of Gfap-expressing neural progenitors arising around the dentate notch migrate and form the granule cell layer in the developing hippocampus. *J. Comp. Neurol.*, **522**, 261–283.

Sekine, K., Honda, T., Kawauchi, T., Kubo, K., & Nakajima, K. (2011) The outermost region of the developing cortical plate is crucial for both the switch of the radial migration mode and the Dab1-dependent “inside-out” lamination in the neocortex. *J. Neurosci.*, **31**, 9426–9439.

Sekine, K., Kawauchi, T., Kubo, K.-I., Honda, T., Herz, J., Hattori, M., Kinashi, T., & Nakajima, K. (2012) Reelin controls neuronal positioning by promoting cell-matrix adhesion via inside-out activation of integrin alpha5beta1. *Neuron*, **76**, 353–369.

Sekine, K., Kubo, K., & Nakajima, K. (2014) How does Reelin control neuronal migration and layer formation in the developing mammalian neocortex? *Neurosci. Res.*, **86**, 50–58.

Senturk, A., Pfennig, S., Weiss, A., Burk, K., & Acker-Palmer, A. (2011) Ephrin Bs are essential components of the Reelin pathway to regulate neuronal migration. *Nature*, **472**, 356–360.

Sibbe, M., Kuner, E., Althof, D., & Frotscher, M. (2015) Stem- and Progenitor Cell Proliferation in the Dentate Gyrus of the Reeler Mouse 3–11.

Simo, S. & Cooper, J.A. (2013) Rbx2 regulates neuronal migration through different cullin 5-RING ligase adaptors. *Dev. Cell*, **27**, 399–411.

Song, J., Olsen, R.H.J., Sun, J., Ming, G.-L., & Song, H. (2016) Neuronal Circuitry Mechanisms Regulating Adult Mammalian Neurogenesis. *Cold Spring Harb. Perspect. Biol.*, **8**.

Soriano, E. & Del Rio, J.A. (2005) The cells of cajal-retzius: still a mystery one century after. *Neuron*, **46**, 389–394.

Sotelo, C. (2004) Cellular and genetic regulation of the development of the cerebellar system.

Prog. Neurobiol., **72**, 295–339.

Super, H., Soriano, E., & Uylings, H.B. (1998) The functions of the preplate in development and evolution of the neocortex and hippocampus. *Brain Res. Brain Res. Rev.*, **27**, 40–64.

Tabata, H. & Nakajima, K. (2003) Multipolar migration: the third mode of radial neuronal migration in the developing cerebral cortex. *J. Neurosci.*, **23**, 9996–10001.

Takano, T., Xu, C., Funahashi, Y., Namba, T., & Kaibuchi, K. (2015) Neuronal polarization. *Development*, **142**, 2088–2093.

Taniguchi, H., He, M., Wu, P., Kim, S., Paik, R., Sugino, K., Kvitsiani, D., Fu, Y., Lu, J., Lin, Y., Miyoshi, G., Shima, Y., Fishell, G., Nelson, S.B., & Huang, Z.J. (2011) A resource of Cre driver lines for genetic targeting of GABAergic neurons in cerebral cortex. *Neuron*, **71**, 995–1013.

Teixeira, C.M., Kron, M.M., Masachs, N., Zhang, H., Lagace, D.C., Martinez, A., Reillo, I., Duan, X., Bosch, C., Pujadas, L., Brunso, L., Song, H., Eisch, A.J., Borrell, V., Howell, B.W., Parent, J.M., & Soriano, E. (2012) Cell-autonomous inactivation of the reelin pathway impairs adult neurogenesis in the hippocampus. *J. Neurosci.*, **32**, 12051–12065.

Terrillion, C.E., Abazyan, B., Yang, Z., Crawford, J., Shevelkin, A. V, Jouroukhin, Y., Yoo, K.H., Cho, C.H., Roychaudhuri, R., Snyder, S.H., Jang, M.-H., & Pletnikov, M. V (2017) DISC1 in Astrocytes Influences Adult Neurogenesis and Hippocampus-Dependent Behaviors in Mice. *Neuropsychopharmacology*, **42**, 2242–2251.

Tissir, F. & Goffinet, A.M. (2003) Reelin and brain development. *Nat. Rev. Neurosci.*, **4**, 496–505.

Toni, N. & Schinder, A.F. (2015) Maturation and Functional Integration of New Granule Cells into the Adult Hippocampus. *Cold Spring Harb. Perspect. Biol.*, **8**, a018903.

Trommsdorff, M., Gotthardt, M., Hiesberger, T., Shelton, J., Stockinger, W., Nimpf, J., Hammer, R.E., Richardson, J.A., & Herz, J. (1999) Reeler/Disabled-like disruption of neuronal migration in knockout mice lacking the VLDL receptor and ApoE receptor 2. *Cell*, **97**, 689–701.

Uchida, T., Baba, A., Perez-Martinez, F.J., Hibi, T., Miyata, T., Luque, J.M., Nakajima, K., & Hattori, M. (2009) Downregulation of functional Reelin receptors in projection neurons implies that primary Reelin action occurs at early/premigratory stages. *J. Neurosci.*, **29**, 10653–10662.

Urban, N. & Guillemot, F. (2014) Neurogenesis in the embryonic and adult brain: same regulators, different roles. *Front. Cell. Neurosci.*, **8**, 396.

Waites, C.L., Craig, A.M., & Garner, C.C. (2005) Mechanisms of vertebrate synaptogenesis. *Annu. Rev. Neurosci.*, **28**, 251–274.

Wang, S., Brunne, B., Zhao, S., Chai, X., Li, J., Lau, J., Failla, A.V., Zobiak, B., Sibbe, M., Westbrook, G.L., Lutz, D., & Frotscher, M. (2018) Trajectory Analysis Unveils Reelin's Role in the Directed Migration of Granule Cells in the Dentate Gyrus. *J. Neurosci.*, **38**, 137–148.

Wasser, C.R. & Herz, J. (2017) Reelin: Neurodevelopmental Architect and Homeostatic Regulator of Excitatory Synapses. *J. Biol. Chem.*, **292**, 1330–1338.

Won, S.J., Kim, S.H., Xie, L., Wang, Y., Mao, X.O., Jin, K., & Greenberg, D.A. (2006) Reelin-deficient mice show impaired neurogenesis and increased stroke size. *Exp. Neurol.*, **198**, 250–259.

Yoshida, M., Assimacopoulos, S., Jones, K.R., & Grove, E.A. (2006) Massive loss of Cajal-Retzius cells does not disrupt neocortical layer order. *Development*, **133**, 537–545.

Zhao, C., Deng, W., & Gage, F.H. (2008) Mechanisms and Functional Implications of Adult Neurogenesis. *Cell*, **132**, 645–660.

Zhao, C., Teng, E.M., Jr, R.G.S., Ming, G., & Gage, F.H. (2006) Distinct Morphological Stages of Dentate Granule Neuron Maturation in the Adult Mouse Hippocampus **26**, 3–11.

Zhao, S., Chai, X., & Frotscher, M. (2007) Balance between neurogenesis and gliogenesis in the adult hippocampus: role for reelin. *Dev. Neurosci.*, **29**, 84–90.

Zhao, S. & Frotscher, M. (2010) Go or stop? Divergent roles of Reelin in radial neuronal migration. *Neuroscientist*, **16**, 421–434.

Zhao, X.-F., Kohen, R., Parent, R., Duan, Y., Fisher, G.L., Korn, M.J., Ji, L., Wan, G., Jin, J., Puschel, A.W., Dolan, D.F., Parent, J.M., Corfas, G., Murphy, G.G., & Giger, R.J. (2018) PlexinA2 Forward Signaling through Rap1 GTPases Regulates Dentate Gyrus Development and Schizophrenia-like Behaviors. *Cell Rep.*, **22**, 456–470.

Zhou, L., Jossin, Y., & Goffinet, A.M. (2007) Identification of small molecules that interfere with radial neuronal migration and early cortical plate development. *Cereb. Cortex*, **17**, 211–220.